Department of Chemistry

Tracer and interdiffusion measurements of some common salts in aqueous solutions and in porous ceramic media

Jori Ahl

Aalto University

DOCTORAL DISSERTATIONS

Aalto University publication series
DOCTORAL DISSERTATIONS 134/2014

Tracer and interdiffusion measurements of some common salts in aqueous solutions and in porous ceramic media

Jori Ahl

Doctoral dissertation for the degree of Doctor of Science in Technology to be presented with due permission of the School of Chemical Technology for public examination and debate in Auditorium Forest Products Building 2 at the Aalto University School of Chemical Technology (Espoo, Finland) on the 17th of October, 2014, at 12 noon.

Aalto University
School of Chemical Technology
Department of Chemistry
Research Group of Physical Chemistry and Electrochemistry

Supervising professor
Professor Kyösti Kontturi

Thesis advisor
Professor Simo Liukkonen

Preliminary examiners
Assistant Professor Javier Cervera, University of Valencia, Spain
Professor Derek Leaist, St. Francis Xavier University, Canada

Opponent
Professor Vicente M. Aguilella Fernández, Universitat Jaume I de Castellón, Spain

Aalto University publication series
DOCTORAL DISSERTATIONS 134/2014

ISBN 978-952-60-5846-7
ISBN 978-952-60-5847-4 (pdf)
ISSN-L 1799-4934
ISSN 1799-4934 (printed)
ISSN 1799-4942 (pdf)
http://urn.fi/URN:ISBN:978-952-60-5847-4

Unigrafia Oy
Helsinki 2014

Finland

Aalto University

Abstract

Aalto University, P.O. Box 11000, FI-00076 Aalto www.aalto.fi

Author
Jori Ahl

Name of the doctoral dissertation
Tracer and interdiffusion measurements of some common salts in aqueous solutions and in porous ceramic media

Publisher School of Chemical Technology

Unit Department of Chemistry

Series Aalto University publication series DOCTORAL DISSERTATIONS 134/2014

Field of research Physical Chemistry

Manuscript submitted 25 February 2014 **Date of the defence** 17 October 2014

Permission to publish granted (date) 17 June 2014 **Language** English

☐ **Monograph** ☒ **Article dissertation (summary + original articles)**

Abstract

There was a need for tracer diffusion measurement data in ternary $MgCl_2$-NaCl-H_2O system to test theoretical models of electrolytes and also need for interdiffusion coefficients in porous ceramic materials to be used in a simulation program to predict moisture and concentration profiles under different environmental conditions. In this work diffusion in aqueous solutions in absence and presence of porous ceramic brick medium was investigated with the Closed Capillary (CCM) and Diaphragm Cell Methods (DM). The measuring techniques, the apparatus as well the calculation method of diffusion coefficients were developed and optimized. The tracer diffusion coefficients of ^{22}NaCl were determined as a function of $MgCl_2$ concentration in aqueous solutions at 298.15 K in a large concentration region. The Onsager limiting law was verified for the first time for a 2:1 electrolyte. The ionization effect of water was taken into account by resolving the relevant Nernst-Planck equations.

The interdiffusion coefficients of NaCl were measured in ceramic bricks new red brick (NRB), old light brick (OLB) and old dark brick (ODB). The effect of concentration and temperature and the salts NaCl, KCl, $NaNO_3$, $CaCl_2$, Na_2SO_4, $MgCl_2$, Na_2CO_3 for diffusion coefficients were investigated. Numerical computer simulation and data analysis were carried out together to obtain both analytical and numerical solutions. For salt diffusion in fully saturated brick under isothermals condition a mathematical model was developed.

In this thesis the CCM was for the first time applied to the measurement of the diffusion coefficients in a porous medium. By taking the experimentally shown sorbed part of the salt flux into account, a Freundlich-like adsorption isotherm could be determined with the help of the calculated adsorption capacity function of NaCl in NRB at 298.15 K. Overall the main conclusion of this experimental thesis is that the methods of DM and CCM developed and optimized here are both excellent techniques for the salt diffusion coefficient measurements in porous ceramic media. In CCM as an absolute method the porosity of the medium can even be unknown.

Keywords tracer diffusion coefficient, closed capillary method, sodium-22 chloride tracer, salt diffusion in porous media, interdiffusion coefficient in fired ceramic brick

ISBN (printed) 978-952-60-5846-7 **ISBN (pdf)** 978-952-60-5847-4

ISSN-L 1799-4934 **ISSN (printed)** 1799-4934 **ISSN (pdf)** 1799-4942

Location of publisher Helsinki **Location of printing** Helsinki **Year** 2014

Pages 164 **urn** http://urn.fi/URN:ISBN:978-952-60-5847-4

A! Aalto-yliopisto

Tiivistelmä

Aalto-yliopisto, PL 11000, 00076 Aalto www.aalto.fi

Tekijä
Jori Ahl

Väitöskirjan nimi
Elektrolyyttien tracer- ja interdiffuusiomittauksia vesiliuoksissa ja huokoisissa keraamisissa väliaineissa

Julkaisija Kemian tekniikan korkeakoulu

Yksikkö Kemian laitos

Sarja Aalto University publication series DOCTORAL DISSERTATIONS 134/2014

Tutkimusala Fysikaalinen kemia

Käsikirjoituksen pvm 25.02.2014 **Väitöspäivä** 17.10.2014

Julkaisuluvan myöntämispäivä 17.06.2014 **Kieli** Englanti

☐ **Monografia** ☒ **Yhdistelmäväitöskirja (yhteenveto-osa + erillisartikkelit)**

Tiivistelmä

Väitöskirjan lähtökohtana oli tarve kokeellisille diffuusiokertoimille ternäärisissä $MgCl_2$-NaCl-H_2O liuoksissa ja binäärisissä yleisissä suolaliuoksissa huokoisissa väliaineissa. Näitä spesifisiä tracer- ja interdiffuusiokertoimia tarvitaan teoreettisten mallien testaamiseen elektrolyyteissä sekä parametreinä kosteus- ja suolakonsentraatioprofiileja huokoisessa väliaineessa erilaisissa ympäristöolosuhteissa ennustavissa simulaatio-ohjelmissa. Näiden haluttujen diffuusiokertoimien mittaamiseksi kehitettiin ja optimoitiin suljetun kapillaarin (CCM) ja diafragmakennon (DM) laskenta- ja mittausmenetelmiä sekä laitteistoa.

^{22}NaCl:n tracerdiffuusiokertoimet määritettiin $MgCl_2$:n vesiliuoksissa konsentraation funktiona lämpötilassa 298,15 K. Teoreettinen Onsagerin rajalaki (OLL) todistettiin kokeellisesti ensimmäistä kertaa 2:1 elektrolyytille. Veden ionitulon vaikutus diffuusiokertoimiin hyvin laimeissa liuoksissa rajalakialueella osoitettiin sekä kokeellisesti että teoreettisesti ratkaisemalla Nernst-Planck -yhtälöt veden ionisaatio huomioon ottaen. Väitöskirjassa CCM menetelmää sovellettiin myös ensimmäistä kertaa diffuusiokertoimien määrittämiseen huokoisessa väliaineessa.

NaCl:n interdiffuusiokertoimet mitattiin keraamisissa väliaineissa: uusi suomalainen punatiili (NRB), vanha vaalea tiili (OLB) ja vanha tumma tiili (ODB). Elektrolyyttien NaCl, KCl, $NaNO_3$, $CaCl_2$, Na_2SO_4, $MgCl_2$, Na_2CO_3 diffuusiokertoimet sekä konsentraation ja lämpötilan vaikutus mitattiin. Kokeellisten diffuusiokertoimien, numeerisen analyysin ja tietokonesimulaation avulla esitettiin matemaattinen malli täysin elektrolyytillä kyllästetyssä tiliväliaineessa vakiolämpötilassa. Loppupäätelmänä voidaan todeta, että sekä DM että CCM ovat kumpikin hyviä ja tarkkoja menetelmiä suolojen diffuusiokertoimien määrityksiin myös huokoisessa keraamisessa materiaalissa. Absoluuttisena menetelmänä CCM:ssä väliaineen huokoisuutta ei edes tarvitse tietää.

Avainsanat tracerdiffuusiokerroin, suljetun kapillaarin menetelmä, natrium-22-kloridi merkkiaine, suolan diffuusio huokoisessa materiaalissa, interdiffuusiokerroin poltetussa keraamisessa tiilessä

ISBN (painettu) 978-952-60-5846-7 **ISBN (pdf)** 978-952-60-5847-4

ISSN-L 1799-4934 **ISSN (painettu)** 1799-4934 **ISSN (pdf)** 1799-4942

Julkaisupaikka Helsinki **Painopaikka** Helsinki **Vuosi** 2014

Sivumäärä 164 **urn** http://urn.fi/URN:ISBN:978-952-60-5847-4

Dedicated to Ia, Ea and Noa

PREFACE

The experimental part of this thesis was performed in two periods. The first, utilizing the Closed Capillary Method (CCM), was carried out at the Laboratory of Physical Chemistry and Electrochemistry from 1990 to 1996. The second part of the research, using the Diaphragm Cell Method (DM), was accomplished by the author during the years 1998–2004 in the Laboratory of Structural Engineering and Building Physics of the Department of Civil and Environmental Engineering. Concurrently to the DM measurements, the CCM measurements were continued during the years 2000–2004 in the Laboratory of Physical Chemistry and Electrochemistry of the Department of Chemical Technology. The author performed all the experimental work in both laboratories.

First, I would like to express my gratitude to my supervisor, Professor Kyösti Kontturi, for providing me with the chance to finish my thesis and all the guidance, advice and encouragement over the years. Also, I am very grateful to Emeritus Professor Simo Liukkonen for the invaluable contribution, interest in my work and the endless patience and support during the work. The numerous and often prolonged but always fruitful discussions have given the author deeper understanding of the science of physical chemistry. I owe a special debt of gratitude to Professor José A. Manzanares for his advices, suggestions and kind help, which have been of utmost importance for the completion of the work.

I would also like to give special thanks to my co-author in two publications of this thesis: Professor Xiaoshu Lü with whom I have had the pleasure to work. I wish to thank Professor Lasse Murtomäki for all the valuable remarks and constructive critical comments concerning the manuscript. I would also like to acknowledge the help and ideas given by Professor Martti Viljanen and the possibility to work in his laboratory of Structural Engineering and Building Physics. The grammatic corrections made by Dr. Benjamin Wilson is greatly appreciated.

In addition, my sincere thanks to the personnel at both the laboratories of Physical Chemistry and Electrochemistry and Structural Engineering and Building Physics for all the practical help and kindness during these years. I am also indebted to all my past and present colleagues, friends and every person not mentioned here who has helped me reach this goal.

Finally, I want to thank my wonderful wife, Sari, and our dear children, Ia, Ea and Noa, for their support, understanding and endless patience in giving me time and space to complete my tortuous diffusion journey, which have been slow but luckily irreversible process. This thesis is dedicated to all of you. The cover image taken by Ia is appreciated.

Espoo, May 2014.

Jori Ahl

CONTENTS

LIST OF PUBLICATIONS

This thesis is based on the five publications listed below. The publications are referred to in the text by their Roman numerals (I-V). In addition to these publications, this thesis includes previously unpublished work, which mainly concerns tracer and interdiffusion measurements as well as calculations with CCM. This unpublished research concerns measurements firstly at infinite dilution of aqueous solutions (continuing the measurements made in publication I) and secondly, in a porous ceramic brick medium extending the measurements made in publications II and III. In addition this thesis details the development and original application of CCM to the built environment.

I. Ahl, J. and Liukkonen, S. Tracer Diffusion of Sodium-22 Chloride in $MgCl_2$-H_2O-Solutions, *Z. Phys. Chem*. **211** (1999) 69-83.

II. Ahl, J. Salt Diffusion in Brick Structures. Part I. Measurements with NaCl, *J. Mater. Sci*. **38** (2003) 2055-2061.

III. Ahl, J. Salt Diffusion in Brick Structures. Part II. The Effect of Temperature, Concentration and Salt, *J. Mater. Sci*. **39** (2004) 4247-4254.

IV. Lü, X. and Ahl, J. Studying of Salt Diffusion Coefficient in Brick - Analytical and Numerical Methods, *J. Mater. Sci*. **40** (2005) 3795-3802.

V. Ahl, J. and Lü, X. Studying of Salt Diffusion Behavior in Brick, *J. Mater. Sci*. **42** (2007) 2512-2520.

AUTHOR'S CONTRIBUTION

Jori Ahl has planned and carried out the experimental work in all publications. He has also written the publications and participated in interpretation of the experimental results. Publication I was written with S. Liukkonen and Publications IV and V were written in collaboration with X. Lü.

Espoo, May 2014.

Professor Kyösti Kontturi

1 INTRODUCTION

The term tracer diffusion refers to the diffusion of one species (e.g., atom, ion or molecule, which may be radioactive) which has a very low concentration in an otherwise uniform solution. Under these conditions, the diffusion of a tracer species depends only on its own concentration gradient. In the history of diffusion studies, the measurement of tracer diffusion coefficients is a relatively new field. The first diffusion coefficient measurements were performed by Graham [1, 2] and Fick [3, 4] between 1829-1855, whereas the first tracer diffusion measurements only date from 1947-1952 (Adamson, Anderson, Saddington, Stokes, Nielsen, Cobble) [5-8]. This research was also preceded by Onsager's pioneering works concerning the microscopic and macroscopic theories of diffusion [9-12]. Although subsequently there have been a number of excellent studies within the literature concerning tracer diffusion [13-16], data relating to thermodynamic and transport properties of electrolyte solutions are insufficient [17, 18]. The first critical examination of tracer diffusion data compiled from the literature was by Mills and Lobo in 1989 [19], but it is worth noting however even in this compilation that the values of tracer diffusion coefficients measured under 0.1 mol/dm^3 are lacking for many salt ions in general electrolytes, whilst values under 10^{-3} mol/dm^3 are almost totally absent.

Furthermore, there has been a need for systematic studies of multicomponent transport properties experimentally. In particular there have been very few mixed electrolyte systems for which all the necessary transport data over a wide range of concentration was available [20]. These experimental and numerical values are required for the understanding and modeling a wide variety of chemical, geochemical, and industrial processes [20, 21]. In addition, the same data is also essential in order to be able to calculate and test the theoretical models of statistical mechanical electrolytes [22-26]. Experimental mutual diffusion data are part of the input information required for calculation of the generalized transport coefficients of irreversible thermodynamics [27, 28] such as the ionic Onsager l_{ij} coefficients [29-31], the R_{ij} friction coefficients [29, 31], and also velocity correlation coefficients [32-35]. Numerical values for the generalized transport coefficients can, in turn, be used as a guide for extending and refining available basic theories and as test systems for developing more accurate approximation methods [36, 37].

In 1984 the NaCl-$MgCl_2$-H_2O electrolyte system at 25°C was chosen as a suitable ternary aqueous mixture at a temperature of as part of an international collaboration between leading laboratories [19, 38]. This higher valence mixture provided a more severe test of the then current theories and as a ternary system it was also important as a model of seawater, its evaporates and concentrated brines, as a typical seawater composition corresponds to a 9.6:1 ratio (0.489 mol/dm^3 NaCl and 0.051 mol/dm^3 $MgCl_2$) [39]. Multivalent cations, like Mg^{2+}, also have a substantial influence on water structure and dynamics within an aqueous salt solution [40] and as a result a number transport property studies in the ternary

$NaCl\text{-}MgCl_2\text{-}H_2O$ have been performed [19, 39, 41-46]. In contrast, there have been only two publications, by Mills et al. [39] and Albright et al. [47], concerning tracer diffusion measurements of the Na^+ ion in a ternary $NaCl\text{-}MgCl_2\text{-}H_2O$ system. These measurements were done only in the strong supporting electrolyte region ($[MgCl_2] > 0.5$ mol/dm^3, where the brackets denote molar concentration).

One of the aims of this work was to measure the tracer diffusion coefficients of Na^+ ion in the ternary $NaCl\text{-}MgCl_2\text{-}H_2O$ system over a large concentration region and to test the Onsager limiting law for 2:1 electrolyte for first time [publication I]. In order to explain the tracer diffusion results obtained in the very dilute region under 10^{-4} mol/dm^3 of $MgCl_2$ additional binary diffusion measurements were performed and the measured binary diffusion coefficients for NaCl at a salt concentration of 10^{-6} mol/dm^3 in the $NaCl\text{-}H_2O$ system were compared to the values calculated from the Nernst-Planck equations when taking into account the ionization of water.

Over the years a number of different experimental methods have been utilized for the determination of the tracer diffusion coefficient. These include: electro analytical methods e.g. polarographic and voltammetric methods [18], diaphragm techniques, the two capillary techniques, the optical refraction techniques based on the Gouy and Rayleigh interference phenomena [48-50] and the NMR spin echo method [51-53]. In particular, the latter has been confined to nuclei with suitable magnetic moments and it has been used mainly for diffusion experiments in inorganic and organic compounds [51, 54] or in electrolyte solutions [18]. In electrolyte solutions the Diaphragm Cell [5,55], the Open-Ended Capillary [6,56] and the Closed Capillary [57,58] methods have, in the main, been used in the determination of the radioactive ion diffusion coefficient.

Nevertheless these techniques have their drawbacks as, both the diaphragm and open-ended capillary methods always have a systematic error due to either the calibration of diaphragm, (also known as the immersion effect) or the flow of inactive solution over the open end of the capillary, the so called ΔL effect [59-62]. Unlike the previous two methods the set-up of the Closed Capillary Method (CCM) means its primary source of error results from the statistical nature of radioactive decay [63, 64].

The first part of the thesis is based on the closed capillary technique developed by Passiniemi, Liukkonen, Noszticzius and Rastas [65-69]. In publication I, the CCM was further developed and tested. A whole new diffusion cell was designed with better temperature control, cell geometry, lead shields and particular emphasis was placed on how to calculate the tracer diffusion coefficient from the experimental dependence of the pulse counts versus time. The previously used calculation based on the Guggenheim Method from reaction kinetics suffered statistical problems due to the decreasing pulse counts differences as a function of time [70]. Three different methods including the Guggenheim were statistically tested with F- and t-tests. Statistical and fittings errors related to these calculation methods were evaluated and the method leading to the most exact diffusion

coefficient values was determined. The calculation method that provided the most reliable diffusion coefficient values was then applied to the tracer diffusion measurements of $^{22}NaCl$ in aqueous $MgCl_2$ (publication I) and also in a study by Ahl and Liukkonen [71]. This calculation method was also applied to the interdiffusion measurements of $^{22}NaCl$ in the aqueous NaCl (unpublished data).

The second part of this thesis deals with salt diffusion measurements in a porous brick matrix. In the capillaries within brick, aqueous electrolyte solutions can cause brick wall deterioration due to changing climatic conditions. The movement of salts within brick depending on its water content and these salts may be precipitated on the outer wall as efflorescence or concentrated under the paint layer covering brick as subfflorescence. This white, powdery crust of crystallized salts and other different types of surface damage may appear in brick walls as a result of these concentrating salting out phenomena. The effects of temperature, moisture and different salt types on the deterioration of brickwork have been investigated using salt stress tests on brick samples [72]. In addition, the distribution of different salts and their deteriorating effects in bricks have been studied [72, 73]. A number of theories of different decay mechanisms in porous building materials due to salts and moisture action have been proposed [72-75] and the possible sources of efflorescent salts, measures needed to control efflorescence, means to remove salting out from the brick wall have also been presented. In summary the phenomenon of salt deterioration in porous materials is a complicated subject but it is well known and has been reported by many researchers [76-81].

Structure durability determination is an important calculation in building science and environmental engineering as porous materials like bricks are commonly used in building industry their deterioration by the action of water and salt should be predictable. In order to reach this goal, the salt transport process needs to be modeled and this requires appropriate experimental transport data. As diffusion is an important transport mechanism in porous materials the ability to be able to precisely estimate diffusion coefficients is important [82]. However from a study of the salt behavior in brick literature, it can be concluded that research in this area is minimal.

Most of the related studies in the field of civil engineering are limited primarily to specific applications with regard to chloride ion behavior and transport in concrete [83-86]. In particular the diffusion coefficients of different salts measured in a brick medium as a function of concentration and temperature are needed as these coefficients may be used in simulation programs to predict moisture and concentration profiles in brick under different environmental conditions. The mechanism of salt transport in porous material can be further complicated as in addition to diffusion convection, thermal convection, migration, capillary suction accompanied by physical and chemical binding of salts on the pore walls and possible surface diffusion can also play a role. In order to measure the effect of one particular transport process all other transport processes must be excluded experimentally or mathematically as in all practical situations - at normal pressures - diffusion contributes both to the transport of salts into and within the

brick structures. In publications II and III the diffusion of salt and the diffusion measuring techniques in porous brick media are developed and studied.

In publication II a method for measuring the diffusion rate of salt in ceramic material is presented and tested with different thicknesses of brick samples and different initial salt concentrations. The method is based on the principle of porous diaphragm technique first introduced by Northrop and Anson [87] and developed by McBain [88], Hartley [89] and Stokes [7]. Originally this method was used for measurements of salt diffusion coefficients in aqueous solutions and the diffusion cell developed as part of this work is based on equipment designed to measure the diffusion coefficient of salt through polymer membranes [90], diffusion coefficient of the chloride ion in cementitious materials [91, 93], and through bricks [94-99]. During the design of the new diffusion cell emphasis was placed on optimizing the geometrical structure, mechanical vibrations and temperature control of the cell. In addition polarization effects on the electrodes and the leakage of electrolyte over specimen were strictly controlled. By using this new cell the interdiffusion coefficient was determined for NaCl in three different ceramic brick materials of NRB, OLB and ODB.

In publication III the developed Diffusion Cell Method (DM) was used to measure the interdiffusion coefficients for other common water-soluble salts found in porous brick media. The interdiffusion coefficients were measured for seven different aqueous electrolyte solutions: NaCl, KCl, $NaNO_3$, $CaCl_2$, Na_2SO_4, $MgCl_2$ and Na_2CO_3. The effect of temperature and concentration on the diffusion coefficient in a porous brick medium were investigated by determining the diffusivity change of NaCl in new Finnish red brick. The mutual relation between the diffusion coefficient in porous brick and the viscosity of the aqueous salt solution was analyzed. The concept of salt diffusion coefficient and diffusion mechanism inside the isotropic macro-porous brick matrix with a continuous pore space is discussed in terms of the pore space characteristics: porosity, a tortuosity and a constrictivity factor.

In publication IV more measurements were carried out and measurement data with different parameters were studied in a more systematic way. The diffusion of salt was studied under isothermal conditions and constant concentration by means of diffusion cell measurements and mathematical methods. NaCl was chosen as the major salt type, as it is one of the main salt components found in building materials. When completely saturated at constant pressure, the convective transport can be neglected; hence a pure diffusion mechanism by concentration gradient is established. The diffusion coefficient is a fundamental parameter from which the transport rate and the depth of salt as a function of time can be predicted and calculated. The mathematical methods involve analytical and numerical calculations of the diffusion process in combination with measurement data. Mathematical model was constructed and its analytical solution was obtained. The analytical and numerical data were compared with the measurement data and showed a good correlation.

Publication V extends the previous work to include more salts commonly found in ceramic engineering bricks. As a representative sample a new red brick (NRB) manufactured commercially for buildings was selected. Dependence of the interdiffusion coefficient on temperature, concentration and other factors was evaluated from the measurements. Starting from the previously verified mathematical model, the diffusion coefficients for different types of salts and effect of temperature and ambient salt concentration on diffusion coefficient are presented. Once again analytical and numerical data corresponded with the measurements.

Prior to publications II-V, we also applied the analytical and numerical methods to study the diffusion of salts in porous brick [100]. However, the measurements were performed with the first generation diffusion cell, which had some systematic errors and resulted in incorrect diffusion coefficients values.

The diffusion coefficients measured in the presence of a fully saturated homogeneous porous brick medium and in the absence of a porous medium in free water were compared and discussed with the help of the measured and estimated parameters of porosity ε, constrictivity ξ and tortuosity τ. A material parameter explaining the relation of diffusion coefficients in the presence and absence of porous brick were obtained for the different porous brick media investigated. The ranking for the effective diffusion coefficients measured for different salts were demonstrated to depend on the solution viscosity (η) and the apparent hydration number (h_a) of the salt in porous brick medium.

In the third - yet unpublished - part of this thesis, the CCM was for the first time applied to the measurement of an electrolyte diffusion coefficient in a porous matrix. The appropriate diffusion cell for porous brick samples with a variable counting efficiency was developed using an optimized counting efficiency function measured with a two dimensional radioactive ^{22}NaCl plane source. The new linear least-square calculation method developed in publication I was applied to the measured intensity data $I = I(t)$ and the apparent differential and integral interdiffusion and tracer diffusion coefficients of ^{22}NaCl were measured as a function of concentration. The apparent integral interdiffusion coefficients obtained with this non-stationary-state CCM were compared with the effective interdiffusion coefficients measured with the stationary-state DM. It was found that both of these integral diffusion coefficients described the binary diffusion of NaCl inside porous NRB under the same conditions (c, T, p) and by taking the binding of part of the salt flux into account a Freundlich-like adsorption isotherm could be determined.

2 DIFFUSION PHENOMENA IN ELECTROLYTES

There is currently a lot of confusion in the diffusion terminology used throughout the published literature as the same terms are used interchangeably to mean different things resulting in a lack of clarity as to what kind of diffusion has been measured. In order to simplify the ambiguous nomenclature the diffusion systems in this work are divided into either binary or multicomponent diffusion systems. In the binary diffusion system the concepts of self-diffusion and interdiffusion can be distinguished, whereas for the multicomponent diffusion system involves multicomponent diffusion, tracer diffusion and intradiffusion models.

2.1 Binary diffusion

The term self-diffusion has always been related to diffusion in pure one-component liquids, i.e. the translational motions of species due to their thermal energy. As a result the self-diffusion coefficient is, in effect, a measure of how fast molecules diffuse among themselves in a one component system, for example the diffusion of water in water. In order to measure a diffusion coefficient in practice one has to select particles by labeling in a way that does not change any of the associated physical or chemical properties. For self-diffusion measurements this typically involves using different enantiomers or isotopes of molecules for which the dynamic properties are approximately the same, for instance the enantiomers of some organic molecules differ from each other only by their optical rotation or in the case of isomers by their mass. In general, one is concerned with the effect of isotopic mass on the diffusion process. For ions, the effect of the difference in mass of the labeled and unlabeled species is usually very small (e.g. $^{22}Na^{+}$, $^{23}Na^{+}$ and $^{24}Na^{+}$) and is not normally measurable within the precision of diffusion experiments [101]. Experimental evidence indicates that this assumption is reasonable for most systems where the isotopic masses of the diffusing components differ by less than 5 % as for greater mass differences, the possibility of isotope effects cannot be excluded [13]. In particular there are clear differences between the self-diffusion rates of the various isotopic forms of water which, in addition to the differences in molecular weight, moments of inertia and strength of the hydrogen bonds are significantly altered (e.g. HDO, D_2O, HTO, $H_2{}^{18}O$) and corrections have to be applied to obtain the value for H_2O [102, 103].

In essence such labeling results in a binary diffusion system and in principle, any system composed of labeled and unlabeled species has to be considered as a binary system. According to Weingärtner, only if the labeled species are present in trace amounts does the diffusion coefficient become equal to self-diffusion coefficient. If the diffusion coefficient measured depends solely on the concentration of the labeled species then the term mutual diffusion should be used [103]. Longsworth's [104, 105] measurements on H_2O-D_2O mixtures indicated measurable effects for the ratio of D_2O in H_2O. In this case the self-diffusion

coefficient of water is found by an extrapolation of D_2O concentration to zero as the real self-diffusion coefficient must be concentration independent.

The other form of diffusion present is the interdiffusion, which occurs between the two chemically distinct species within the binary system. There are numerous synonyms for interdiffusion coefficients used in the literature including binary diffusion, mutual diffusion, salt diffusion, electrolyte diffusion, hetero diffusion, chemical diffusion, isothermal diffusion and concentration diffusion coefficients depending on the publication and the binary system studied. All of these coefficients describe the diffusion of a substance or electrolyte as a whole. If there is a salt concentration gradient in a binary electrolyte system then the constraint of maintaining electrical neutrality ensures that positive and negative ions move from the region of higher to lower concentration at the same speed, hence there is only one interdiffusion coefficient in this type of system. Due to the concentration dependence of diffusion coefficient, the expressions integral and differential are sometimes added as a prefix [106]. The term integral interdiffusion coefficient is related to the average value when a large concentration difference involved, whereas the differential interdiffusion coefficient term is used when there is a much smaller concentration difference. However, the boundary value for when concentration difference results in either integral or differential interdiffusion is somewhat arbitrary [36, 104].

2.2 Multicomponent diffusion

The most common form of diffusion found in nature and many practical diffusion applications is multicomponent diffusion. In the multicomponent diffusion system there are more than two components and diffusion processes may involve the simultaneous diffusion of many solutes. For example, two electrolytes with a common ion in an essentially non-ionized solvent like H_2O form a ternary system, whereas two electrolytes without a common ion in H_2O form a quaternary solution for diffusion [36]. In multicomponent diffusion systems the electrostatic interaction can cause complex multicomponent effects as instead of a single electrostatic interaction trapping one anion and one cation as in a binary case, there now is a myriad interactions binding together all the ions in the system.

In addition the concentration gradient of one component can have an influence on the diffusion flow of another component as the ion which is the highest mobility can either accelerate the movement of oppositely charged ions, or inhibit diffusion of similarly charge ions. In some cases such mobile ions can also cause another ion to move against its concentration gradient from a region of low into a region of high concentration. These resulting multicomponent or ternary effects are caused by coupled diffusion with non-zero cross-term diffusion coefficients. For example, the use of the solvent mixture water-acetone increases significantly the diffusion rate of Na_2SO_4 when compared to binary case without acetone [107].

The multicomponent diffusion system changes to the tracer multicomponent diffusion system as the concentration of one component is allowed to approach

zero. In the case of a three-component system, which may be composed both of electrolytes and nonelectrolytes, the term ternary tracer system is used. In these ternary tracer systems the experiments are easier to perform than in the case of a ternary electrolyte system, for example, where four diffusion coefficients are required to determine the diffusion. In tracer diffusion experiments a very small amount of tracer (which is usually radioactive or somehow possible to identify) is added to part of the liquid system that is in equilibrium prior to the addition and it is essential that the labeled species is in trace amounts and not isotopic to any of the other species in the solution [108]. In the literature for the tracer diffusion coefficient is also referred to as the trace ion, single ion and ionic diffusion coefficient [19].

In tracer diffusion, the influence of the diffusion potential on the flux of the tracer ions is negligible. The species (ions and solvent) in tracer systems have independent diffusion coefficients that differ from those of electrolyte diffusion of the whole in binary systems. It should also be noted that the tracer diffusion coefficients essentially do not depend on the reference frame like cell-fixed or Fick's reference frame. Furthermore, since the activity coefficient of the tracer ion does not change in a virtually uniform solution, the thermodynamic factor $\partial ln a_i / \partial ln x_i$, which appears in the equations describing mutual diffusion, becomes unity. In tracer ion diffusion the electrophoretic effect is either zero or negligible so the relaxation effect is the only long-range interionic force to consider due to the extremely low concentration of the diffusing radioactive species and the movement of the tracer ion relative to a background of non-diffusing ions [12, 13, 18, 109].

The third diffusion form in the multicomponent diffusion system is intradiffusion, a term first introduced by Albright and Mills [13] to facilitate the description of diffusion in certain multicomponent systems. It is defined as the mutual diffusion between two chemically equivalent components within a multicomponent system. In this context chemically equivalent relates to the negligible differences in diffusion between these two components in the system. Usually this is done by replacing a portion of one component present by an isotopically labeled form of the same component (e.g. NaCl with ^{22}NaCl) and hence the movement of the new component maybe followed separately. In some cases the intradiffusion coefficient will be numerically equal to the tracer diffusion, however, it should be emphasized that the meanings of the two terms differ significantly. In tracer diffusion, attention is focused on a diffusing component which may or may not have a chemically equivalent component in the system and which is in very low concentration in an essentially homogeneous environment. In contrast, in an intradiffusion process the intradiffusion coefficient is independent of the ratio of the concentrations of the two components and depends only on the sum of their concentrations and the concentrations of the other components of the system. Moreover, in intradiffusion, the labeled component does not have to be present in trace amounts as is essential in tracer diffusion. The term intradiffusion is also related to the term self-diffusion, which can be defined as a special case of intradiffusion in a two-component binary system [110].

3 TRACER ELECTROLYTE SYSTEM

The diffusion phenomena (other than self-diffusion) are caused by a movement of substances under concentration gradients in a mixture with respect to each other. This movement at a microscopic level in a uniform liquid or solution is caused by the rapid random thermal motion of the ions and molecules, whereas macroscopically it can be observed indirectly as a Brownian motion. In experimental terms in order to measure the diffusion phenomenon a gradient of some kind is needed as the driving force for diffusion is the gradient of the chemical potential arising from the maximization of mixing entropy. The chemical potential is a function of the activity coefficient and the concentration and it can be determined by experiments (the activity coefficient usually considered to be unity) with respect to the standard chemical potential. However, the diffusion flow (flux) of a component cannot be determined directly but rather its divergence can be measured from the change in concentration with respect to time, $-\nabla \cdot J = \partial c/\partial t$.

In purely macroscopic terms substances are treated either as components or ionic constituents. A component is a substance which amount can be varied independently according to Gibbs phase rule, whereas ionic constituents or ionic species (ions) are the charged parts of a component. They are able to move with respect to each other although their concentrations cannot be varied against the electroneutrality condition.

3.1 Transport equations

The diffusion flow in a fluid mixture of *n* thermodynamic components can be described by using the linear phenomenological transport equations of irreversible thermodynamics [10,28,29,111]. It is also possible to use the empirical or practical flow equations which are extensions of Fick's law and involve the concentration gradients of the diffusing components and their diffusion coefficients D_{ij}. In this thesis the latter formalism has been chosen.

Diffusion is always measured relative to a reference frame and there are a variety of reference velocities e.g. number fixed velocity, solvent velocity (Hittorf's reference system) and volume-average velocity (Fick's reference system) [29]. At constant pressure and temperature the diffusion process in a multicomponent system can be described by the empirical Fick's equation generalized to a reference frame velocity v^r [112]:

$$J_i^r = C_i(v_i - v^r) = -\sum_{j=1}^{n-1} D_{ij} \nabla C_j, \qquad i = 1, 2, \ldots, n-1 \tag{1}$$

where $J_i^r, C_i, v_i, v^r, D_{ii}$ and D_{ij} are the flux density, concentration and velocity of component *i*, the reference velocity, the main-term diffusion coefficient of component *i* and the cross–term diffusion coefficient, respectively. In this thesis

we study diffusion processes in the absence of convection, so that the cell-fixed and the Hittorf reference frames become essentially equivalent. For the sake of clarity, no superscripts are then used on the flux densities to indicate the reference frame. Furthermore, no overhead arrows are written on vector quantities like flux densities or velocities.

The Nernst-Planck equations [113-115] are often applied to study electrolyte diffusion. They can be derived from the general phenomenological transport equations using certain assumptions which are reasonable in the dilute concentration range. The Nernst-Planck equations for the ionic flux densities are:

$$j_i = -u_i RT \nabla c_i - c_i u_i z_i F \nabla \Phi , \qquad i = 1, 2, \ldots, m \tag{2}$$

where $u_i, z_i, R, T, F,$ and Φ are the electric mobility and charge number of the ionic species i, the universal gas constant, the absolute temperature, the Faraday constant, and the electric potential, respectively. The number m of ionic species is different from the number of n of components.

The electric potential gradient $\nabla\Phi$ includes, in addition to the term caused by the external electric field, also the term caused by the internal electrical fields produced by the motion of oppositely charged ions (diffusion potential). The gradient $\nabla\Phi$ can be determined from the local electroneutrality condition and the relationship between ionic fluxes and electric current I:

$$\sum_{i=1}^{n} z_i c_i = 0 \tag{3}$$

$$\sum_{i=1}^{n} z_i j_i = \frac{I}{F} . \tag{4}$$

In an infinitely dilute solution (as indicated by a superscript 0) the electrical and diffusional ionic conductivities are equal and the Nernst-Einstein equation:

$$D_i^0 = RT u_i^0 = \frac{RT \lambda_i^0}{z_i^2 F^2} \tag{5}$$

is applicable [115]. The Nernst-Planck equations can then be presented as:

$$j_i = -D_i \nabla c_i - \frac{z_i F}{RT} D_i c_i \nabla \Phi , \qquad i = 1, 2, \ldots, m . \tag{6}$$

This remarkable fact that the diffusion coefficients of electrolytes can be predicted from their electrical properties was first recognized by Nernst [113, 114]. In Eq. (5), D_i^0, and λ_i^0 are the diffusion coefficient and the molar conductivity of the ionic species i at infinite dilution, respectively. The limiting molar conductivity λ_i^0 can be found by extrapolation to the infinite dilution from mobility (the moving-boundary method) or transport number measurements (the Hittorf method) [116].

3.2 Moderate dilution: $MgCl_2$-NaCl-H_2O

In the ternary electrolyte system $MgCl_2$-NaCl-H_2O, there are $n = 3$ components identified as 0, 1 and 2. Since the concentrations of the two electrolytes can be varied independently (at constant temperature and pressure), there are $n - 1 = 2$ independent electrolyte diffusion fluxes and $(n - 1)^2 = 4$ independent electrolyte diffusion coefficients. In the finite dilution concentration range considered in this section, 10^{-4} mol/dm$^3 \leq C \leq 10^{-2}$ mol/dm^3, the dissociation of water does not need to be taken into account.

The Fick diffusion equations for the system $MgCl_2$(1)-NaCl(2)-H_2O(0) are:

$$J_1 = -D_{11}\nabla C_1 - D_{12}\nabla C_2 \tag{7}$$

$$J_2 = -D_{21}\nabla C_1 - D_{22}\nabla C_2 \tag{8}$$

where J_1 , J_2 , C_1 and C_2 are the flux densities and molar concentrations of $MgCl_2$ and NaCl, respectively. The following relations are deduced between the limiting ternary interdiffusion coefficients for the components and the ionic limiting molar conductivities and the ionic diffusion coefficients [112]:

$$D_{11} = \frac{RT}{4F^2}\frac{6\lambda_1^0\lambda_3^0C_1+(\lambda_1^0\lambda_2^0+\lambda_1^0\lambda_3^0)C_2}{(\lambda_1^0+2\lambda_3^0)C_1+(\lambda_2^0+\lambda_3^0)C_2} = D_1 + t_1(D_3 - D_1) \tag{9}$$

$$D_{12} = \frac{RT}{2F^2}\frac{(\lambda_3^0-\lambda_2^0)\lambda_1^0C_1}{(\lambda_1^0+2\lambda_3^0)C_1+(\lambda_2^0+\lambda_3^0)C_2} = \frac{1}{2}t_1(D_3 - D_2) \tag{10}$$

$$D_{21} = \frac{RT}{2F^2}\frac{(4\lambda_3^0-\lambda_1^0)\lambda_2^0C_2}{(\lambda_1^0+2\lambda_3^0)C_1+(\lambda_2^0+\lambda_3^0)C_2} = \frac{1}{2}t_1(D_3 - D_2) \tag{11}$$

$$D_{22} = \frac{RT}{F^2}\frac{(\lambda_1^0\lambda_2^0+2\lambda_2^0\lambda_3^0)C_1+2\lambda_2^0\lambda_3^0C_2}{(\lambda_1^0+2\lambda_3^0)C_1+(\lambda_2^0+\lambda_3^0)C_2} = D_2 + t_2(D_3 - D_2) \tag{12}$$

where

$$t_1 = \frac{4D_1C_1}{4D_1C_1+D_2C_2+D_3(2C_1+C_2)} \tag{13}$$

$$t_2 = \frac{D_2C_2}{4D_1C_1+D_2C_2+D_3(2C_1+C_2)} \tag{14}$$

are the transport numbers of Mg^{2+} and Na^+. Notice that the subscripts 1 and 2 in the concentrations refer to the components $MgCl_2$ and NaCl, respectively, and the subscripts 1, 2 and 3 in the ionic conductivities and the ionic diffusion coefficients refer to the ionic species Mg^{2+}, Na^+ and Cl^-, respectively. Although these relations are strictly valid only in dilute solutions, for the sake of clarity no superscripts are used on the diffusion coefficients.

The ternary system $MgCl_2$-NaCl-H_2O becomes a tracer system when the concentration of one component vanishes. By allowing C_2 to approach zero the diffusion coefficients D_{ij} become gradually independent of the concentrations and consequently the diffusion coefficients in Eqs. (9)-(12) at $C_2 = 0$ become:

$$D_{11} = \frac{RT}{F^2}\frac{3\lambda_1^0\lambda_3^0}{2\lambda_1^0+4\lambda_3^0} = \frac{3D_1D_3}{2D_1+D_3} \tag{15}$$

$$D_{12} = \frac{RT}{2F^2}\frac{\lambda_1^0(\lambda_3^0-\lambda_2^0)}{\lambda_1^0+2\lambda_3^0} = \frac{D_1\ (D_3\ -D_2\ )}{2D_1\ +D_3} \tag{16}$$

$$D_{21} = 0 \tag{17}$$

$$D_{22} = \frac{RT}{F^2}\ \lambda_2^0 = D_2 \tag{18}$$

The theoretical diffusion coefficients can be calculated from the values of the ionic molar conductivities using Eqs. (15)-(18). With the literature values λ_1^0 = 106.8 S cm^2/mol (literature values vary between 106.1-107.4 S cm^2/mol) [117-120], λ_2^0 = 50.1 S cm^2/mol [116] and λ_3^0 = 76.4 S cm^2/mol [120] the calculated diffusion coefficients are D_{11}^0= 1.255×10^{-5} cm^2/s, D_{12}^0= 0.144×10^{-5} cm^2/s, and D_{22}^0= 1.334×10^{-5} cm^2/s. The main term diffusion coefficients D_{11}^0 and D_{22}^0 are the values of the interdiffusion coefficient of $MgCl_2$ and that of the tracer diffusion coefficient of the Na^+ ion at infinite dilution. In general, the cross-term diffusion coefficients are not symmetric i.e. $D_{ij} \neq D_{ji}$ as shown here with D_{12} and D_{21} [108].

The ternary system $MgCl_2$(1)-NaCl(2)-H_2O was studied experimentally in publication I. Radioactive, γ-emitting ^{22}NaCl was used as the tracer electrolyte and $MgCl_2$ as supporting electrolyte. The cross-term D_{21} describes the contribution of the concentration gradient of $MgCl_2$ to the diffusion flow of NaCl. Since the concentration gradient of $MgCl_2$ cannot drive a coupled flow of NaCl in a solution where there is no NaCl, Eq. (17) shows that D_{21} = 0 when C_2 = 0. Therefore, Eq. (8) reduces to:

$$J_2 = -D_{22}\nabla C_2 \tag{19}$$

that is, the diffusion flow J_2 of the tracer NaCl depends only on its own concentration gradient ∇C_2 as there are no couplings with other component flows. It has also been shown that tracer flow does not depend on the choice of the reference system [15, 16]. At infinite dilution, where the ions are far enough apart to be without influence on one another, the tracer diffusion coefficient D_{22} can be calculated from Eq. (18).

At finite dilution, where the short-range ion-ion Coulombic interactions must be taken into account, the tracer diffusion coefficient D_{22} depends on the supporting electrolyte concentration $C_1 = C$ and there is at present no satisfactory fundamental theory for its evaluation [19]. The tracer diffusion coefficient

$D_{22} = D_{22}(C)$ could be either measured or approximated by using Eq. (12) with the $\lambda_i = \lambda_i(C)$ data, if available. Such data is rarely available and, in particular, is currently unavailable for the Na^+ ion. Estimation of $\lambda_i = \lambda_i(C)$ can be done, for example, by applying the purely empirical linear equation, $\lambda_i = \lambda_i^0 - K\sqrt{C}$, first found by Kohlrausch [121] to describe the variation of the conductivity of strong electrolytes with concentration in dilute solutions. By replacing the concentration with the ionic strength for conductivity data of ions of higher than univalent type the modified Kohlrausch law can be given as [122]:

$$\lambda_2 = \lambda_2^0 - k_{\lambda 2}\sqrt{I_c} \tag{20}$$

where $k_{\lambda 2}$ is a coefficient,

$$I_c = \frac{1}{2}\sum c_i z_i^2 \tag{21}$$

is the ionic strength in molarity-scale, and c_i and z_i are the molar concentration and charge number of ionic species i. From Eqs. (12) and (20), D_{22} can then be presented as [122]:

$$D_{22} = D_{22}^0 - k\sqrt{I_c} \tag{22}$$

In 1927 Onsager derived, mainly from the data of Kohlrausch [123], a more precise and complicated theoretical equation for the limiting conductivity (improving the theory of Debye and Hückel [124, 125]) by including the electrophoretic effect in addition to the relaxation effect [11, 126, 127]. Later on Onsager also derived a limiting equation for the diffusion coefficient of an ion present in trace amounts in an otherwise uniform electrolyte solution [12]. Gosting and Harned [128] and Wang [59] subsequently showed that this formula could be applied to the case of concentration dependence in tracer- and self-diffusion. The ionic diffusion theory of Onsager is essentially an extension of the Debye and Hückel interionic attractions and repulsions theory of strong electrolytes involving the relaxation and electrophoretic effects, which was well known from conductivity theory. In deriving the equations Onsager made a number of simplifying assumptions of a physical nature and mathematical approximations, such as taking only the first term of a mathematical series. This is equivalent to neglecting the cross-product of the electrophoretic and relaxation effects terms. The expressions of Onsager are therefore only strictly valid as limiting equations and may be expected to hold only for very dilute solutions. For symmetrical, singly charged 1-1 electrolytes the theory will restrict the molarity to $C \leq 10^{-2}$ mol/dm^3 and unsymmetrical multi-charged electrolytes to even $C \leq 10^{-3}$ mol/dm^3 [129], hence the theory is not extendable to concentrated solutions.

In a tracer diffusion system the activity coefficient is practically constant, the diffusion potential and electrophoretic effects are negligible and the relaxation effect can be calculated. For example, in the case of an ion whose transport number is very small the Onsager general limiting law, which varies with

different types of electrolytes, can be expressed for the tracer ion in the form of [113]:

$$D_{ii} = \frac{RT\lambda_i^0}{F^2 z_i^2}\left[1 - \frac{2.801 \times 10^6}{(\varepsilon_r T)^{\frac{3}{2}}}\left(1 - d^{1/2}\right) z_i^2 \sqrt{I_c}\right] \tag{23}$$

where ε_r, and $d(u_i)$ are the relative permittivity of the solvent and the mobility function. The prefactor of the brackets in the right hand side of this equation is the limiting value of the diffusion coefficient of the tracer ion. The second negative term express the time of the relaxation effect and the coefficient of the square root of the ionic strength is the theoretical limiting slope. The definition of the dimensionless mobility function $d(u_i)$ is rather complicated, especially in the general case of Onsager's treatment as it is a function of the mobilities and valences of all the various ions present. Gosting and Harned [128] show that it can be expressed in the terms of the limiting molar conductivities λ_i^0 and charge numbers z_i of the ions. Here the function is expressed with three kinds of ions present, $Mg^{2+}(1)$, $Na^+(2)$ and $Cl^-(3)$, as:

$$d(u_2) = \frac{|z_2|}{|z_1|+|z_3|}\left[\frac{\lambda_1^0}{|z_2|\frac{\lambda_1^0}{|z_1|}+|z_1|\frac{\lambda_2^0}{|z_2|}} + \frac{\lambda_3^0}{|z_2|\frac{\lambda_3^0}{|z_3|}+|z_3|\frac{\lambda_2^0}{|z_2|}}\right]. \tag{24}$$

Using the previously given literature values for the ionic molar conductivities at infinite dilution, the value of the mobility function becomes $d(u_i)$= 0.433.

The Onsager Limiting Law (OLL) can be given for the diffusion coefficient of the tracer ion $Na^+(2)$ in an aqueous $MgCl_2$ solution at 25 °C in the form:

$$D_{22} = [1.334 - 0.620(mol/dm^3)^{-1/2}\sqrt{C_1}] \times 10^{-5}\ cm^2/s \tag{25}$$

where we have used that $I_c = 3C_1$ is the ionic strength of the $MgCl_2$ supporting electrolyte.

3.3 Very dilute solutions: $MgCl_2$-NaCl-HCl-H_2O

In the concentration range $C \leq 10^{-4}$ mol/dm^3, the concentration of the OH^- and H^+ ions (or more precisely H_3O^+ ions) may become comparable with that of the electrolyte ions in aqueous solutions. Here we study again the system $MgCl_2$-NaCl-H_2O at 25 ºC, but now the dissociation of water

$$K_w = c_{H^+}c_{OH^-} = 1.008 \times 10^{-14}\ \frac{\text{mol}^2}{\text{dm}^6} \tag{26}$$

is taken into account. Due to the high mobilities of the hydrogen and hydroxide ions their effect could be detectable at concentrations considerably higher than 10^{-7} mol/dm^3. Especially, if there is a spatial pH change from neutral to acidic or basic during the experiment, the cross-term contributions could become

significant. Usually the issue of water dissociation is neglected in diffusion measurements as they are rarely performed below concentrations of 10^{-2} to 10^{-3} mol/dm^3 [19]. However, Mills [130] made a series of experiments at concentration between 2×10^{-5} and 3×10^{-8} mol/dm^3 and these comprised interdiffusion measurements of ^{22}NaCl and $Mg^{82}Br_2$ electrolytes diffused out of a capillary into pure water. In both cases the effect of water ionization on the measured integral binary diffusion coefficients became noticeable at concentrations below 10^{-4} mol/dm^3. These experimental results of binary diffusion measurements were then subsequently analyzed by Woolf et al. [131], Woolf [132] and Passiniemi et al. [133].

For two fully dissociated electrolytes in partially ionized water, the number of independent components is $n = 4$: $MgCl_2$(1), NaCl(2), HCl(3) and H_2O(0). Then, there are $n - 1 = 3$ three fluxes and $(n - 1)^2 = 9$ diffusion coefficients. It is assumed that there exists no isotope effect, i.e., the difference between the diffusion coefficients of the radioactive ^{22}NaCl tracer and the inactive ^{23}NaCl is immeasurable within the precision of the experiments [101]. The Fick equations, Eq. (1), for this system are:

$$J_1 = -D_{11}\nabla C_1 - D_{12}\nabla C_2 - D_{13}\nabla C_3 \tag{27}$$

$$J_2 = -D_{21}\nabla C_1 - D_{22}\nabla C_2 - D_{23}\nabla C_3 \tag{28}$$

$$J_3 = -D_{31}\nabla C_1 - D_{32}\nabla C_2 - D_{33}\nabla C_3 \tag{29}$$

The following relations between the component diffusion coefficients in Eqs. (27)-(29) and the ionic diffusion coefficients can be derived:

$$D_{11} = \frac{D_1\left[6C_1D_4 + C_2(D_2+D_4) + C_3(D_3+D_4) + K_W C_3^{-1}(D_5-D_4)\right]}{2C_1(2D_1+D_4) + C_2(D_2+D_4) + C_3(D_3+D_4) + K_W C_3^{-1}(D_5-D_4)} \tag{30}$$

$$D_{12} = \frac{2C_1D_1(D_4-D_2)}{2C_1(2D_1+D_4) + C_2(D_2+D_4) + C_3(D_3+D_4) + K_W C_3^{-1}(D_5-D_4)} \tag{31}$$

$$D_{13} = \frac{2C_1D_1\left[(D_4-D_3) + K_W C_3^{-2}(D_4-D_5)\right]}{2C_1(2D_1+D_4) + C_2(D_2+D_4) + C_3(D_3+D_4) + K_W C_3^{-1}(D_5-D_4)} \tag{32}$$

$$D_{21} = \frac{2C_2D_2(D_4-D_1)}{2C_1(2D_1+D_4) + C_2(D_2+D_4) + C_3(D_3+D_4) + K_W C_3^{-1}(D_5-D_4)} \tag{33}$$

$$D_{22} = \frac{D_2\left[2C_1(2D_1+D_4) + 2C_2D_4 + C_3(D_3+D_4) + K_W C_3^{-1}(D_5-D_4)\right]}{2C_1(2D_1+D_4) + C_2(D_2+D_4) + C_3(D_3+D_4) + K_W C_3^{-1}(D_5-D_4)} \tag{34}$$

$$D_{23} = \frac{C_2D_2\left[D_4-D_3 + K_W C_3^{-2}(D_4-D_5)\right]}{2C_1(2D_1+D_4) + C_2(D_2+D_4) + C_3(D_3+D_4) + K_W C_3^{-1}(D_5-D_4)} \tag{35}$$

$$D_{31} = \frac{2C_3D_3(D_4-D_1)}{2C_1(2D_1+D_4) + C_2(D_2+D_4) + C_3(D_3+D_4) + K_W C_3^{-1}(D_5-D_4)} \tag{36}$$

$$D_{32} = \frac{C_3 D_3 (D_4 - D_2)}{2C_1(2D_1+D_4)+C_2(D_2+D_4)+C_3(D_3+D_4)+K_W C_3^{-1}(D_5-D_4)} \quad (37)$$

$$D_{33} = \frac{D_3[2C_1(2D_1+D_4)+C_2(D_2+D_4)+2C_3 D_4\,]}{2C_1(2D_1+D_4)+C_2(D_2+D_4)+C_3(D_3+D_4)+K_W C_3^{-1}(D_5-D_4)} \quad (38)$$

where the values i = 1, ..., 5 of the subscript in the ionic diffusion coefficients D_i refer to the ionic species Mg^{2+}, Na^+, H^+, Cl^- and OH^-, respectively; the same applies below to the ionic molar conductivities λ_i^0.

In addition, the Nernst-Einstein equation, Eq. (5), was used to relate the molar conductivity and the diffusion coefficient. The literature values used for the equivalent molar conductivity of hydrogen and hydroxide ions were: λ_3^0 = 349.8 S cm^2/mol and λ_5^0 = 197.6 S cm^2/mol [134]. The nine theoretical diffusion coefficients calculated from Eqs. (30)-(38) at 298.15 K are given graphically in Fig. 1 for constant C_2(NaCl) and C_3(HCl) concentrations as a function of $MgCl_2$ concentration. The negative diffusion coefficients D_{13} and D_{23} are multiplied by −1 and the diffusion coefficient D_{33} is divided by 5 in order to get them on the same scale with other diffusion coefficients. The ionic diffusion coefficient D_3 of the hydrogen ion is relatively large value because of the rapid proton jump mechanism [108]. Since D_{13} and D_{23} are proportional to D_3, they are also relatively large. The negative cross-term diffusion coefficients indicate the reverse coupling effect between the diffusion currents of salt ions and the hydrogen ions.

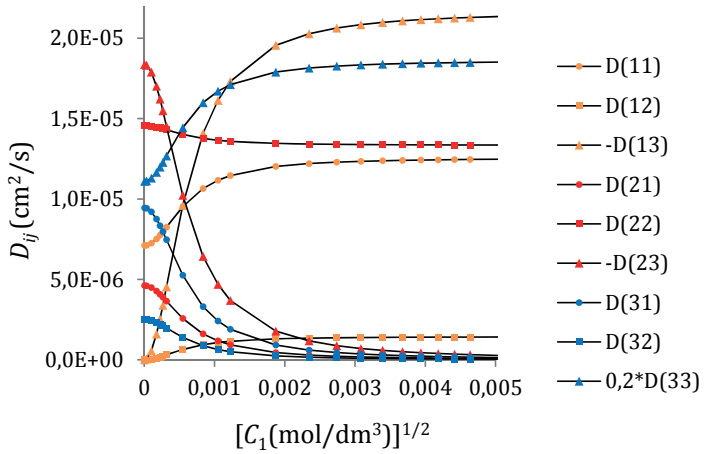

Fig. 1. The nine diffusion coefficients D_{ij} of the quaternary $MgCl_2$-NaCl-HCl-H_2O system calculated at 25 °C as a function of the concentration of the supporting electrolyte of C_1($MgCl_2$). The concentrations of NaCl and HCl are held constant at a typical experimental values of $C_2 = 0.341\times10^{-6}$ mol/dm^3 and $C_3 = 1\times10^{-7}$ mol/dm^3.

The diffusion flow of NaCl is $J_2 = -D_{21}\nabla C_1 - D_{22}\nabla C_2 - D_{23}\nabla C_3$, Eq.(27). Figure 2 shows the diffusion coefficients D_{21}, D_{22} and D_{23} calculated from the ionic diffusion coefficients and from the Onsager Limiting Law, Eq.(25), for $MgCl_2$ concentrations lower than 10^{-4} mol/dm^3. The coefficient D_{23} describes the

effect of the concentration gradient of HCl on the flow of NaCl. Due to the large negative value of D_{23} this effect can be quite pronounced even with a small ∇C_3. The main-term diffusion coefficient, D_{22}, which describes the contribution of the concentration gradient of NaCl to its flow, increases with decreasing $MgCl_2$ concentration.

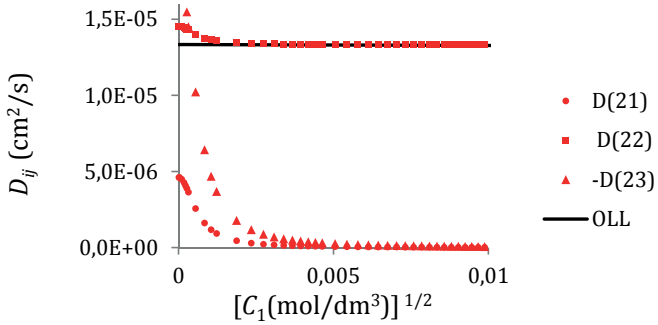

Fig. 2. The diffusion coefficients of the NaCl diffusion flow in the quaternary system $MgCl_2$-NaCl-HCl-H_2O calculated at 25 °C as a function of the supporting electrolyte concentration, $C_1(MgCl_2)$. The concentrations of NaCl and HCl are held constant at typical values of $C_2 = 0.341\times10^{-7}$ mol/dm^3 and $C_3 = 1\times10^{-7}$ mol/dm^3.

Let us consider the behavior of the Onsager Limiting Law at infinite dilution with the effect of water ionization. In Onsager's general treatment [12] water is considered as a structureless solvent that acts as either a provider of the volume in which the solute particles move or conductor medium for the mobile ions with a dielectric constant ε_r. The ambient electrolyte with all the ions present can still be taken into a consideration in the limiting equation with the mobility function Eq. (24) and with the ionic strength Eq. (21). Here the functions $d(u_i) = f(z_i, \lambda_i)$ and $I_c = f(z_i, c_i)$ can be expressed with Mg^{2+}(1), Na^+(2), H^+(3), Cl^-(4) and OH^-(5) ions and with Na^+-ion tracer as follows:

$$d(u_2) = \frac{|z_2|}{|z_1|+|z_3|+|z_4|+|z_5|}\left[\frac{|z_1|\lambda^0_{1,eq}}{|z_2|\lambda^0_{1,eq}+|z_1|\lambda^0_{2,eq}} + \frac{|z_3|\lambda^0_{3,eq}}{|z_2|\lambda^0_{3,eq}+|z_3|\lambda^0_{2,eq}} + \frac{|z_4|\lambda^0_{4,eq}}{|z_2|\lambda^0_{4,eq}+|z_4|\lambda^0_{2,eq}} + \frac{|z_5|\lambda^0_{5,eq}}{|z_2|\lambda^0_{5,eq}+|z_5|\lambda^0_{2,eq}}\right] \quad (39)$$

$$I_c = 3C_1 + C_2 + \tfrac{1}{2}C_3(1 + K_w C_3^{-2}) \quad (40)$$

where $\lambda^0_{i,\mathrm{eq}} = \lambda^0_i/|z_i|$ is ionic equivalent conductivity, and C_1, C_2, and C_3 are the concentrations of the supporting electrolyte, the tracer electrolyte and HCl, respectively. In this case, the mobility function has a value of $d(u_i)$ = 0.240 compared to a value of $d(u_i)$= 0.433 in the previous case, where the ionization effect of water is neglected. The value of the ionic strength is significantly dependent on the concentrations of ambient ions. At neutral or near neutral pH the ionization effect of water is greater for $d(u_i)$ than for I_c. By using Eq. (39), the coefficient k in Eq. (25) for D_{22} when water dissociation is taken into account is k = 0.240×10^{-5} (cm^2/s)(mol/dm^3)$^{-1/2}$, which is smaller than the value k =

0.358×10^{-5} (cm^2/s)(mol/dm^3)$^{-1/2}$ corresponding to no water dissociation. The ionic strength to be used in Eq. (22) when water dissociation is considered is that in Eq. (40), but it can be approximated by $I_c \approx 3C_1$ for $6 < \text{pH} < 8$ just like in Eq. (25). The Onsager Limiting Law (OLL) with and without the effect of the water ionization is presented in Fig. 3 with the tracer diffusion coefficient D_{22} plotted as a function of the ionic strength of the ambient electrolyte.

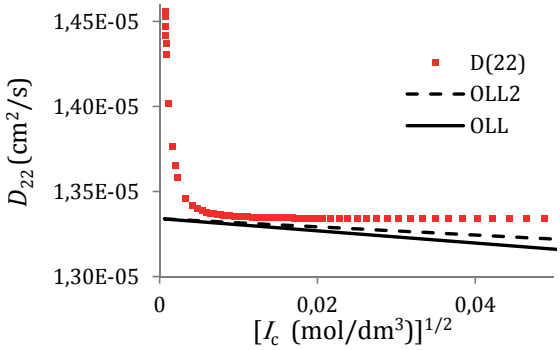

Fig. 3. The diffusion coefficient D_{22} in the system $MgCl_2$-NaCl-HCl-H_2O calculated from Nernst-Planck equations as a function of the ionic strength. The concentrations of NaCl and HCl are $C_2 = 0.341\times10^{-6}$ mol/dm^3 and $C_3 = 10^{-7}$ mol/dm^3. The straight lines are the OLL: $D_{Na^+}/(10^{-5}$ cm^2/s) = 1.334 – 0.358 $[I_c/(\text{mol/dm}^3)]^{1/2}$ and the OLL with the effect of ionization of water (OLL2): $D_{Na^+}/(10^{-5}$ cm^2/s) = 1.334 – 0.240 $[I_c/(\text{mol/dm}^3)]^{1/2}$ at 25 °C.

The quaternary electrolyte system $MgCl_2$(1)-NaCl(2)-HCl(3)-H_2O(0) becomes a quaternary tracer system when the NaCl concentration C_2 approaches zero. The cross-term diffusion coefficients D_{21} and D_{23} in Eqs. (33) and (35) tend then towards zero and Eq. (34) leads to $\lim_{C_2\to0} D_{22} = D_2$, which calculated at 25°C as $D_{22}^0 = 1.334\times10^{-5}$ cm^2/s using the Nernst-Einstein equation and the limiting conductivity of the Na^+ ion $\lambda_2^0 = 50.1$ S cm^2/mol. Equation (28) reduces then to $J_2 = -D_{22}^0\nabla c_2$. This result is the same as seen previously in the ternary tracer electrolyte system, however the above quaternary tracer electrolyte system can only implemented theoretically by reducing C_2 to zero mathematically. The challenge is to prove the OLL experimentally with measurements at infinite dilution. Nevertheless, it is not possible to measure the diffusion coefficient D_{22} with zero tracer concentration and to prevent the effect of ionization of water at infinite dilution. In addition, the ratio C_2/C_1 increases with decreasing supporting electrolyte concentration and can cause couplings between diffusion flows due to the low specific activity available for the ^{22}Na tracer. With lower tracer concentrations the measured pulse amounts are not high enough to satisfy the required levels of accuracy and precision.

The ionic diffusion coefficients for the NaCl tracer flux density, Eq. (28), were calculated at different concentrations C_1, C_2 and C_3 at $C_1 \le 10^{-4}$ mol/dm^3, using the relations with the ionic diffusion coefficients that can be derived from the Nernst-Planck equations. The calculated values of D_{ij} are given in Table 1 and the main diffusion coefficient D_{22} is also displayed graphically in Fig. 4.

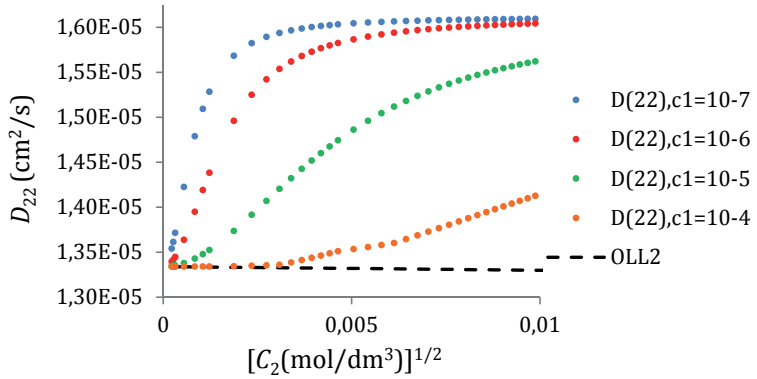

Fig. 4. Calculated diffusion coefficient D_{22} at 25 °C in the system $MgCl_2$-NaCl-HCl-H_2O as a function of the NaCl concentration. The HCl concentration is $C_3 = 10^{-7}$ mol/dm^3. The straight line marked as OLL2 is $D_2/(10^{-5}\ \mathrm{cm^2/s}) = 1.334 - 0.240\ [I_c/(\mathrm{mol/dm^3})]^{1/2}$.

As it can be seen from Table 1 and Fig. 4, the calculated D_{22} are higher than those given by OLL and the cross coefficients D_{21} and D_{23} deviate from zero. These changes from the ideal quaternary tracer electrolyte system increase as a function of decreasing $C_1(MgCl_2)$ concentration. The possible difference between the calculated and measured values of D_{22} may result from measurement inaccuracies within the diffusion capillary system, which develops unknown concentration gradients of ∇C_1 and ∇C_3. These gradients then contribute with the non-zero diffusion coefficients of D_{21} and D_{23} to the NaCl tracer flow. The measurements presented in the following chapters are interpreted according to this theoretical background with the help of the Nernst-Planck equations applied to the ionic flows in the infinite dilute concentration.

Table 1. Diffusion coefficients D_{21}, D_{22} and $-D_{23}$ of the NaCl flow in the system of $MgCl_2$-NaCl-HCl-H_2O calculated at 25 °C at different concentrations of $MgCl_2$ (C_1), NaCl (C_2) and HCl (C_3). The units of the concentrations C_i are 10^{-6} mol/dm^3 and those of the diffusion coefficients D_{ij} are 10^{-5} cm^2/s.

D_{21}	$C_3 = 0.1$				$C_3 = 1$				$C_3 = 10$			
	$C_2 = 0.1$	0.5	1	5	$C_2 = 0.1$	0.5	1	5	$C_2 = 0.1$	0.5	1	5
$C_1 = 0.1$	0.142	0.460	0.640	0.929	0.028	0.128	0.229	0.610	0.003	0.015	0.030	0.135
$C_1 = 1$	0.041	0.176	0.301	0.700	0.019	0.088	0.162	0.502	0.003	0.014	0.029	0.129
$C_1 = 10$	0.005	0.024	0.048	0.202	0.004	0.021	0.042	0.181	0.002	0.010	0.019	–0.088
$C_1 = 100$	0.001	0.003	0.005	0.025	0.001	0.003	0.005	0.025	0.000	0.002	0.004	0.021
D_{22}	$C_3 = 0.1$				$C_3 = 1$				$C_3 = 10$			
	$C_2 = 0.1$	0.5	1	5	$C_2 = 0.1$	0.5	1	5	$C_2 = 0.1$	0.5	1	5
$C_1 = 0.1$	1.372	1.456	1.503	1.580	1.342	1.368	1.394	1.495	1.335	1.338	1.342	1.370
$C_1 = 1$	1.345	1.380	1.414	1.519	1.339	1.357	1.377	1.467	1.335	1.338	1.342	1.368
$C_1 = 10$	1.335	1.340	1.347	1.387	1.335	1.340	1.345	1.382	1.335	1.337	1.339	1.357
$C_1 = 100$	1.334	1.335	1.335	1.341	1.334	1.335	1.335	1.340	1.334	1.335	1.335	1.340
$-D_{23}$	$C_3 = 0.1$				$C_3 = 1$				$C_3 = 10$			
	$C_2 = 0.1$	0.5	1	5	$C_2 = 0.1$	0.5	1	5	$C_2 = 0.1$	0.5	1	5
$C_1 = 0.1$	0.565	1.832	2.546	3.700	0.079	0.355	0.632	1.687	0.008	0.042	0.083	0.371
$C_1 = 1$	0.161	0.699	1.170	2.787	0.052	0.244	0.450	1.388	0.008	0.040	0.078	0.354
$C_1 = 10$	0.020	0.097	0.190	0.804	0.012	0.059	0.116	0.501	0.005	0.026	0.052	0.244
$C_1 = 100$	0.002	0.010	0.020	0.099	0.001	0.007	0.014	0.068	0.001	0.006	0.012	0.059

4 BINARY DIFFUSION IN POROUS BRICK MEDIA

In this chapter the diffusion in a binary salt-H_2O system in porous brick media is studied. The effect of brick material, its mineralogical composition and the geometry of the pore structure on porous brick media diffusion are discussed. The binding of ions on the surface of brick pores and the possible influence on the measured diffusion coefficient are examined.

4.1 Fired brick materials

One of the scopes of the present thesis was to develop measurement techniques for diffusion in bricks and to determine yet unknown salt diffusion coefficients in brick matrix under different environmental conditions. From the point of view of the diffusion coefficients measurement the brick matrix can be considered to be like a black box without any precise knowledge of its mechanical or chemical structure. However, to understand the diffusion mechanisms and to describe the salt diffusion processes inside the porous brick it is still necessary to look at the properties of the brick matrix.

Historically brick making depended completely on manual labor, from quarrying the raw material through forming the brick to firing it, in contrast, modern brick making is a highly industrialized process raw materials, shaping techniques and firing cycles differ greatly in industrialized processes, but the quality is higher and the brick are more homogenous than ever before.

The raw material for brickmaking is clay or shale. Shale is hard and rocklike material but when ground and mixed with water it reverts to the consistency of soft and plastic clay. The most important minerals in clay are quartz sand grains, aluminum and iron oxides/hydroxides and different clay minerals [75,135]. The iron oxides - FeO, Fe_2O_3, Fe_3O_4 - and hydroxides - $Fe(OH)_2$, $Fe(OH)_3$ - and related compounds are the main reason for the formation of different red colors during the firing process. Chemical analysis of Finnish clay shows that the most important components in Finnish brick raw materials are (mean values from literature): SiO_2 (59%), Al_2O_3 (16%) and Fe_2O_3 (6%) with minor components including: FeO, MgO, CaO, Na_2O, K_2O and H_2O (approximately 3 % of each) [72,136-138].

Diffusion measurements were performed using 3 different ceramic brick materials including old dark brick (ODB) and the old light brick (OLB), which represent brick materials found in old masonry and the new Finnish red brick (NRB) as an example of modern brick material. The elemental analysis of the modern NRB is displayed in Fig. 5. Prior to analysis the bricks were purified and dried to a constant weight as outlined in the publication II. The concentration of elements on the surface prior to any experiment was analyzed by SEM-EDS (Scanning Electron Microscope - Energy-Dispersive X-ray Spectroscopy) using a 12 keV

beam energy at 5 mm intervals along the carbonated brick surface. The analysis beam area was about 0.5 mm^2 at a magnification of x100 and duplicate points were measured to ensure reproducibility. Results of the main elements found are given as mean values based on three different specimens from the broken surface of the brick. The element analyses made for the brick specimen used in this work concur with chemical analyses of typical Finnish clay used as the raw material for brickmaking and there was no chloride contaminants e.g. as a form of NaCl detected prior to exposure to the electrolyte used in the diffusion experiments.

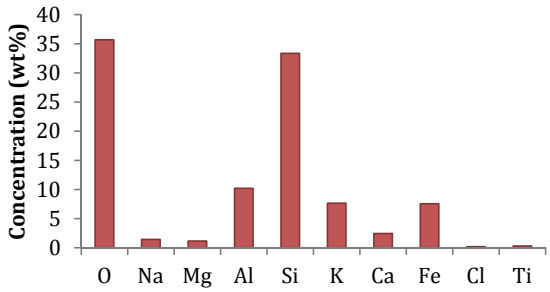

Fig. 5. Concentrations of the main elements analyzed from the broken surface of NRB, expressed as mass fraction. Analysis was performed with SEM-EDS for three pure specimens with duplicate points at different locations. Mean value is given.

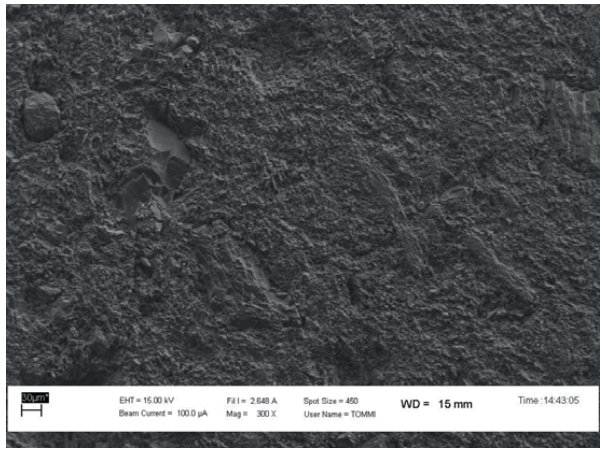

Fig. 6. SEM microphotograph taken from the surface of the pure uncontaminated ceramic NRB. The scale bar is 30 µm and magnification ×300.

The SEM images obtained for NRB are presented in Figs. 6-9. In Fig. 6 the micrograph from the surface of pure and dry untreated brick is presented. Figure 7 shows a brick surface, which has been soaked in concentrated NaCl solution and dried prior to the SEM micrograph. The effect of NaCl sorption (see Section 4.4 below) on the surface structure of ceramic brick medium can be seen from the micrographs displayed in Figs. 8 and 9 at two different magnifications. Here the brick specimen was immersed in concentrated NaCl solution then rinsed with

water for 24 h in order to remove any soluble salt. Some NaCl salt residue was still detectable on the brick surface as can been seen from the NaCl crystal structure in Fig. 9 (at ×5000 magnification). The porosities of the NRB samples taken from the same brick featured in these images were about 0.23.

The other structural characteristics of the porous brick materials used in this work are given in publication II. From these mean literature values it can be seen that porosity, the specific internal surface area and pore-size distribution are all interrelated. The smaller the pore-size of the brick medium, the larger the inner pore surface area and the porosity values are, respectively. This relationship is not universal but it is true of the brick materials examined in this thesis.

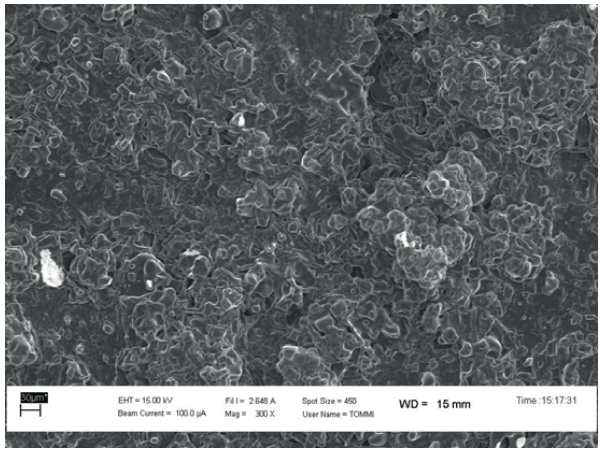

Fig. 7. SEM microphotograph taken from the surface of ceramic NRB soaked in concentrated NaCl solution. The scale bar is 30 µm and magnification ×300.

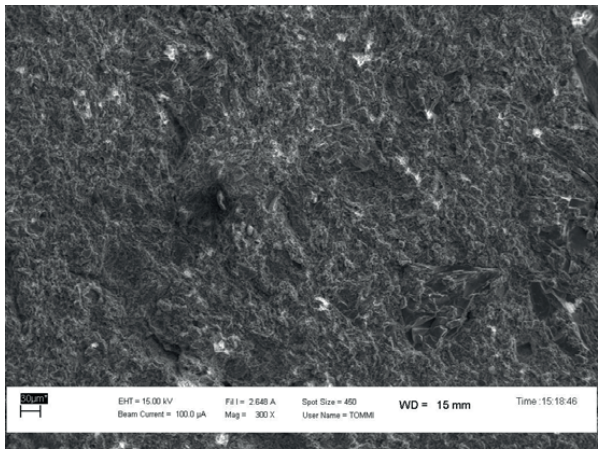

Fig. 8. SEM microphotograph taken from the surface of ceramic NRB soaked in concentrated NaCl solution then rinsed with water for 24 h. The scale bar is 30 µm and magnification ×300.

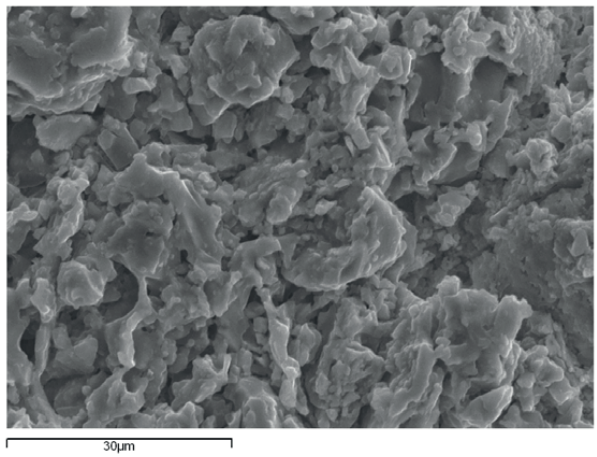

Fig. 9. Same material and conditions as in Fig. 8, at magnification ×5000.

4.2 Porosity

The most important physical features of the brick medium from the point of view of diffusion are the pore structure characteristics like porosity, pore-size distribution, pore geometry and connectivity between the pores [139]. The pore structure and morphology of brick is mainly formed during the drying process of the clay. The rest of the latent water and the OH^- groups from the clay minerals are liberated and any organic material is burned during the firing process. Depending on how high this firing temperature is the porosity of dark fired bricks is smaller than the porosity of the normal or light fired bricks as with increasing firing temperature the pores become coarser and porosity decreases.

The typical pore size distribution - determined by mercury intrusion porosimetry (MIP) [140] - for NRB varies within 95% between pore radius of 0.45–1.8 µm (r_{mean} =1 µm). For OLB the pore radius was observed to be between 0.01-1 µm (r_{mean} =0.04 µm) and for ODB between 0.1-30 µm (r_{mean} =8 µm), respectively. Although MIP is a fast and easy technique, it can be inaccurate as it overestimates the fine pore volume and an underestimates the wide pore volume of the pores (the ink-bottle effect) [141, 142], however no other pore-size distribution determination for Finnish NRB was found. Previously Nielsen [75] has used both the digital image analyzing (DIA) techniques with the scanning electron micrographs and MIP-techniques to determine the pore-size distribution of new British red brick. The results showed that the pore-size distribution determined with DIA-techniques gave slightly higher pore radius values, as expected, but that the form of the distribution was unchanged.

The porosity ε (also denoted as ε_{eff} [93]) is defined as volume fraction accesible to the diffusing ions, i.e. the fraction of the brick volume that contains solution

$$\varepsilon = \frac{V_{pore}}{V_{brick}} \approx \frac{A_{pore}}{A_{brick}}. \quad (41)$$

The approximation in Eq. (41) follows from the assumption of homogeneous mean pore structure. That is, the mean area fraction of the pores on any cross section is approximately independent of the x coordinate. In other words, in any thin slice along the diffusion direction, the tortuosity is approximated as unity.

The porosity was determined for each brick material. The water saturation method was used where one end of the brick specimen under investigation was exposed to ion exchanged water at a temperature of 25 °C. The water soaked into the brick sample capillaries until fully saturated and then weighed. In order to ensure complete removal of all the air from the pores the sample was then placed connected to vacuum pump whilst immersed in ion exchanged water, then weighed again. Finally the sample was left immersed in the water for 24 h to ensure filling of any pores still containing entrapped air. After a constant weight was attained (which usually was reached even without using the vacuum pump for the more coarse porous materials NRB and ODB) the porosity of the individual sample was calculated from the volume and the mass change of the specimen. The porosities determined for NRB were usually between 0.21-0.26; for ODB between 0.12-0.20 and for OLB between 0.28-0.31, respectively.

The measured values of the water-saturation porosity show a good correlation to the results found by Nielsen [75]. Even though in this study the pore-size distributions measured with DIA techniques differed from that determined with the MIP techniques, the porosities measured by these two methods were similar to each other and also with the porosities determined by the water saturation method. Although this comparative investigation was performed using new British red brick (ε = 0.28-0.29) the result is assumed to also apply to NRB.

In principle with some materials both the MIP and DIA techniques could give higher values for the porosity due to the inclusion of possible dead end pores and enclosed cracks as it is difficult to discern between these through-pores. The advantage of the water saturation method is that it is immune to these usually air filled dead end pores with have no straight connection to the surface. This is critical as only the through-pores contribute to the transport properties of the diffusion in brick medium [143], therefore the open or the effective porosity ε_{eff} determined by water saturation is the best way to measure the volume fraction of the brick specimen accessible to the diffusing ions.

4.3 Tortuosity factor

There has been a lot of discussion about how to relate the diffusion coefficient measured in the presence porous medium, $D_{\text{p,}}$ to the diffusion coefficient measured in the absence of porous medium, D_{a}. The empirical fact is that the

diffusion coefficient can be very different for different porous media and differ greatly to that measured in the absence of porous medium. This is a complicated subject and the discussion here will be restricted to bulk unidirectional binary salt diffusion in homogeneous, isotropic, macroporous and fully aqueous solution saturated media with a continuous pore space. Hoogschagen [144] denoted the ratio $Q = D_p/D_a$ as diffusibility. In order to predict the diffusibility many equations have been proposed most of which are based on pore space models or empirical correlations like giving Q as a unique function of the porosity ε. In addition, pore space characteristics like the constrictivity ξ and the tortuosity τ, as well as interaction parameters like the interaction coefficient γ, have been presented as parameters for the diffusibility equation. Many variants of this function $Q = f(\gamma, \varepsilon, \xi, \tau)$ are presented in the literature but so far no universally accepted material parameter or matrix factor function has been determined.

The constrictivity ξ describes the form of the pores and accounts for the fact that the cross section of a segment varies over its length. The tortuosity τ takes account of the length of the tortuous diffusion path in the porous medium. Usually τ is defined as the ratio of the real diffusion path to the shortest distance between the end and start points of the path in the porous medium. However, throughout the literature there are a number of variations for tortuosity including the inversion of the previous definition and terms like apparent and real tortuosity are used [143-147].

The interaction coefficient γ is thought to account for the influence of the overlapped interaction force field exerted by the pore walls on the diffusing ions and molecules in the pores. The effect of this kind of a parameter is diminished if the number of collisions between the ions and molecules is significantly greater than the number of collisions with the pore walls. The interaction coefficient γ is therefore also dependent on the ratio of the pore size to the diffusing species and solvent molecules as well as the concentration and ionic charge dependent effective thickness of the surface layer (the Debye length κ^{-1}).

One commonly utilized form of diffusibility is $Q = \varepsilon \xi \tau^{-2}$ as defined by Brakel and Heertjes [148]. This type of geometrical factor has been used in many diffusion coefficient measurements made, for example, in porous matrices like crushed rock, cementitious materials and concrete [149]. In the case of porous ceramic brick only one expression for the function of Q was found [94] and involved a comparison of the ratio of the diffusion coefficients measured in NRB and in bulk water $Q = \varepsilon \tau \gamma$ for which a value of $\approx 1/7$ was obtained. As there was no determination of the factors τ and γ in the article and based on the diffusion measurements outlined in this thesis the given relationship would seem to be incorrect. In addition, the equation also overestimates the interaction phenomena that are not a critical consideration in macro porous brick.

As there was no possibility to determine the constrictivity factors or the interaction coefficients for the ceramic brick media (and no similar investigations in the literature) it was decided to evaluate the material in terms of tortuosity values instead. These tortuosity measurements were done by comparing the

conductivity of the solution in absence of the porous brick to the value measured in the presence of the brick medium. The hypothesis was that the parameters affecting the impedance or conductivity through the brick are the porosity and the tortuosity. By knowing the porosity and the conductivities, the tortuosity could be calculated by the equation [150]:

$$\tau = \varepsilon \frac{R_p}{R_a} = \varepsilon \frac{\kappa_a}{\kappa_p} \tag{42}$$

where R is the impedance and κ is the conductance. The subindices p and a refer to the presence or absence of porous brick, respectively.

The cell constant $k = L/A$ of the conductivity apparatus (Consort K320) measuring chamber was 3.720 cm^{-1} determined with 0.01 mol/dm^3 KCl solution (κ = 1413 µS/cm) at a constant measuring temperature of 25.00±0.05 °C. The calculated tortuosity values for the various bricks in different salt concentrations C are given in Figs. 10 and 11. The calculation involved measuring five points within the concentration region of 10^{-4} to 1 mol/dm^3 and the results give a tortuosity value - via the least-square method with τ as a linear function of ln$C$ with correlation coefficients of 0.908-0.967 for different salts (Fig. 10) and 0.966-0.997 for the different brick materials (Fig. 11). The plots of τ vs. $C^{1/2}$ show a sharp decay below $C \approx 0.01$ mol/dm^3 and the calculated tortuosity becomes less than unity at $C \approx 0.001$ mol/dm^3.

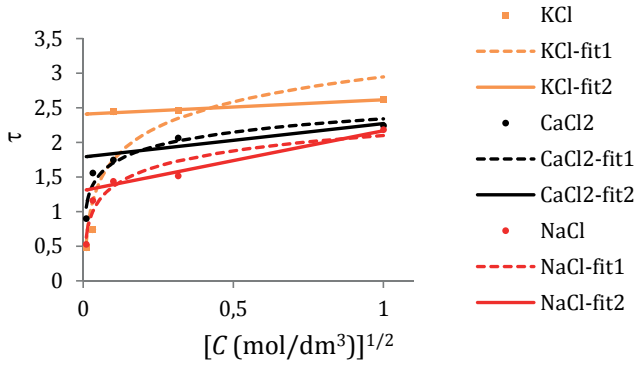

Fig. 10. The tortuosity τ of NRB in different electrolytes at 25 °C. The fitting curve, fit1 is a nonlinear logarithmic regression fit with 5 measurement points in the concentration region of $C = (10^{-4}\text{-}1)$ mol/dm^3. The fitting line, fit2 is a linear regression fit with only 3 points in the concentrated region of C = (0.01-1) mol/dm^3. The measurement points shown are mean values.

This result implies that in more dilute solutions (≤ 0.01 mol/dm^3) charge increasingly passes through the surface double layer, which has smaller impedance when compared to bulk solution. The surface charge (negative in NRB) increases the electrical conductivity of porous material the more dilute the electrolyte solution in the pores [150]. This is possible because the Debye length increases sharply below an electrolyte concentration of 0.02 mol/dm^3 and

moreover the Debye length for a 1:1 type of electrolyte is always larger than that of a 1:2 type of electrolyte. The smallest values for the tortuosity were calculated for the 1:1 type electrolytes KCl and NaCl, while the calculated tortuosity curve for $CaCl_2$ was not so pronounced. The influence of the effective thickness of the double layer (the Debye length κ^{-1}) in the dilute concentration region can also be seen in the calculated tortuosities in the different brick materials. The smallest values were calculated for the OLB with the smallest mean pore radius of r_{pore} = 40 nm and the largest surface to volume ratio ($A/V = 2/r_{pore}$) whereas the highest values were calculated for the ODB with the largest r_{pore} = 8000 nm and the smallest surface to volume ratio.

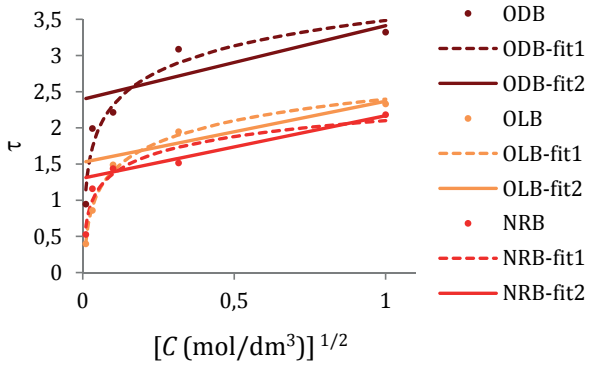

Fig. 11. The tortuosity τ of ODB, OLB and NRB as a function of NaCl concentration at 25 °C. The fitting curve *fit1* is a nonlinear logarithmic regression fit with five measurement points in the concentration region between 10^{-4} and 1 mol/dm^3. The fitting line *fit2* is a linear regression fit with only three points in the concentrated region between 0.01 and 1 mol/dm^3. The measurement points shown are mean values.

Calculated tortuosity values $\tau < 1$ have been reported when surface diffusion has been significant [151, 152]. This demonstrates that there is a connection between the electrical and diffusional mobilities and the effective thickness of the double layer in dilute electrolyte concentrations as the unexpected surface diffusion may increase the measured diffusion coefficient in a porous medium, the surface conductivity may also increase the measured conductivity giving $\tau < 1$, see Eq. (42). In order to exclude the possible effect of the surface conductivity the tortuosities were finally calculated only with 3 points from a concentration between (10^{-2} - 1) mol/dm^3 and the correlation coefficients with the linear least-square method were 0.900-0.991 for different salts (Fig. 10) and 0.818-0.991 for different brick materials (Fig. 11), respectively.

The mean value of the tortuosity calculated at 25 ºC by the conductivity method was taken from the linear fitting region and designated as apparent tortuosity, τ_a. In the electrolyte concentration region between 0.01 and 1 mol/dm^3, their measured values were: 2.9 for NaCl in ODB, 1.9 for NaCl in OLB, 1.7 for NaCl in NRB, 2.0 for $CaCl_2$ in NRB, and 2.5 for KCl in NRB. There were only a few tortuosity determinations for brick media in the literature and of those only one determined by the conductivity method and only one for NRB (ε = 0.24). The

following mean values for tortuosity as a function of salt and concentration in aqueous solution were found in the literature [140, 150]: in NaCl calculated tortuosities were τ = 2.4 (0.01 mol/dm^3), τ = 3.8 (1 mol/dm^3) and τ = 5.2 (6 mol/dm^3); in KNO_3 calculated were τ = 2.5 (0.01 mol/dm^3) and τ = 4.0 (1 mol/dm^3) and in LiCl τ = 4.0 (1 mol/dm^3), respectively. These literature values for tortuosity are larger than those in this work but overall they follow the same trend as the calculated tortuosity decreases with the decreasing electrolyte concentrations in the pores. These results demonstrate that tortuosity in ceramic brick would require a more systematic study and also new methods of measurement in order to clarify the influence of the pore morphology tortuosity on the diffusibility, however this was beyond the scope of this thesis.

4.4 Sorption effect

Sorption is frequently involved when solid-liquid interfaces are present in experiments as an interface between a solid phase and solution tends to sorb solute in order to minimize the excess free energy of the surface and here the generic term sorption means either physical or chemical adsorption, absorption or ion exchange reactions. Additionally, it is often difficult to distinguish between these processes without careful experimental data of chemical and surface analyses, however these are rarely available for the system under investigation and interpretation of the data available is often complicated [153]. Sorption may occur also in the case when electrolyte solution is in contact with the surface of porous material and has previously been investigated (along with the diffusion of ions) in porous media like crushed rock and bentonite clay [154], sodium montmorillonite [155], compacted sodium bentonite [156], soils [157], membranes [115, 158, 159] and concrete [160-164]. Overall there is still a lack of published experimental data in the literature dealing with the sorption of salts on porous brick media, with only the work of Nielsen [75], who measured moisture sorption isotherms by hygroscopic water intake for bricks and calcareous sandstones, available.

Most substances acquire a surface electric charge when brought into the contact with a polar solution and surfaces in contact with aqueous media are more often negatively charged than positively charged [153]. The surface charge of the porous fired brick has also been found to be negative, indicating cations sorption on the pore walls and possible cation-exchange properties. The magnitude of these surface charge densities, q, were determined with streaming potential measurements and found to be between $-4.43 \leq q \leq -3.75$ mC/m^2 with the pore-size area of 0.2-1.0 μm [150]. The potential between the charged surface and the electrolyte solution is known as the electrokinetic or zeta potential according to the double-layer theory. Due to electroneutrality, anions will either remain in close proximity to the sorbed cations or form a second adsorption layer leading to a new cation layer and so on away from the surface. The electric double layer can be generally regarded as consisting of two regions: an inner region that may include adsorbed ions and a diffuse region in which ions are distributed according to the electrical forces and random thermal motion. The sorption effects in porous

materials tend to increase with decreasing pore size, which increases the porosity and the wall area and hence the pore wall interactions with aqueous solution [91].

Some preliminary experiments carried out in this work indicated that sorption of NaCl occurred on the surface of brick specimens. This sorption was detected by γ-ray counter which measured a high residual activity of ^{22}NaCl sorbed on the used brick tube samples after thorough rinsing with portable water. The diameters of the investigated NRB tube samples were 11.70 mm with lengths of approximately 40 mm ($V \approx 4.3$ cm^3, $\varepsilon \approx 0.23$). Each of the specimens was measured separately and for example an experiment was performed where the initial equilibrium γ-activity of 0.05 mol/dm^3 ^{22}NaCl, $A_0 = 3.551\times10^6$ counts/0.5h, decreased to $A = 1.265\times10^5$ counts/0.5h after 3 months in the water rinsing treatment (as the outer surface was covered with lacquer the salt was only able to leave the brick cylinder from the ends). By taking the background activity and half-life period of decay into account, the residual ^{22}NaCl amount were calculated to be on the average about 3 wt. % of the original amount. This average value determined from the activity measurements provided an estimation of the sorbed amount of NaCl on the pore walls inside brick tube. Similar brick tubes were also subsequently used in the CCM diffusion measurements.

In addition to these whole tube experiments flat surfaces were also exposed to NaCl solutions and involved immersing purified brick samples with broken surface into the salt solution under study and allowing it to soak into the matrix via capillary action. The surface was then dried and the amount of NaCl sorbed on the surface was analyzed by SEM-EDS. Parallel samples were also prepared but with the addition of 24 h rinsing of the brick surface with water after the salt solution exposure. The dimensions of the cracked NRB samples were approximately 33 mm × 12 mm × 5 mm ($V \approx 2.0$ cm^3, $\varepsilon \approx 0.23$). The brick samples were sputter-coated with a thin carbon layer under vacuum. The SEM-EDS measurements were performed 12 keV beam energy at 5 mm intervals along the brick surface with a beam area of about 0.5 mm^2 at a magnification of ×100; duplicate points were measured to ensure reproducibility.

From the results presented in Figs. 12 and 13 it can be presumed that NaCl sorption occurs on the brick surface with the physisorbed salt presumed to be mainly removed by the rinsing water step, while the chemisorbed salt remained on the surface (Figs. 8 and 9). The concentration of the salt solution soaked into the pores appeared not to have a remarkable effect on the residual amount of NaCl detected although the movement of the salt with the waterfront in the drying process was observable in the specimen with a electrolyte concentration C = 0.6 mol/dm^3. The low concentration of chlorine detected indicates that ion-exchange reactions take place on the surface of brick as part of the chloride counter-ions appear to have been substituted with e.g. nitrate, carbonate or sulfate anions (not analyzed) of the rinsing water. An interesting phenomenon was detected in the last two samples where 0.1 mol/dm^3 concentrations of two organic additives (2-hydroxy- and 2-methoxybenzaldehydes) were dissolved in the 0.6 mol/dm^3 NaCl solution resulting in the profound inhibition of NaCl sorption

Moreover, the additional 24 h water rinsing step did not seem to influence the residual concentration level of NaCl detected.

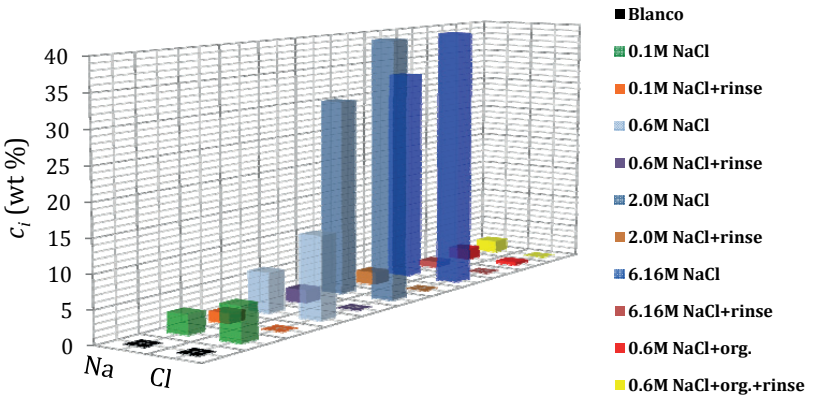

Fig. 12. Elemental content of Na and Cl (as weight percent) on the surface of NRB analyzed with SEM-EDS. The diagram represents data from 5 specimens exposed to aqueous NaCl solutions of different concentrations and 5 equivalent surfaces that were subjected to an additional 24 hour rinsing with streaming water after the exposure.

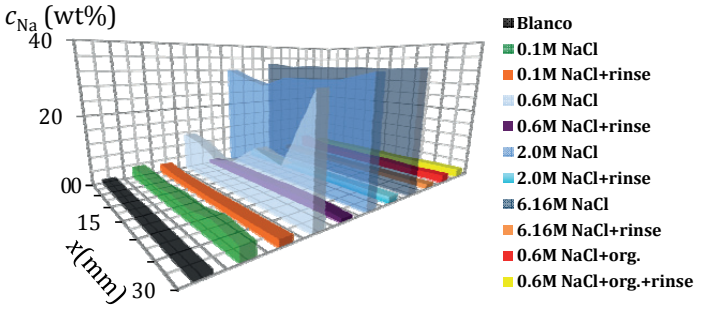

Fig. 13. Na content as a function of *x* coordinate along the surface of the NRB specimen as analyzed with SEM-EDS. The diagram represents 11 surfaces exposed to different treatments. The streaming water flowed in the *x* direction.

In SEM images taken from the brick surface both after the salt solution treatment and after rinsing with water the areas of adsorbed organic layer can be seen (Figs.14 and 15). These two organic additives are known for their ability to adsorb onto the surfaces, influence on crystal growth rate and formation and ability to reduce the surface area [165]. These results highlights the possibility that new impregnating substances that influence the surface phenomena in porous brick could be developed to produce desirable surface properties. The effects of various additives on the process of structure formation at different stages of the ceramic heat treatment process have already been investigated [166] and similar sorption effects are present when salt solution is in contact with porous brick medium. The residual amount of salt that penetrated into the specimens was estimated to average about 2-3 wt. %. This amount can be thought to be the order of magnitude

of the NaCl sorption on the porous NRB. The effect of sorption on the diffusion measurements is discussed in the following sections.

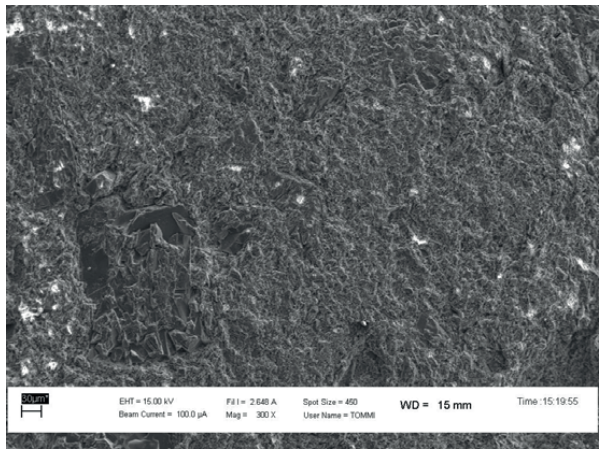

Fig. 14. SEM micrograph taken from the surface of NRB specimen after immersion in a solution of 0.6 mol/dm^3 NaCl + 0.1 mol/dm^3 2-hydroxybenzaldehyde in acetone + 5% 2-methoxybenzaldehyde in water. The scale bar is 30 µm and magnification ×300.

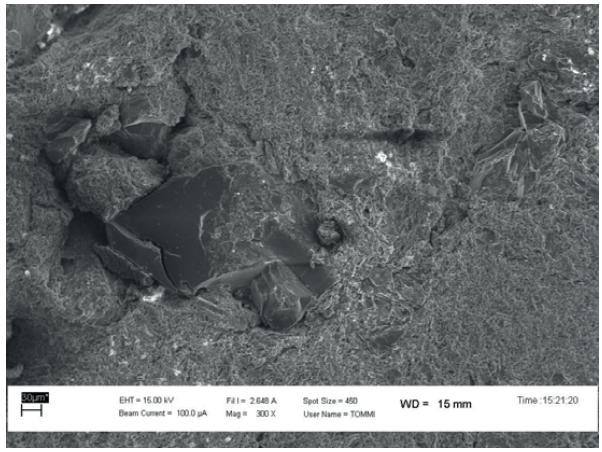

Fig. 15. Same material and immersion conditions as in Fig. 14. After treatment the specimen was rinsed for 24 h and dried. The scale bar is 30 µm and magnification ×300.

4.5 Steady-state diffusion of NaCl-H_2O in porous media

Let us first consider the system NaCl-H_2O in stationary state. As explained in section 4.4, sorption occurs when porous NRB is in contact with an aqueous NaCl solution. However, sorption is still assumed to have a negligible effect on the measured diffusion coefficient in concentrated solutions when using the stationary-state DM method. This means that the sorption equilibrium is assumed to be achieved prior to the onset of the steady state. Following immersion the

initial incoming salt flux may adsorb on the pore walls and these binding effects act as a NaCl sink, which in turn slows down the establishment of the stationary state. For the DM experiment, it took between 20-60 h to reach the steady state.

The above consideration of the influence of the sorption effects applies only to the fully saturated porous system. In partially saturated hygroscopic capillary-porous materials with broad pore-size distribution like ceramic brick, the main mechanisms of moisture transfer are sorption phenomena and capillary effects. These types of moisture transfer include the simultaneous movement of water vapor and liquid salty water in the porous material and are therefore highly dependent on the moisture saturation level and the hysteresis phenomena between adsorption and desorption [168].

In a completely saturated brick medium in contact with the ambient solution phase, the sorbed NaCl is assumed to be immobile and the salt flux density only depends on the gradient of the concentration C_f of free NaCl in the pore:

$$J_{brick} = -D_{ss} \frac{dC_f}{dx} \tag{43}$$

where D_{ss} is the diffusion coefficient determined under steady-state conditions. The only movement is the very rapid reversible sorption and desorption processes in the immobile surface layer as any possible surface diffusion effect is considered to be negligible as it difficult to measure or separate its part from the total diffusion flux. Surface diffusion can be thought of as a part of the flux measured under the influence of $\mathrm{d}C_f/\mathrm{d}x$.

All the concentrations used in this thesis are referred to the pore volume. The flux density J_{brick} in Eq. (43) is referred to the total brick area normal to the x direction, and not to the pore cross section area. The flux density referred to the pore cross section area is:

$$J = \frac{1}{\varepsilon} J_{brick} = -\frac{D_{ss}}{\varepsilon} \frac{dC_f}{dx} = -D_e \frac{dC_f}{dx} \tag{44}$$

where

$$D_e = \frac{D_{ss}}{\varepsilon} \tag{45}$$

is the effective diffusion coefficient measured under steady-state conditions in a porous brick medium. Similar definitions have also been utilized by Tang [163], Nilsson [162,167] and Nilsson et al. [169] who used the term intrinsic diffusion coefficient for D_{ss}/ε. Other terminologies have also been used. For example, Glass et al. [93] used the term intrinsic diffusion coefficient for D_{ss} and the term pore-system diffusion coefficient for D_{ss}/ε. Atkinson et al. [170] uses the term pore-solution diffusion coefficient for D_{ss}/ε. Andrade et al. [171] and also Brakel et al. [148] have used the term effective diffusion coefficient for D_{ss}. Due to these differences in naming convention and definition in the diffusion measurements of

porous media, care should be taken when making comparisons between measured and published values. Numerous diffusion coefficients can be found in the literature but few have been clearly defined. Strict dimension analyzes for the diffusion coefficients in porous media have been performed by Nilsson [162, 167] and Tang [163].

4.6 Non steady-state diffusion of NaCl-H_2O in porous media

The diffusion of NaCl under non-stationary conditions is described by Fick's second equation:

$$\frac{\partial c_f}{\partial t} = -\frac{\partial J}{\partial x} = D_e \frac{\partial^2 c_f}{\partial x^2} \tag{46}$$

which results from the combination of Fick's first law and the equation of continuity describing the mass conservation. In Eq. (46) the adsorption effect has not been taken into account. This equation was used in the binary (unpublished) and tracer diffusion measurements in closed quartz capillaries (publication I). No adsorption effect was found when comparing the diffusion coefficients measured with different capillaries diameters of 0.70 and 1.40 mm at very low $MgCl_2$ concentrations ~10^{-5} mol/dm^3 (unpublished). This contrast with the findings of Gosman et al. [172] who discovered an adsorption effect in commercial Pyrex glass capillaries when comparing the diffusion coefficients measured with different capillaries diameters of 1.000 and 1.904 mm at very low NaCl concentrations of about 10^{-5} mol/dm^3.

Possible sorption processes do have an influence on the measured diffusion coefficients in a non-steady-state system as sorption may occur when salt penetrates through the porous medium from the high concentration side to the low concentration side. The salt is believed to be captured by the pore walls especially on the low or zero concentration side where there are relatively more areas available for salt binding when compared to the high concentration side. The binding mechanisms, which retard the observed diffusion, have not been investigated but physical adsorption is assumed to be the main sorption process. Therefore, the effect of sorption must be taken into account when studying NaCl diffusion in brick with the CCM.

The total salt concentration inside the pore, walls included, is the sum of the free and adsorbed salt concentration

$$C = C_s + C_f \,. \tag{47}$$

Under adsorption equilibrium conditions, the concentrations C_s and C_f are related by an adsorption isotherm. Since adsorption is fast compared to mass diffusion, it can be assumed that C_s and C_f are also related by the adsorption isotherm when studying mass transport and hence the ratio between their (time) variations can be described by the adsorption capacity:

$$S = \left(\frac{dC_s}{dC_f}\right)_{eq} \approx \frac{\partial C_s/\partial t}{\partial C_f/\partial t} \ . \tag{48}$$

Thus, when adsorption is taken into account, Eq. (46) must be modified to:

$$\frac{\partial C}{\partial t} = (1+S)\frac{\partial C_f}{\partial t} = -\frac{\partial J}{\partial x} = D_e \frac{\partial^2 C_f}{\partial x^2} \ . \tag{49}$$

The adsorption capacity describes the ability of a porous brick medium to adsorb further salt when the free salt concentration increases in the pore solution. It was denoted as binding capacity by Tang [163] and Nilsson et al. [162, 167, 169] in their studies with chloride transport in concrete. Olin [154] and Muurinen [156] derived a similar term, which they designated as the capacity factor term α.

Equation (49) can be transformed to:

$$\frac{\partial C_f}{\partial t} = D_{app} \frac{\partial^2 C_f}{\partial x^2} \tag{50}$$

where

$$D_{app} = \frac{D_{ss}}{\varepsilon(1+S)} = \frac{D_e}{1+S} \tag{51}$$

is the apparent diffusion coefficient. While the effective diffusion coefficient D_e depends on the influence of the porous structure of the brick medium (e.g. porosity, constrictivity, tortuosity) the apparent diffusion coefficient D_{app} in addition also depends on the adsorption effects in the porous brick medium. A similar definition has also been used by Andrade [173] and other researchers to calculate chloride diffusion coefficients in different types of concrete. While their effective diffusion coefficient in steady-state experiments [174-178] encounters only ionic transport, the apparent obtained from non-stationary experiments does also take into account binding of chlorides with cement phases [179-181].

Equations (50) and (51) were used in binary differential, binary integral and tracer diffusion measurements in closed brick tubes with the CCM (unpublished). In CCM the source of the NaCl is inside of the closed brick tube.

5 CLOSED CAPILLARY METHOD IN POROUS BRICK MEDIA

As there were no reliable values measured for diffusion coefficients of salts in brick media within the literature, the Closed Capillary Method (CCM) was used for the salt diffusion coefficient measurements in porous fired brick media in order to allow the evaluation and comparison of the results obtained in publications II-V with the modified Diaphragm Cell Method (DM). In addition to obtaining comparable data via an independent method the idea was also to determine if this method would be applicable to other types of diffusion not previously studied. In this thesis the CCM was, for the first time, applied to the measurement of salt diffusion coefficients in pore solutions inside a porous medium and due to the cylinder structure of the brick specimens used in the experiments the method could also be called the closed cylinder method. The integral interdiffusion coefficients with the same concentration gradients of NaCl as measured with the DM were also measured with the CCM. Moreover, differential interdiffusion coefficients of NaCl and tracer diffusion coefficients for the Na^+ ion were determined in the NRB-medium as a function of concentration at an ambient temperature of 25 °C.

The very first experiments using the idea of closed capillary were performed by Harned et al. [191] who measured the interdiffusion coefficient of KCl in water with the conductometric method. Similar closed capillary concepts were utilized by both Timmerhaus et al. [57] and Zhukhovitskii et al. [192] for their studies of the self-diffusion of CO_2 in the gas phase and self-diffusion experiments of silver isotope in solid silver, respectively. Some preliminary experiments in liquids with closed capillary were made by Noszticzius [58] prior to the development of the continuous CCM by Passiniemi, Liukkonen, Noszticzius and Rastas [65-69]. The CCM used by Passiniemi et al., was further developed by Ahl [193], Ahl and Liukkonen [publication I], Chakrabarti et al. [194] and all versions were applied to diffusion measurements of tracer-ions in aqueous electrolyte solutions. In addition to these measurements the method has also been applied to biological applications in aqueous solutions by Simonin et al. [195] who used modified CCM to measure the diffusion coefficient of large human blood lipoproteins. These macromolecules were indirectly labeled by the attachment a fatty acid molecule labeled with the β–emitter ^{131}I radioisotope. However CCM has not been previously used for the measurements of inter- or tracer diffusion coefficients in porous matrices.

5.1 Measuring cell and apparatus

In this work the CCM for the determination of diffusion coefficients in electrolyte solution - both in the absence and presence of a porous medium - employs the continuous monitoring of the radioactivity in the diffusion cell. The radiochemical used was gamma-active ^{22}Na, which decays to ^{22}Ne via positron emission (90%)

and with the competitive orbital electron capture mode (10%) [196]. The decay schemes are as follows [197]:

$$^{22}_{11}Na \xrightarrow{\beta^+} {}^{22}_{10}Ne + {}^{0}_{+1}e + {}^{0}_{0}\vartheta_e \tag{52}$$

$$^{22}_{11}Na + {}^{0}_{-1}e \xrightarrow{EC} {}^{22}_{10}Ne + {}^{0}_{0}\vartheta_e \tag{53}$$

where β^+, EC and ϑ_e represent the positron emission, the electron capture and the electron neutrino, respectively. The 551 keV positron annihilation radiation and 1275 keV positron emission peaks from the ^{22}Na γ-spectrum were utilized from the 10 V voltage output of the gamma active detector system. The measured γ-spectrum of ^{22}Na is presented in Fig. 16. The half-life of the radioisotope is 2.602 years and the value of the decay constant is 8.447×10^{-9} s^{-1}.

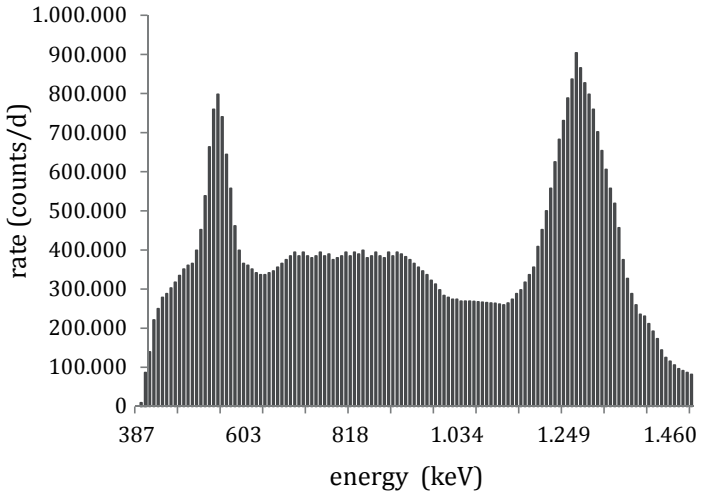

Fig. 16. Measured γ ray spectrum of ^{22}Na. The spectrum was obtained with a planar type thallium-activated sodium iodide scintillation counter coupled to a multichannel pulse-height analyzer. The 551 keV and 1275 keV energy peaks were utilized for pulse counting via the multichannel scaling mode of the spectrometer.

A schematic drawing of the apparatus for measuring the diffusion coefficient in a porous medium is shown in Fig. 17. The diffusion cell including the closed brick tube was thermostated in a water-bath at 298.15 ± 0.01 K. The measuring system for γ-counting consists of a planar NaI(Tl) scintillator detector (2 in × 2 in), photomultiplier at the base (EG&G Ortec 266) and high voltage (650 V) source (EG&G Ortec ACE Mate 925-Scint). The multichannel analyzer (EG&G Ortec Adcam Analyst Model 100U) was in the multichannel scaling mode.

The position of the closed brick tube with respect to the lead shields and NaI(Tl) scintillator was chosen on the basis of the counting efficiency function. This function, also called the registration function $r(x)$, makes it possible to follow the

changes of the radioactivity during the diffusion experiment and was experimentally determined by using a two-dimensional radionuclide plane source of ^{22}NaCl that was able to move horizontal to the radial (x) direction over the flat scintillator. The radioactive plane source was made by immersing a thin filter paper in the bulk ^{22}NaCl solution, drying and attaching it to the end of a blank plastic cylinder with the same dimensions as the brick tube specimen. The optimal registration function was found through trial and error by varying the positions of the γ-detector and lead shields with respect to the radionuclide source and recording the counts. The registration function and the horizontal position of the brick tube in relation to this function are given in Fig. 18. The optimal vertical position of the brick tube with respect to the NaI(Tl) scintillator was discovered to be 108 mm and the optimal thickness of the lead-acryl piston in between the brick and the scintillator 86 mm.

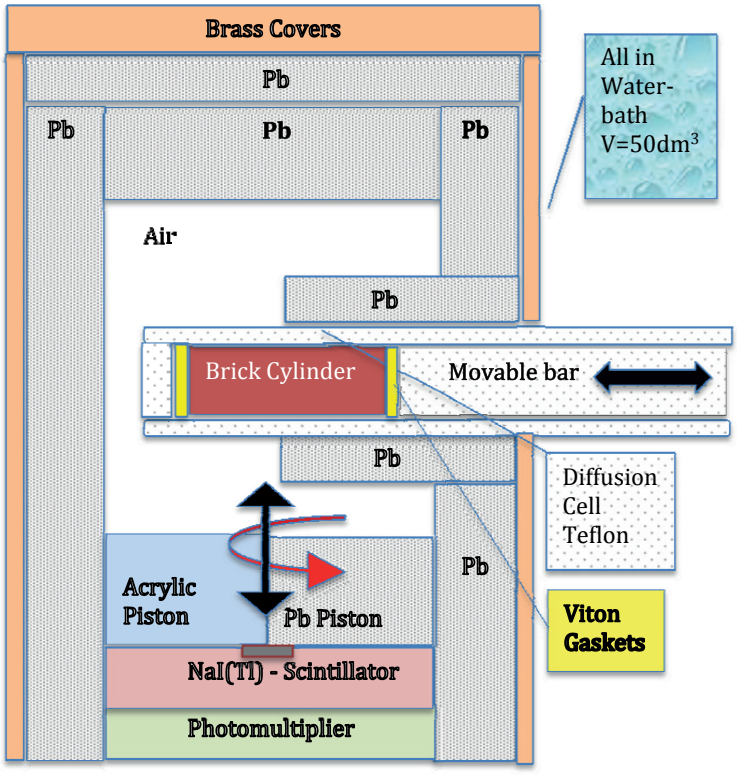

Fig. 17. Schematic drawing of the apparatus for measuring the diffusion coefficients with the closed capillary method in a porous medium. The whole apparatus was thermostated in water-bath at 25.00 ± 0.01 °C. The final vertical positions of the brick specimen, the lead-acrylic piston (Φ = 62 mm) and the planar NaI(Tl)-scintillator (2 in × 2 in) are not absolute as they were adjusted in order to optimize the gamma registration function. The thickness of the lead-acrylic piston was varied between 36-86 mm and could be rotated ±20°.

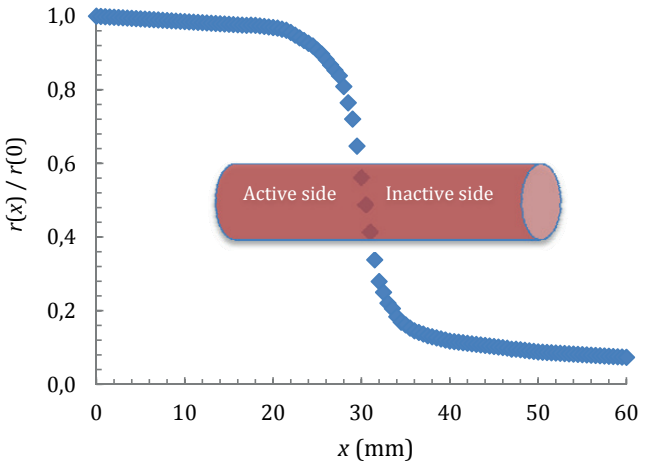

Fig. 18. Measured registration function with a ^{22}NaCl plane source and associated optimal horizontal position of the closed brick cylinder. The registration function $r(x)$ is given as a relative dimensionless $r(x)/r(x = 0)$ function, where $r(x = 0) = 13335$ Bq.

The diffusion measurements were made with cleaned and inspected NRB-tubes with a lacquered outside and a uniform diameter of $\Phi = 11.64$ mm and lengths between $L = 39.88$-40.12 mm. The length of each cylindrical brick specimen was precisely measured prior to the diffusion measurement with the calibrated digital measuring instrument at 25 °C. The calibration was done against an optical measuring microscope (Tesa Microhite) with an accuracy of ±0.02 mm. Basic aqueous salt solutions (Merck, pro analyze) were prepared by first weighting out the appropriate salt and dissolving it in Milli-Q-water that had been degassed by boiling for 30 min. The radioactive solutions were made of a sample of carrier free ^{22}NaCl solution produced by Amersham Radiochemical Center (UK) and also, as reference check, by Dupont (USA). A small amount (10 mm^3) from 1.00 mCi active solution of ^{22}NaCl was placed in a 10 cm^3 bottle and gently heated under the infrared lamp to remove the solvent water. The resulting solid of ^{22}NaCl was subsequently dissolved into aqueous salt solution of known concentration under investigation and this active solution was used to fill half of the brick cylinder. Both the active and the inactive solutions were kept in the same kind of measuring bottles under the same conditions ($V = 10$ cm^3, $t = 27$ °C, Argon atmosphere) prior to filling the brick tube in order to prevent air bubble formation during the diffusion tests. A more detailed description of the preparation of the measuring solutions and the brick specimen, the equipment and the laboratory procedures related to these measurements are provided in publications I-III and in the author's licentiate thesis [193].

All of the experiments were started with a check to ensure that the background activity level in the measuring chamber (≈ 10 Bq) was less than 2% of the registered activity of the diffusion measurement. The brick specimen under

investigation was first gently immersed about 1 mm from one end under the surface of the inactive measuring solution. After the solution front, due to the capillary effect, had reach the halfway mark the solution was rapidly changed to the active one and the specimen remained immersed until the previously dry end of the brick specimen became fully moisten with the first inactive solution. A small drop of inactive solution was left on the end of the brick and the surface of the lacquered active cylinder end was gently wiped with moisten tissue paper. As the solution to the diffusion equation with CCM is based on a boundary value problem [publication I] there is no need for a sharp initial concentration distribution between the active and inactive solutions - a state which would difficult to achieve in the case of a porous brick medium. Although the formation of a three dimensional initial concentration distribution can be tolerated (as has been shown) from the viewpoint of optimal conditions the position of initial boundary at the middle of the brick cylinder is more favorable [66]. Nevertheless a series of experiments using the sliding cell technique (first introduced by Chakrabarti et al. [194]) were still performed using a combination of two brick cylinders of half size filled with inactive and active solution, respectively, however the results were less accurate and repeatability was poor.

The diffusion brick tube specimen once filled with the experimental inactive and active solutions was closed tightly using Viton gaskets at both ends and put in a supporting measuring cell. The closed diffusion cell was screwed in to the movable bar and the whole assembly was placed in the previously determined optimal horizontal position (Fig. 18). Small turbulence at the interface of the liquids resulting from the filling process decayed quickly and was insignificant after the first half an hour of measuring but in order to ensure reliability the initial measuring point in each measurement was ignored.

5.2 Tracer diffusion measurements

In the tracer diffusion measurement a very small amount of tracer is added to part of the liquid system, which is in equilibrium prior to the addition. In practice with the porous brick system used in this work the upper half of the brick cylinder was filled at the beginning of the experiment with inactive solution and the lower half with the radioactive solution. Measurement of any change in the activity was based on the position dependent counting efficiency of the radioactivity detector system. As the concentration of the supporting NaCl electrolyte in both sides of the brick cylinder was the same and under isothermal and isobaric conditions the diffusion flow of the ^{22}NaCl tracer only depended on its own concentration gradient, see Eq. (19). The ternary tracer diffusion system inside the porous brick tube was NaCl(1)- ^{22}NaCl(2) in H_2O(0). The mean concentration of ^{22}NaCl tracer was of the order of 5×10^{-8} mol/dm^3. The tracer diffusion coefficients were measured in the NaCl concentration region between 0.005 and 3.08 mol/dm^3.

5.3 Interdiffusion measurements

Interdiffusion occurs in binary systems and in the CCM data presented in this thesis the diffusion coefficient is calculated from the changes of the radioactivity during the diffusion. By adding some radioactive salt to the binary salt-H_2O solution the diffusion system becomes either ternary or quaternary, unless the salts are isotopes of each other and the diffusive behavior of the two isotopes are interchangeable as is the case with the isotopes of ^{22}NaCl and ^{23}NaCl. The mass effect of the isotopes $^{22}Na^+$, $^{23}Na^+$ and $^{24}Na^+$ on the diffusion processes has previously been shown to be very small and normally immeasurable [101]. Furthermore, the Cl^- counter-ion is the same in both salt isotopes and its ionic diffusion coefficient, D_{Cl^-} provides half of the binary diffusion coefficient of the NaCl salt. In this work the isotope effect was therefore omitted and the diffusive behavior of ^{22}NaCl and ^{23}NaCl were presumed to be identical resulting in the diffusion system being treated as a binary system with only one diffusion coefficient D_{NaCl} [68], which was measured as a function of concentration with the CCM. The binary diffusion system inside the porous brick tube was NaCl(12) in H_2O(0), where NaCl(12) represents both ^{23}NaCl and ^{22}NaCl. The mean concentration of the radioisotope ^{22}NaCl in the brick cylinder was ca. 5×10^{-8} mol/dm^3.

In practice the upper half of the brick cylinder was filled at the beginning of the experiment with inactive NaCl solution (concentration C_1) and the lower half with NaCl solution mixed with a very small amount of radioactive ^{22}NaCl tracer (concentration C_2); the subscripts 1 and 2 refer here to upper and lower half of the cylinder, respectively. These two different solutions were in total internal equilibrium prior to filling of the brick cylinder and the start of the experiment. In the differential interdiffusion experiments, the salt concentration difference C_2-C_1 was small. The mean NaCl concentration, $C_{\mathrm{mean}} = 0.5(C_2+C_1)$, was varied between 0.05 and 3.08 mol/dm^3. In the integral interdiffusion experiments, the concentration C_1 was zero and $C_{\mathrm{mean}} = 0.5C_2$ was varied between 0.0005 and 3.08 mol/dm^3.

5.4 Calculation of the diffusion coefficients

In the case of tracer diffusion measurements in the system ^{23}NaCl(1)- ^{22}NaCl(2)-H_2O(0), where there is a concentration gradient with respect only to the radionuclide. This is because in tracer diffusion there are no gradients related to inactive components. Furthermore, in tracer diffusion D_{app} does not depend on tracer concentration but rather on the constant concentration of supporting ^{23}NaCl electrolyte.

The diffusion in porous brick medium in CCM is described by Eq. (50). In the case of a radioisotope as the diffusing species the half-life of the nuclide must be taken into account and the Fick's second law is applied in the form:

$$\frac{\partial C_f}{\partial t} = D_{app}\nabla^2 C_f - \lambda C_f \tag{54}$$

where D_{app} is the apparent diffusion coefficient of the tracer ion $^{22}Na^{+}$ or the tracer component $^{22}NaCl$ present in the existing diffusion system [68], C_f is the concentration of the free tracer ion $^{22}Na^{+}$ or component $^{22}NaCl$ and λ is the decay constant of ^{22}Na, respectively.

In the case of a interdiffusion measurement in NaCl(12)- H_2O(0), where NaCl(12) represents both $^{23}NaCl$ and $^{22}NaCl$, there is a concentration gradient with respect to the NaCl salt as a whole. Then, C_f is the sum of concentrations of free $^{23}NaCl$ and $^{22}NaCl$. Without the isotope effects, diffusion proceeds as for a binary salt and the major contribution to C_f comes from the inactive $^{23}NaCl$, with the used salt concentrations of $[^{23}NaCl] \geq 5\times10^{-4}$ mol/dm^3 and $[^{22}NaCl] \leq 5\times10^{-8}$ mol/dm^3; note that the tracer concentration C_f needs not to be statistically small for Eq. (54) to be valid [15, 198, 199]. Furthermore, in interdiffusion D_{app} does depend on C_f and the concentration gradient (integral and differential diffusion).

Equation (54) may be solved in a closed cylinder using cylindrical coordinates in order to calculate the concentration as a function of position and time, $c(r, \theta, x, t)$ [200, 201]. In this thesis, the determination of the concentration changes was based on the use of radionuclides with any measured changes in the activity of the nuclides based on the position dependent counting efficiency, $h(r, \theta, x, t)$ of the nuclear detector system. Cylindrical factors caused by the disturbances in the filling process disappear after an induction period for capillaries and cylinders with small r/L ratio and it has been shown that only a one dimensional counting efficiency function, $h(x)$, is adequate [67]. Thus the intensity $I(t)$ can be given in the following form [65, 67, 71]:

$$I(t) = I_\infty + \sum_{m=1}^{\infty} I_m \, exp\left(-k_m D_{app} t\right) \tag{55}$$

where I_∞, I_m, and k_m are the intensity of the equilibrium concentration ($I_\infty = I_0$), the constant intensity term and the eigenvalue k_m (which depend on diffusion cell geometry). The infinite sum of Eq. (55) always converges because of the negative arguments of the exponentials.

The diffusion coefficient can be measured with any convenient specimen geometry and there are a number of possible diffusion geometries for which there already exist solutions including the commonly used cylinder geometry [200, 202, 203]. For cylinders or capillaries with both ends and the surface of the rod closed, the condition $1.85/r > \pi/L$ holds and the eigenvalues are $k_m = (m\pi/L)^2$ with m= 1,2,3, … [67, 198]. For the brick tubes used in this work for the CCM (diameter Φ = 1.164 cm, length L = 4 cm) the values are $1.85/r$ = 3.179 cm^{-1} and π/L = 0.785. The intensity equation for the closed brick cylinder is then:

$$I(t) = I_\infty + \sum_{m=1}^{\infty} I_m \, exp\left(-\frac{m^2\pi^2}{L^2} D_{app} t\right) \tag{56}$$

After about 30-40 h from the beginning of the experiment only the first term in the series predominates and the other terms may be ignored. Then, D_{app} was

calculated with the experimental results $I = I(t)$ from the slope $(-\pi^2 D_{\mathrm{app}}/L^2)$ of the equation:

$$ln[I(t) - I_\infty] = ln\,(I_1) - \frac{\pi^2 D_{app}}{L^2} t \tag{57}$$

where the I_∞ term was first solved with the initial nonlinear regression analysis from the start of the experiment with three sum terms of Eq. (56) using the Levenberg-Marquardt method [204].

Equation (57), with the iterated I_∞ term, proved to be statistically the best equation for calculating the tracer and interdiffusion coefficients measured with the CCM in porous brick media. The method based on this equation was previously known as the linear least-square calculation method (publication I, [71], [193]). In practical diffusion experiments long time pulse counts coming from the diffusion cell during certain time intervals Δt are measured rather than short time intensities at time t. It is also important to correct the measured pulse counts against background activity, the half-life of the tracer and the dead-time of the pulse counter as have been done in this work. In the least-square regression method used the increasing uncertainty of the experimental data points as a function of time was also taken into account [205] by including the statistical error of the linear least-square calculation method to the minimized function. The aim was then to minimize the function S_N, the sum of the squares of the ratio of each residual in $[\ln[I(t_i) - I_\infty] - est_i]$ to the corresponding assessed error as:

$$S_N = \sum_{i=1}^{240} \left[\sqrt{ln(I(t_i) - I_\infty)}\,[ln(I(t_i) - I_\infty) - est_i\,]\right]^2 \tag{58}$$

where the function S_N to be minimized relates to all 240 data points $I(t_i)$, each of which is a pulse count collected in a 30 min interval over a measuring period of 5 days. The term est_i is the least-square regression estimate for the term of $\ln[I(t_i) - I_\infty]$.

The optimization of the pulse counting intervals Δt and also the statistical reasons for using Eq. (57) are presented in more detail in the publication I and also in [71, 193]. The mathematics used for solving the diffusion equation Eq. (54) and the above derivations are well known [200, 201, 204, 206] and the theoretical background for the important relation between the diffusion coefficient, the cell geometry and the counting efficiency function have been broadly interpreted previously in the works of Rastas and Kivalo [207], Liukkonen et al. [208] and Liukkonen, Noszticzius and Passiniemi et al. [65-67].

6 RESULTS AND DISCUSSION

This experimental work consists of three separate experimental parts concerning diffusion measurements. The first part deals with the tracer diffusion measurements with the CCM in pure salt-water solutions in the absence of porous media (Sections 6.1-6.3). The second part consists of the interdiffusion measurements of salts in porous brick media with the stationary-state DM (Sections 6.4-6.7) and the final part relates to the novel application of non-stationary-state CCM for the measurement of the diffusion coefficients in porous brick media (Sections 6.8-6.10).

6.1 Tracer diffusion: $MgCl_2$-$^{22}NaCl$-H_2O

In publication I closed capillary measuring techniques, including apparatus and diffusion coefficient calculation method from an infinite series solution have been presented, further developed and tested. The diffusion coefficients were found to be most accurately determined by a new linear least-square calculation method that produced a standard error of ≤ 0.1%. The tracer diffusion coefficients of ^{22}Na ions in the system $MgCl_2(1)$-$^{22}NaCl(2)$-$H_2O(0)$ were determined as a function of the $MgCl_2$ concentration (C_1) in aqueous solutions at 25 °C, over a large concentration region. The main results from concentrations between 1 and 10^{-4} mol/dm^3 were evaluated by the total differential method and are given in the Table 2. The measured diffusion coefficients are given as mean value ± mean standard deviation [209] in all tables in this thesis. The solution concentrations used were analyzed using atom absorption spectrophotometry.

Table 2. Experimental tracer diffusion coefficients of ^{22}Na ions in 10^{-5} cm^2/s units calculated with the linear least-square method for a $MgCl_2$ concentration C_1 between 1 and 0.0001 mol/dm^3 at 298.15±0.01 K.

C_1(mol/dm^3)	0.994	0.0997	0.00982	0.00101	0.000101
single exp. D	0.995±0.001	1.247±0.002	1.272±0.002	1.314±0.003	1.328±0.002
	0.993±0.002	1.245±0.003	1.274±0.002	1.317±0.002	1.327±0.001
	0.996±0.003	1.244±0.002	1.271±0.003	1.313±0.002	1.329±0.002
	0.994±0.002	1.247±0.002	1.270±0.002	1.313±0.002	1.326±0.002
	0.991±0.002	1.244±0.003	1.271±0.001		1.329±0.002
	0.995±0.002	1.244±0.002	1.272±0.002		
			1.273±0.002		
mean D	0.994±0.001	1.245±0.001	1.272±0.001	1.314±0.001	1.328±0.001

This thesis reports the first diffusion coefficients measurements at dilute concentrations (C_1 < 0.5 mol/dm^3) for $MgCl_2$ solutions. However, our measurements for a 1 mol/dm^3 solution gave a value of (0.988±0.001)×10^{-5} cm^2/s that agreed with values previously determined by Mills et al. (0.985±0.005) ×10^{-5} cm^2/s and Albright et al. (0.989±0.002)×10^{-5} cm^2/s [39, 19] with a diaphragm cell and optical interferometry methods, respectively. The Onsager Limiting Law, Eq. (22), was verified to the tracer diffusion of $^{22}NaCl$ at low concentrations of $MgCl_2$ - the first time for a 2:1 electrolyte. For the asymmetrical electrolyte $MgCl_2$ the

limiting law was observed to hold true to molarities of $C_1 \leq 10^{-2}$ mol/dm^3. This was demonstrated by comparing the measured tracer diffusion coefficients at concentrations between 10^{-2}-10^{-4} mol/dm^3 and fitting them with the Onsager Limiting Law by the least squares method. The regression line and the measuring points are presented in publication I (Fig. 8). The experimental D_{22}^0 value for Na^+ ion - from the intercept - was $(1.334\pm0.002)\times10^{-5}$ cm^2/s and agreed with the Nernst limiting value $D_{22}^0 = 1.334\times10^{-5}$ cm^2/s, which should be equal for all types of supporting electrolytes.

It is well known that in deriving the equations of the limiting law Onsager made a number of mathematical approximations like neglecting the cross product of the electrophoretic and relaxation effects terms. The expressions of Onsager are therefore only strictly valid as limiting equations and may be expected to hold only for very dilute solutions. This can be clearly seen by presenting both the relative tracer diffusion coefficients (D/D^0) and the reciprocals (η_0/η) of the relative viscosities as a function of the square root of the concentration. Both of the curves fall progressively in the order of KCl, NaCl, LiCl and $MgCl_2$ (Figs. 9 and 10 in publication I) indicating a significant mutual relation between the viscosity and the measured values of tracer diffusion coefficients. The marked change of the D_{Na^+} from the Onsager Limiting Law at concentrations greater than 0.01 mol/dm^3 is certainly caused in part by the increase in viscosity of the supporting electrolyte as the rise in ionic strength increases viscous force, which influences the electrophoretic effect and retards the motion of ions [210].

The relation between the size and the mobility of ion was first suggested by Stokes [211] who calculated frictional resistance in terms of the dimensions of the very large solid spherical particle and the viscosity of the ideal continuous medium. Another important equation first derived by Einstein [212] demonstrated that $D = kT/f$, where f is the frictional coefficient, showing the relationship between diffusion coefficient and viscosity. In this Stokes-Einstein formula the concept of viscous resisting force were applied to the motion of a colloidal particle, with a size significantly greater than the solvent molecules, through a fluid. The analogous relationship between the tracer diffusion coefficient and viscosity for individual smaller ions diffusing through larger solvent molecules had previously been recognized by Onsager, Fuoss, Gordon [213] and Broersma [214]. Moreover, an equation for concentrated solutions that calculates the viscosity effect on the electrophoretic term has also been proposed [215].

6.2 Tracer diffusion: $MgCl_2$-^{22}NaCl-HCl-H_2O

For supporting electrolyte concentrations below 10^{-4} mol/dm^3 the measured Na^+ tracer diffusion coefficient exceeded the limiting value $D^0 = 1.334 \times 10^{-5}$ cm^2/s. A similar result was also found by both Passiniemi [68] and Wang et al. [63] who, using CCM, measured values of $D^0 = 1.338 \times 10^{-5}$ cm^2/s and $D^0 = 1.445 \times 10^{-5}$ cm^2/s, respectively, results that lie above the Onsager Limiting Law. Passiniemi used aqueous NaCl solutions and Wang et al. aqueous NaI solutions.

As explained in Section 3.3, in this concentration range we have to consider the components $MgCl_2$(1), NaCl(2), HCl(3) and H_2O(0). The experiments in very dilute solutions were complicated by the fact that the accuracy and precision degenerates as a result of the low concentrations of radioactive tracer used. In principle, we consider tracer concentrations $C_2 < 0.01C_1$. However, this level was not sufficient to produce good statistics when $C_1 < 10^{-4}$ mol/dm^3 and the amount of tracer had to be increased. This increase tracer amount improved the statistics but lead to results that, at first, seemed contradictory. This increase in tracer concentrations also effects of the level of water ionization resulting in additional cross-term contributions (see Table 1). The main results for concentrations below 10^{-4} mol/dm^3 are given in Table 3.

Table 3. Experimental diffusion coefficients of Na^+ ions in 10^{-5} cm^2/s units calculated at 298.15±0.01 K with the linear least-square method for $MgCl_2$(1) supporting electrolyte in the range 10^{-5}-10^{-6} mol/dm^3 and different NaCl(2) concentrations. The inner radius of the quartz capillaries was 0.70 mm; except for the set of six experiments at C_2/C_1 = 6.82%, $C_1 = 9.98\times10^{-6}$ mol/dm^3, where it was 0.35 mm.

$C_1(10^{-6}$ mol/dm$^3)$	9.98 (0.35 mm)	9.98	1.00
C_2/C_1(%)	6.82	6.82	26.80
single exp.	1.453±0.010	1.478±0.002	1.338±0.010
D	1.468±0.004	1.495±0.002	1.351±0.013
	1.476±0.005	1.515±0.003	1.334±0.014
	1.486±0.006	1.502±0.003	1.351±0.009
	1.489±0.004		
	1.476±0.006		
mean *D*	1.475±0.005	1.498±0.008	1.344±0.004

$C_1(10^{-6}$ mol/dm$^3)$	9.98	9.98	9.98
C_2/C_1(%)	3.42	6.83	13.63
single exp.	1.431±0.005	1.493±0.004	1.559±0.004
D	1.429±0.005	1.498±0.003	1.535±0.003
	1.448±0.005	1.482±0.004	1.520±0.003
		1.499±0.007	
mean *D*	1.436±0.006	1.493±0.004	1.538±0.010

Good statistics were not obtained until the proportion of the tracer concentration was raised significantly as shown by the high tracer concentrations measurements in Table 3 (C_2/C_1 = 26.80%, $C_1 = 1.00\times10^{-6}$ mol/dm^3). These measurements in a supporting electrolyte of 10^{-6} mol/dm^3 gave a mean value for D_{Na^+} of 1.344×10^{-5} cm^2/s that was a significant deviation from the Nernst limiting value as the pure tracer diffusion coefficients D_{21} and D_{23} should be zero or at least as small as possible. From the Nernst-Planck equations, Eqs. (33)-(35), under these conditions the calculated values D_{ij} are compared to the tracer flow equation $J_2 = -D_{21}\nabla C_1 - D_{22}\nabla C_2 - D_{23}\nabla C_3$, Eq. (28), where the subscripts 1, 2 and 3 denote $MgCl_2$, NaCl and HCl, respectively. The component diffusion coefficients were calculated at three different pH ($\approx -\log_{10}C_3$) and the results in 10^{-5} cm^2/s units were: (i) pH 6, D_{21} = 0.0493, D_{22} = 1.347, D_{23} = –0.136; (ii) pH 7, D_{21} = 0.1020, D_{22} = 1.361, D_{23} = –0.406; and (iii) pH 8, D_{21} = 0.0846, D_{22} = 1.356, D_{23} = –10.636. The relatively large values of D_{23} indicate that this situation is not

exactly that of tracer diffusion, i.e. the approximation $J_2 \approx -D_{22}\nabla C_2$ cannot be used. The experimental accuracy of measured diffusion coefficients in the $MgCl_2$ solution of 10^{-6} mol/dm^3 could not be evaluated because the actual concentration gradients ∇C_1 and ∇C_3, and hence the different contributions to the measured flow J_2, are not known.

For closed capillary measurements small capillary diameters are preferable in order to eliminate the possible convection currents caused by mechanical sources e.g. the thermostat stirrer motor. However, these smaller capillaries have a larger surface to volume relation $2/r$ which can result in surface phenomenon like surface diffusion that can increase the measured diffusion coefficient value. In order to exclude surface diffusion or any other microstructure surface effects a series of parallel measurements using capillaries with radius of r = 0.35 mm and r = 0.70 mm were performed (upper panel in Table 4). As can be seen the values measured in the narrower capillaries were smaller. Although the reason for this is still undetermined, it seems that surface diffusion for the r = 0.70 mm capillaries was negligible. Although no surface diffusion effects have been reported previously for quartz capillaries used in this work, a faster surface diffusion of Na^+ ions has previously recorded in commercial Pyrex glass capillaries [172].

Finally, in order to measure pure tracer diffusion coefficients a series of measurements was carried out with different tracer concentration (lower panel in Table 4). The limiting value was ascertained by plotting tracer diffusion coefficient against the square root of NaCl tracer concentration and extrapolating linearly to zero. The results are depicted graphically in Fig. 19. The equation of the least-squares fitted slope is D_{Na^+}(cm^2/s) = 1.341×10^{-5} + 1.724×10^{-3} $C_2^{1/2}$, where C_2 denotes here the value of the NaCl concentration in mol/dm^3 units, with a correlation coefficient of r = 0.986 and the intercept on the ordinate gives $D^0_{Na^+}$ = $(1.341 \pm 0.008)\times10^{-5}$ cm^2/s.

At this order of dilution the concentration of the tracer, the supporting electrolyte and the ions resulting from the water ionization become comparable and the extrapolated diffusion coefficient, which is higher than the Nernst limiting value 1.334×10^{-5} cm^2/s, obtained from the OLL will contain contributions from cross-term coefficients. For dilute $MgCl_2$ concentrations ($C_1 \leq 10^{-4}$ mol/dm^3) the absolute values of D_{23} are greater than the values of D_{21} as can be seen from Table 1. As the value of 1.341×10^{-5} cm^2/s was obtained by extrapolating to the zero concentration of NaCl the condition $C_2/C_1 < 1\%$ holds and the value can be considered as the pure tracer diffusion coefficient of the sodium ion at infinite dilution with respect to the supporting electrolyte. The component diffusion coefficients were calculated at three different pH and the results in 10^{-5} cm^2/s units were: (i) pH 6, D_{21} = 0.004, D_{22} = 1.335, D_{23} = –0.012; (ii) pH 7, D_{21} = 0.005, D_{22} = 1.335, D_{23} = –0.020; and (iii) pH 8, D_{21} = 0.005, D_{22} = 1.335, D_{23} = –0.611.

At the beginning of the experiment there is only a concentration gradient with respect to the NaCl and the concentrations of $MgCl_2$ and HCl are constant within the diffusion capillary. As the possible development of other concentration

gradients during the measurement is unknown their possible influence on the diffusion flow of NaCl has to be evaluated from the cross-term coefficients. The coefficients of D_{21}, which represent the effect of the concentration gradient of $MgCl_2$ on the diffusion flow of NaCl, can be taken as zero when compared to the magnitude of the D_{22} coefficients. In contrast, the coefficients of D_{23}, which represent the effect of the concentration gradient of HCl on the diffusion flow of NaCl, must be treated as non-zero as any spatial change in the pH from neutral to basic would probably effect the measured value of D_{Na^+}.

In conclusion it can be stated that the Nernst limiting value for the Na^+-ion in aqueous solutions is very challenging to measure with the CCM and it appears that this will also apply both to other ions and other supporting electrolytes measured with other methods [63, 68]. The use of higher specific activities than were obtainable in this work, would allow the use of smaller tracer amounts could help but the main problem with water ionization still remains. The best way to determine the Nernst limiting value at an infinite dilution is by extrapolation from the 10^{-2}-10^{-4} mol/dm^3 region to a supporting electrolyte concentration of zero; however an extrapolated value from a more dilute region may include cross-term coefficient contributions of hydrogen and hydroxide ions due to their high mobilities.

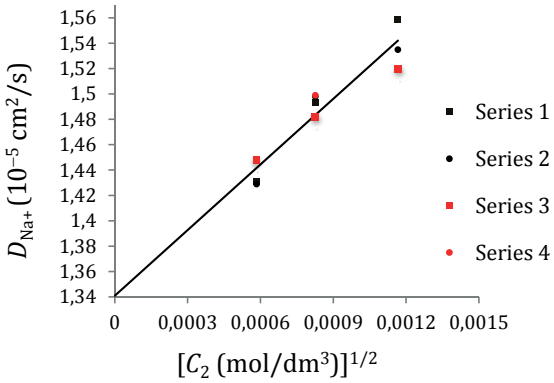

Fig. 19. Determination of the limiting value $D^0_{Na^+}$ = 1.341×10^{-5} cm^2/s at 298.15±0.01 K by extrapolation of the experimental tracer diffusion coefficients to zero. The $MgCl_2$ concentration was 9.98×10^{-6} mol/dm^3 and C_2 denotes the total concentration of ^{22}NaCl and ^{23}NaCl.

6.3 Binary diffusion: ^{22}NaCl-H_2O at extreme dilution

In order to examine the effect of the water ionization on the diffusive behavior in dilute aqueous electrolyte a series of binary diffusion measurements were also performed. These measurements were inspired by those of Mills [130] who used the open-ended capillary method in dilute NaCl solutions (from 2×10^{-3} to 2×10^{-5} mol/dm^3) where a different diffusive behavior was observed. In this work, the radioactive ^{22}NaCl tracer was allowed to diffuse against pure water to allow the

binary salt diffusion coefficient to be determined. It was assumed that no isotope effect exists for the diffusion measurements i.e. either the diffusion coefficient of the radioactive ^{22}NaCl is the same as the inactive ^{23}NaCl or the difference in diffusion coefficients are immeasurable within the precision of diffusion experiments. The measured NaCl diffusion coefficients at NaCl concentrations C_2 = 1.02×10^{-6} and 2.04×10^{-6} mol/dm^3 in the NaCl-H_2O system are given in Table 4.

Table 4. Experimental diffusion coefficients D_{22} in 10^{-5} cm^2/s units for the NaCl-H_2O system at 298.15 ± 0.01 K. The results are calculated from measurements made at very low concentrations of NaCl with the linear least-square method. The NP values have been calculated from the ionic diffusion coefficients of the Nernst-Planck equations taking into account the ionization of water.

$C_2(10^{-6}$ mol/dm$^3)$	1.02	2.04
single exp.	1.522±0.003	1.569±0.004
D_{22}	1.531±0.008	1.563±0.006
	1.532±0.003	1.578±0.005
	1.518±0.005	
mean D_{22}	1.526±0.003	1.570±0.004
NP D_{22}	1.528	1.563

These measured values were then compared to the values calculated from the Nernst-Planck equations taking into account the water ionization, Eq. (34). These calculated values are depicted graphically in Fig. 20 with the experimental values and with the Onsager Limiting Law slopes of the aqueous binary diffusion for NaCl (Onsager-Fuoss Limiting Law, [11]) and for the tracer diffusion of Na^+ in aqueous NaCl (Onsager Limiting Law, [12]). The experimental results show a good correlation with the values calculated from the Nernst-Planck equations taking the ionization of water into account and show that the measured diffusion coefficients are not pure binary diffusion coefficients as would normally be expected. By analogy to Eqs. (12) and (14), the diffusion coefficient in this system can be expressed as $D_{22} = D_2 + t_2 (D_3 - D_2)$, where 2 and 3 denote Na^+ and Cl^-. When NaCl is the only electrolyte present, $t_2 = D_2/(D_2 + D_3)$ and D_{22} becomes the binary diffusion coefficient $D_{22} = 2D_2D_3/(D_2 + D_3) = 1.611\times10^{-5}$ cm^2/s. When the NaCl concentration tends to zero, t_2 also does, and D_{22} takes the tracer value $D_2 = 1.334\times10^{-5}$ cm^2/s. The measured values in between the two limiting law values of tracer and binary diffusion coefficients, which indicates that NaCl is not the only electrolyte present and that the measured diffusion coefficients contain contributions from the highly mobile H^+ and OH^- ions. Previously measured values found in the literature were $(1.55\pm0.02)\times10^{-5}$ cm^2/s at 1×10^{-4} mol/dm^3 [198], $(1.54 \pm 0.03) \times10^{-5}$ cm^2/s at 9×10^{-5} mol/dm^3 [130], $(1.51\pm0.03)\times10^{-5}$ cm^2/s at 2×10^{-5} mol/dm^3 [130] and $(1.47 \pm 0.04)\times10^{-5}$ cm^2/s at 2×10^{-5} mol/dm^3 NaCl-H_2O solutions [198]. Although these literature values are lower compared to those calculated from the Nernst-Planck equations they also indicate ternary diffusion effects in the infinite dilute region of binary diffusion as can be seen from Fig. 20. Without this ternary effect the measured values should be of the order of the Nernst limiting value 1.611×10^{-5} cm^2/s.

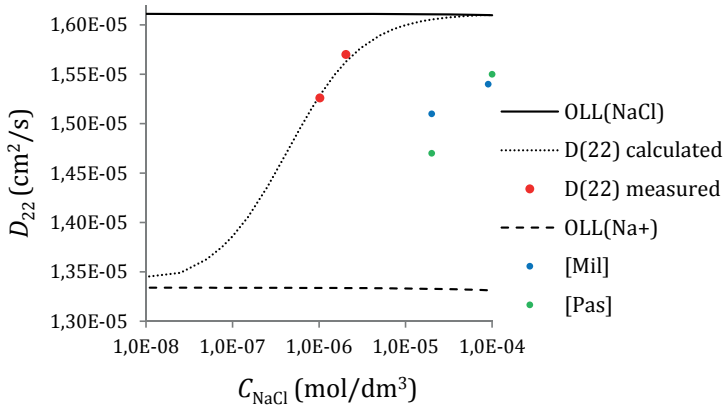

Fig. 20. Experimental and theoretical values of the diffusion coefficient D_{22} in the binary system of NaCl(2)-H_2O at very low concentration of NaCl at 298.15 ± 0.01 K. The theoretical values have been calculated by taking into account the ionization of water. The straight dashed and dotted lines describe the Onsager Limiting Laws for binary NaCl and for the tracer diffusion of Na^+ in aqueous NaCl. The literature values [Mil] and [Pas] given are taken from the publications of Mills [130] and Passiniemi [198].

6.4 Binary diffusion: NaCl-H_2O in brick media

The second part of this thesis consists of the interdiffusion measurements of salts in porous ceramic brick media. The method developed, tested and optimized is a modification of the stationary-state DM used earlier in free aqueous solutions. The measuring techniques, the apparatus as well the calculation method of the diffusion coefficient from Fick's law in a pseudo-stationary state are presented in publication II. The term pseudo-stationary state indicates that at any moment the diffusion flux is not dependent on the space coordinate inside the specimen. The time for reaching of the pseudo-stationary state was about 20-60 h depending on the specimen and the experimental conditions. In a successful one week experiment, which included 500-700 measured data points, the correlation coefficient found when fitting the experimental data to the diffusion equation was larger than 0.9995. The optimum dimensions for the ceramic sample with respect to homogeneity and time to achieve the pseudo-stationary state condition was found to be a 25 mm diameter (Φ) and thickness (L) of 10 mm with the optimum initial salt concentration of the brick sample was discovered to be that of the chamber β used in different diffusion tests. The volume of the brick specimen was 1 cm^3 and the chamber volumes were 25 cm^3 (α) and 2200 cm^3 (β).

By using this modified Diaphragm Cell Method (DM) as outlined, the interdiffusion coefficient was determined for NaCl in aqueous solutions at 25 °C in three different ceramic brick materials: new Finnish Red Brick (NRB), Old Light Brick (OLB) and Old Dark Brick (ODB), respectively. All the aqueous NaCl solutions were prepared by weighing, taking into account the appropriate buoyancy corrections. The change of the concentration in chamber α was

analyzed by monitoring the conductivity as a function of time and the cell constant was found to be 1.702 cm^{-1} after calibration with standard KCl solution.

The measured diffusion coefficients at a salt concentration of 0.05 mol/dm^3 are given as an effective diffusion coefficient, D_e, calculated with the porosity value, ε, measured for each of the specimen prior to the diffusion experiment. Porosities were determined by first using capillary saturation of water followed by sucking water through the specimen with a vacuum pump to ensure full saturation. This method for determining the porosity is also termed open or effective porosity because it measures the volume fraction of the brick specimen accessible to the diffusing ions but not the possible dead end pores or cracks (see Section 4.2). The diffusion coefficients for different the brick materials measured in publication II are presented as single measured values ± fitting errors of the least-square method and from these calculated effective diffusion coefficients ± the standard errors (Table 5). The measured mean effective porosity values are given for each brick materials.

The main result was the value determined for the diffusion coefficient of commercial ceramic NRB, which had a measured effective diffusion coefficient value in 0.05 mol/dm^3 aqueous NaCl at 25 °C of $(0.499 \pm 0.004)\times10^{-5}$ cm^2/s. The corresponding values for the porous medium of OLB and ODB were $(0.453 \pm 0.008)\times10^{-5}$ and $(0.337 \pm 0.009)\times10^{-5}$ cm^2/s, respectively. The level of precision for the measured diffusion coefficients was calculated to be $\leq \pm1\%$ for NRB, $\leq \pm2\%$ for OLD and $\leq \pm3\%$ for ODB, respectively. This decrease in the precision correlated with the increasing heterogeneity of the different brick materials being measured. The quality of the material of NRB, which is an industrially manufactured engineering brick, is more uniform and homogenous than ODB and OLB, which represent brick materials find in old masonry (see Section 4.1). Moreover, there were also a lot of OLB and ODB specimens that were found to be unsuitable due to structural defects that were detected during the diffusion measurements.

No diffusion coefficient values for OLD or ODB were found in the literature and only two diffusion measurement references for porous brick. Nielsen [75] has reported for red brick at room temperature diffusion coefficients of $(1.9 \pm 0.3)\times10^{-5}$ in 2.5 and $(2.8 \pm 0.7)\times10^{-5}$ cm^2/s in 5 mol/dm^3 NaCl, respectively. These values for aqueous NaCl are much higher than the Nernst limiting value of 1.611×10^{-5} cm^2/s at infinite dilution suggesting that there must an error in these measurements. On the other hand, Lempinen et al. [94] reported a value of 0.217×10^{-5} cm^2/s for a 0.5 mol/dm^3 NaCl solution in NRB at room temperature, which is too low compared to value measured in this work even when differences in the concentration and measuring temperature are taken into account. In contrast the diffusion coefficient values determined in this work are based on the many repetitions using systematic and controlled test arrangements.

The difference in the diffusion rate between the different brick materials measured may give rise to some questions as the ranking of the measured diffusion coefficients are not only governed by the porosity parameter alone and use of the

measured tortuosity factors (see Section 4.3) can provide a better explanation. The ranking with values ($D_e(10^5\ cm^2\ s^{-1})$; τ) at the point where $C_{NaCl} = 0.05$ mol/dm^3, t = 25 °C gives values of: NRB (0.499; 1.62), OLB (0.453; 1.75) and ODB (0.377; 2.72). The position of the OLB material in the ranking list also results from both its mean pore size (40 nm), which is significantly the smallest and the largest inner pore surface area (10.9 m^2/g) of all brick media measured. This means greater interaction with the diffusing ions and the porous medium of the brick and it is even possible that chloride ions ingress into the finest tubes is hindered as a result of the negative surface charge of electrical double layer on the brick wall. In more dilute solutions this effect is greater because of the larger effective thickness of the ionic cloud (Debye length ≈ 30 Å at 0.01 mol/dm^3 for 1:1 electrolyte). This lag in the motion of the chloride anions also results in a reduction in the drift velocity of the slower sodium cations, which is the opposite of what is observed in pure unbounded aqueous systems. The result of this phenomenon might then be seen as a smaller diffusion coefficients measured for OLD. This influence of the double layer of the porous medium as a dragging force on the diffusing ions, including the adsorption processes is far more pronounced in more porous media like concrete or rock.

Table 5. Experimental effective diffusion coefficients D_e in 10^{-5} cm^2/s units for 0.05 mol/dm^3 NaCl in different brick materials at 298.15 ± 0.05 K. The brick mean porosity ε and its typical range of variation $\Delta\varepsilon$ are also shown. The errors of the single experiment measurements (≈2×10^{-9} cm^2/s) are not shown whenever they are significantly lower than the dispersion error when evaluating the mean diffusion coefficient.

	NRB	OLB	ODB
$\varepsilon \pm \Delta\varepsilon$	0.225±0.009	0.292±0.004	0.177±0.012
single exp.	0.495	0.445±0.004	0.319±0.008
D_e	0.508	0.469±0.005	0.344±0.006
	0.510	0.446±0.003	0.348±0.007
	0.502		
	0.484		
	0.491		
	0.502		
mean D_e	0.499±0.004	0.453±0.008	0.337±0.009

6.5 Diffusion coefficients of salts in brick media. Concentration and temperature dependence

In publication III the DM presented and tested with different brick materials in aqueous NaCl in publication II was applied to the measurement of other water-soluble salts commonly found in building materials. The diffusion coefficients were also measured for KCl, $NaNO_3$, $CaCl_2$, $MgCl_2$, Na_2SO_4 and Na_2CO_3 in aqueous solutions in NRB at 25 °C and the measured effective diffusion coefficients with the fitting and standard errors are given in Table 6. The diffusion coefficients determined for different electrolytes varied between (0.271-0.544)$\times10^{-5}$ cm^2/s. As there were no literature values measured in a porous ceramic brick medium available, these measured diffusion coefficients of the different salts were compared to the corresponding value measured in the absence

of porous medium in free water at the same mean concentration and at infinite dilution. The value of the diffusion coefficients as a function of salt followed the same trend as measured in free water with only the order of magnitude changed. The value of D_e for the salts of KCl, $NaNO_3$, $CaCl_2$, $MgCl_2$ and Na_2SO_4 were 0.282-0.289 times the values measure in water. The value of D_e for the salts of NaCl and Na_2CO_3 with respect to their free water values did differ somewhat from the other salts giving values of 0.332 (maximum) and 0.271 (minimum) times the diffusion coefficient measured in water at the same concentration, respectively (see Table 1 and Fig. 6 in publication III).

The measured diffusion coefficients decreased in the order of KCl(1), NaCl(2) and $NaNO_3$(3) – the 1-1 alkali metal electrolytes, $CaCl_2$(4) and $MgCl_2$(5) – the 2-1 alkaline-earth metal electrolytes, Na_2SO_4(6) and Na_2CO_3(7) – the 1-2 bivalent anion alkali metal electrolytes. This manner of decrease of the diffusion coefficients is very similar to that observed for the decrease of reciprocal of the relative viscosities (η_0/η) of the same electrolytes under the same conditions (p,T,c). The values of η_0/η are given in Table 6 and are also depicted graphically in publication III (Fig. 7). This variation of the diffusion coefficients and viscosity is also very similar to that observed in pure electrolyte-water solutions under equivalent conditions or even at infinite dilution calculated with the Nernst-Hartley equation [116] and this can be seen by comparing Figs. 6 and 7 in publication III (**N.B.** the numbers 7 and 8 in the abscissa should be 6 and 7). Even the (η_0/η)-values of $NaNO_3$(3) and Na_2SO_4(6), that do not fall on the reciprocal curve of the relative viscosity can be explained by the corresponding rise observable in the diffusion coefficient of these electrolytes in the pure electrolyte-water solution system. Although this is not so clearly seen in the presence of the porous brick, there still seems to be a connection between the binary diffusion and the viscosity in the case of a porous medium as was also observed in the case of the absence of a porous medium between the tracer diffusion and viscosity (Section 6.1).

Table 6. Experimental effective diffusion coefficients D_e in 10^{-5} cm^2/s units of different electrolytes in NRB measured at 0.05 mol/dm^3 and 298.15 ± 0.05 K. The reciprocals of the relative viscosities of salt-water solutions are given as η_0/η, where η_0= 0.8903 mPa s is the viscosity of water at 298.15 K. The errors of the single experiment measurements (≈ 2×10^{-9} cm^2/s) are not shown because they are lower than the dispersion error when evaluating the mean diffusion coefficient.

Salt	KCl	NaCl	$NaNO_3$	$CaCl_2$	$MgCl_2$	Na_2SO_4	Na_2CO_3
η_0/η	0.9999	0.9949	0.9968	0.9835	0.9773	0.9770	0.9729
single exp.	0.541	0.495	0.426	0.322	0.306	0.290	0.266
D_e	0.547	0.508	0.424	0.319	0.304	0.290	0.274
	0.544	0.510	0.424	0.321	0.304	0.292	0.273
		0.502	0.421		0.301	0.295	0.270
		0.484			0.311	0.289	0.272
		0.491					0.268
		0.502					0.270
mean D_e	0.544	0.499	0.424	0.321	0.305	0.291	0.271
	±0.002	±0.004	±0.001	±0.001	±0.002	±0.001	±0.001

The concentration and temperature dependence of D_e in ceramic NRB were also measured and the results are given in Tables 7 and 8. The diffusion coefficients measured as a function of NaCl over the concentration range for C_{mean} (0.05-3.08) mol/dm^3 varied in between (0.415-0.499)×10^{-5} cm^2/s at 25 °C and the measured values in 0.05 mol/dm^3 NaCl as a function of temperature were (0.218-0.499)×10^{-5} cm^2/s, respectively. As there were no pre-existing literature values the free water values in the absence of a porous medium were used as a reference. The variation of D_e as a function of concentration was smaller than its variation as a function of temperature, which remained close to that of NaCl in free solution (see Figs. 8 and 9 in publication III). It means that the minimum values of the measured diffusion coefficients were in the medium range concentration region of about 0.3-1.5 mol/dm^3 both in presence and in absence of the porous medium.

Table 7. Experimental effective diffusion coefficients D_e in 10^{-5} cm^2/s units measured at different NaCl concentrations in NRB at 298.15 ± 0.05 K. The values D_a(10^{-5} cm^2/s) in free water are from Lobo et al. [216]. The errors of the single experiment measurements (≈ 2×10^{-9} cm^2/s) are not shown because they are lower than the dispersion error when evaluating the mean diffusion coefficient.

C (mol/dm^3)	0.05	0.30	1.00	3.08
single exp. D_e	0.495	0.452	0.414	0.492
	0.508	0.455	0.422	0.467
	0.510	0.457	0.409	0.486
	0.502			0.491
	0.484			0.471
	0.491			
	0.502			
mean D_e	0.499±0.004	0.454±0.001	0.415±0.004	0.481±0.006
D_a	1.504	1.473	1.482	1.559

Measured diffusion coefficients also show similar behavior as a function of temperature both presence and absence of the brick medium. The rather strong temperature dependence is due to both the decreasing viscosity of the solution and the increasing thermal kinetic energy of the molecules and ions as the temperature is increased. The temperature dependence in porous brick was $D_e = (1.67t + 7.18)\times10^{-7}$ cm^2/s ($r^2 = 0.990$), whereas the equation in the absence of porous brick was $D_a = (3.23t + 70.9)\times10^{-7}$ cm^2/s ($r^2 = 0.996$) fitted from the literature values [216]. In both equations t is the temperature value in Celsius scale. The diffusion coefficients increased linearly as a function of temperature, and the temperature coefficient in free water was larger than in porous media. This is reasonable based on the assumption that the more confined and hindered space in porous structures, might result in a reduced mean forward speed of the diffusing salt ions. Moreover, in dilute salt solutions the double layer in the porous brick grain surface will bind salt ions and water molecules limiting strongly their Brownian motion as a function of temperature [145].

It is also possible to describe the temperature dependence of the diffusion coefficients with the experimental formula $D = D_0\, e^{-E/RT}$, where E is the activation energy required for a molecule or ion to "push past" some of its neighbors and move into the next Coulombic cage or 'hole' in the solution [217]. It has been shown that the formation of holes required for this particle jump is analogous to the formation of the holes necessary for viscous flow of a liquid. Consequently, the activation energy for diffusion is similar to that for viscous flow and a similar type of formula can also be utilized for the temperature dependence of viscosity [218]. The results from these measurements and calculations showed that the viscosity, diffusion coefficient and temperature in a porous brick medium were related as expected.

Table 8. Experimental effective diffusion coefficients D_e in 10^{-5} cm^2/s units measured in 0.05 mol/dm^3 of NaCl in NRB a different temperatures. The values D_a(10^{-5} cm^2/s) in free water from Lobo et al. [216] has been interpolated to fit the measured (t,C) points. The errors of the single experiment measurements ($\approx 2\times10^{-9}$ cm^2/s) are not shown because they are lower than the dispersion error when evaluating the mean diffusion coefficient.

t (°C)	8.00	13.00	18.00	25.00
single exp.	0.223	0.277	0.369	0.495
D_e	0.214	0.284	0.359	0.508
	0.215	0.270	0.364	0.510
	0.221			0.502
				0.484
				0.491
				0.502
mean D_e	0.218±0.002	0.277±0.004	0.364±0.004	0.499±0.004
D_a	0.967	1.129	1.253	1.504

6.6 Brick and electrolyte characteristics affecting diffusion

In this section the reasons for the smaller diffusion coefficients measured in porous ceramic brick when compared to the unbound free water values are considered and an approximate numerical geometric factor describing these differences are presented. In addition, the reasons for the ranking of different salt diffusion coefficients measured in porous brick are analyzed in terms of solution viscosity and the hydrodynamic radii and hydration of the ions.

6.6.1 Influence of geometry

There has been a lot of discussion about how to relate the diffusion coefficient measured in a porous medium to the diffusion coefficient measured in the absence of a porous medium (see section 4.3). Mainly this discussion has dealt with porous matrices like crushed rock, sedimentary rocks, sandstones, bentonite clay, cementitious materials and concrete. These deliberations led Hoogschagen to define the diffusibility $Q = D_p / D_a$ where the subscripts p and a stand for presence and absence of porous medium. In this work Q can be calculated for the relation between the binary diffusion coefficients measured in fully saturated,

isotropic, fired ceramic brick compared to the corresponding values measured in free unbounded aqueous salt-water system.

In porous media factors restricting the solute diffusion are usually categorized into porosity, ε, tortuosity, τ, constrictivity factor, ξ, and the interaction coefficient, γ. The interaction of the electrolyte ions with the pore surface is not so significant for a macroporous ($\geq$ 50 nm) medium as it for microporous ($\leq$ 2 nm) or mesoporous (2 nm $\geq$ pore size $\leq$ 50 nm) media (definitions adopted by the IUPAC [219]). As a result, the interaction coefficient, γ, the for the macroporous structure of brick media can be reasonably approximated to one, taking into account pore size, the order of magnitude of the diffusing ions and Debye length (see Table V in publication II). The only potential exception to this are the diffusion coefficients measured in OLB (pore size 40 nm, pore surface area 10.9 m^2/g) where a measurable interaction between solute and pore surface could occur. In this case, any measureable interaction can be simplified by considering that the interaction coefficient γ is incorporated into the apparent tortuosity or constrictivity factor parameters. However, the idea that the interaction coefficient is negligible only applies to diffusion coefficients calculated for the stationary state measurements e.g. when the sorption-desorption equilibrium has already been reached (see Sections 4.5 and 4.6).

There are many variants for diffusibility in the literature but the commonly accepted form is: $Q = \varepsilon\, \xi\, \tau^{-2}$ [148]. As the effective diffusion coefficient D_e has previously been defined as D_p/ε, Eq. (45), the formula can be written in the form of:

$$D_e^*(c_i, t) = D_a(c_i, t)\, \frac{\xi}{\tau^2} \tag{59}$$

where D_e^* is the estimate for the measured effective diffusion coefficient D_e, D_a is the diffusion coefficient of the electrolyte in pure bulk water in the absence of porous brick, τ is the tortuosity and ξ is the constrictivity factor evaluated from the function of $\xi = f(B)$.

The mean apparent tortuosity values, τ_a, determined in this work with NaCl salt were chosen as a first approximation for the τ value used in Eq. (59) and these constant values were τ_a = 1.7 for NRB, τ_a =1.9 for OLB and τ_a = 2.9 for ODB (cf. Section 4.4). For the ξ value there were 3 different possibilities available in the form of the function, $\xi = f(B)$, firstly the function of Petersen (hyperbola of revolution) [220] , the function of Currie (sinusoidal) [221] and the function of Michaels (a series of connected cylindrical capillary models) [222]. As a more detailed knowledge of the brick matrix geometry was unavailable, the ξ value in different brick media was approximated by using median values based on results from all three functions. Parameter B is defined as the significant ratio of the maximum and minimum cross section for different pore forms and this was estimated from the pore size distributions determined by the MIP measurements made for NRB, OLB and ODB, resulting in estimated final values for the constrictivity factor of: ξ = 0.85 for NRB, ξ = 0.80 for OLB, ξ = 0.75 for ODB,

respectively [140, 150]. The experimentally measured effective diffusion coefficients D_e and the calculated estimates D_e^* from Eq. (59) as a function of different diffusion systems measured are plotted in Fig. 21.

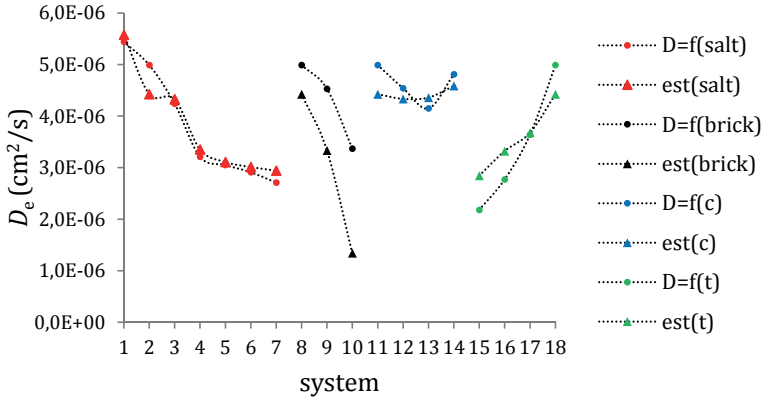

Fig. 21. The measured effective diffusion coefficients D_e compared to calculated estimates D_e^* from Eq. (59). The binary diffusion coefficients are numbered subsequently: as a function of salt: 1 (KCl), 2 (NaCl), 3 ($NaNO_3$), 4 ($CaCl_2$), 5 ($MgCl_2$), 6 (Na_2SO_4), 7 (Na_2CO_3); as a function of brick medium: 8 (NRB), 9 (OLB), 10 (ODB); as a function of concentration: 11 (C = 0.05 mol/dm^3), 12 (C = 0.30 mol/dm^3), 13 (C = 1.00 mol/dm^3), 14 (C = 3.08 mol/dm^3) and as a function of temperature: 15 (t = 8 °C), 16 (t = 13 °C), 17 (t = 8 °C), 18 (t = 25 °C).

As it can be seen in Fig. 21, the estimates calculated from Eq. (59) showed some variation between the measurements. For example, the term $\xi\tau_a^{-2}$ in Eq. (59) explains the relation D_e/D_{abs} in the case of different salt quite reasonably (in green) and it is only the estimates for D_e^*(NaCl) and $D_e^*(Na_2CO_3)$ that are either too low or high. However, by using an alternative value for $\tau(C_{NaCl}$ = 0.05 mol/dm^3) = 1.62 (determined from the logarithmic regression fit in Fig. 11) the resulting estimate D_e^*(NaCl) = 0.487 × 10^{-5} cm^2/s would correlated better with the experimentally measured value of D_e(NaCl) = 0.499 × 10^{-5} cm^2/s. Regardless of the moderate estimates for the different brick media, the estimates for the variations in concentration (in blue) and temperature (in red) were not precise enough. A more accurate material parameter should be found that is not a static constant but dependent at least on concentration and temperature in order to explain the partly contradictory differences in the relation of D_e/D_{abs} discovered here.

The consistent differences between the measured and estimated diffusion coefficients for the different brick materials (in brown) indicate a systematic error in the $\xi\tau_a^{-2}$ term. The τ_a values of 1.60, 1.63 and 1.83 would provide a perfect fit with the ξ values used for the different brick media measured however, particularly in the case of NRB, the value of 1.60 resulted in a poor fitting with any other salt than NaCl. The best correlation with the measured effective diffusion coefficients were finally achieved with the τ_a values of 1.71 for NRB,

1.68 for OLB and 1.83 for ODB, which in turn gave $\xi\tau_a^{-2}$ values of 0.291 for NRB, 0.283 for OLB and 0.224 for ODB. The fitting errors with the material parameters given are plotted according to the binary diffusion system studied in Fig. 22. As can be seen from the plot the chosen parameters estimated the measured diffusion coefficients in porous brick, at best, with an error of ±3% for half of the experimental diffusion coefficients and at worst with an error of 28%. The estimates are poorer when the diffusion coefficients as a function of temperature are considered as the fitting errors are on average ±7%. In the absence of any literature data related to brick media, the material parameter $\xi\tau_a^{-2}$ values of 0.22-0.29 determined here were compared to those of Olin et al. [154] who measured in a crushed rock medium and found corresponding values of 0.01-0.1. This difference is understandable and result from smaller geometrical factors associated with the more porous and tortuous crushed rock.

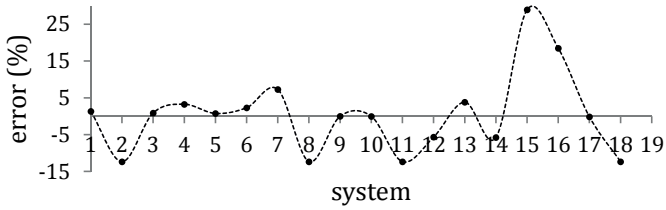

Fig. 22. Fitting errors for the estimates of D_e^* compared to the measured effective diffusion coefficients D_e. The system labels 1-19 correspond to different salts 1(KCl), 2(NaCl), 3($NaNO_3$), 4($CaCl_2$), 5($MgCl_2$), 6(Na_2SO_4), 7(Na_2CO_3); different brick media 8(NRB), 9(OLB), 10(ODB); different concentrations: 11(c = 0.05 mol/dm^3), 12(c = 0.30 mol/dm^3), 13(c = 1.00 mol/dm^3), 14(c = 3.08 mol/dm^3) and different temperatures: 15(t = 8°C), 16(t = 13°C), 17(t = 18°C), 18(t = 25°C). The material parameters $\xi\tau_a^{-2}$ used in the fittings were 0.291 (NRB), 0.283 (OLB) and 0.224 (ODB).

From the results it still seems that a universal constant material parameter or geometrical factor that explains all the differences in interdiffusion coefficients between porous brick matrix and unbounded bulk water is unattainable. Moreover, this issue would require a more detailed investigation and understanding of the pore morphology in brick media to be solved satisfactorily. The work detailed here demonstrates that the $\xi\tau_a^{-2}$ term is the material parameter, which gives a useful first approximation for the salt diffusion coefficient in the porous brick media studied. The only drawback is that the diffusion coefficient in pure aqueous solution is required for the calculation of diffusion coefficient estimate. Still the most accurate way to determine the diffusion coefficient in porous media is through time consuming experimentation.

6.6.2 Influence of ion hydration

The measured effective diffusion coefficients were shown to decrease with the decreasing reciprocals of the relative viscosity (η_0/η) - see Table 6 - meaning that diffusion coefficients are inversely related to the viscosity. This is similar in nature to the Stokes-Einstein formula for the solid spherical particle diffusing

through an inert Newtonian fluid [223] and this equation can be modified for the case of binary salt diffusion in a porous medium to give:

$$D = \frac{\varepsilon kT}{6\pi\eta r_a} \tag{60}$$

where ε is the porosity of the medium, k is the Boltzmann constant, η is the viscosity of the aqueous salt solution in the porous medium and r_{a} the apparent radius of the diffusing binary salt.

It clear from Eq. (60) that the ranking between the measured diffusion coefficients of different salts in porous brick does not only rely on the different viscosities of the aqueous salt solutions, as the viscosities for the salt solutions were between (0.89-0.92)×10^{-3} N s/m^2 and the measured diffusion coefficients were between (0.27-0.54)×10^{-5} cm^2/s. Conversely, the differences between the measured D_e are not based solely on the differences between the actual atomic or hydrodynamic crystal ionic radii of individual atoms composing the salts. This situation can change however, when the solvation effects of the ions are taken into account as the hydrated ions are larger than the continuous layer of surrounding solvent water molecules. The hydration reduces the amount of free water molecules available thereby reducing the effective water concentration and increasing the effective salt concentration in solution. It is known that ion hydration usually comprises of several layers with the innermost water layer being the most immobile. As the hydration of ions most certainly increases the radius of ions involved in diffusion this effect should be included into the radius of r_{a} in Eq. (60).

For ternary tracer diffusion or interdiffusion of neutral molecule this hydration can be easily account for as there is only one diffusing ionic species or component. In contrast, for binary salt diffusion of electrolyte the diffusion potential between cation and anion forces both the cation and anion to diffuse at the same speed with the associated hydrated water meaning that the radius of r_a must include both ions and all the hydrated water. As a result the apparent hydrodynamic radius from Eq. (60) needs to be divided by the radii of both the water molecules and the hydrated salt ions. The main idea is to equalize the total volume obtained from the apparent hydrodynamic radius with the sums of volumes of the individual ions in stoichiometric relation and all the hydrated water molecules. By using this assumption an apparent hydration number can be calculated with known solution viscosity and effective diffusion coefficient. The apparent hydration number, h_{a}, for the salt given can then be solved from the following derived equation of:

$$h_a = r_{H_2O}^{-3}\left[\left(\frac{kT}{6\pi\eta D_e}\right)^3 - (xr_{cation}^3 + yr_{anion}^3)\right] \tag{61}$$

where $r_{\mathrm{H_2O}}$, r_{cation}, r_{anion}, x, y and D_{e} are the radius of water molecule in hydration, the radii of the unhydrated ions and their stoichiometric coefficients, respectively and the effective diffusion coefficient.

Due to the great variation in data for the hydrated ionic radii the bare ionic radii were selected as the degree of hydration of an ion depends primarily on the radius of the bare ions and the charge, which are taken into account through the stoichiometry of the salt. In order to interpret volumes of solvated ions in solution, it is usually also necessary to have values of the respective intrinsic volumes or corresponding radii of the ions in an unsolvated state [224]. The numerical values of the ion radius vary depending on how they are calculated e.g. from the wavefunctions, lattice spacings or crystal structures of various salts. In the case of monatomic inorganic ions, at least four scales of ionic radii are available: the Pauling, the Gourary, the Adrian, and the Goldschmidt scales [224]. In Eq. (61) the Pauling ionic radii was used [134], however for the unsymmetrical polyatomic ions, like SO_4^{2-} and CO_3^{2-} complete and reliable crystal ionic radii are lacking [224]. Hence the missing values were calculated by assuming that the ions are spherical and the Stokes-Einstein equation at infinite dilution applies. Very similar values for the ionic radii can also be calculated from the tabulated molar volumes of these ions in water at 25 °C [225]. Ultimately values of 2.3 and 2.2 Å were chosen for the polyatomic ions SO_4^{2-} and CO_3^{2-} and 3.3 Å for the hydrated water molecule radius [226]. For the different salts investigated the calculated change in apparent hydration number, h_a, and total apparent radii, r_{salt}, with solution viscosities are plotted in Fig. 23. In can be observed that as the apparent radius of the salts goes changes from about 4.5 to 8.8 Å, the apparent hydration numbers goes from 2.3 to 18.6, respectively. This means that the least hydrated salt was KCl with the apparent hydration number of h_a = 2.3, followed by NaCl (h_a = 3.1) and $NaNO_3$ (h_a = 5.1). After these 1-1 electrolytes came the divalent cation salts $CaCl_2$ (h_a = 11.4) and $MgCl_2$ (h_a = 13.2). The most hydrated were clearly the polyatomic salts Na_2SO_4 and Na_2CO_3 with apparent hydration numbers of 15.1 and 18.6, respectively.

In view of all these assumptions the apparent hydration numbers for porous salt diffusion systems calculated appear to be reasonable, although there is considerable variation in the ion hydration number within literature [129, 227]. For example, the strongly hydrated divalent Ca^{2+} and Mg^{2+} ions have given literature values between 6-10 and 6-14, whilst the more weakly hydrated Cl^- ions are given the value of 2. This means that in the binary diffusion case the mean literature values for the salts $CaCl_2$ and $MgCl_2$ have the following stoichiometric coefficients $1 \times 8 + 2 \times 2 = 12$ and $1 \times 10 + 2 \times 2 = 14$, which show a good correlation when compared to the values of 11.4 and 13.2 calculated here.

In spite of the correlation for both the divalent cation and anion salts, the hydration numbers determined for KCl and NaCl are too small when compared to the typical literature values of 3.5-8.4 for Na^+ ion and 3.0-5.4 to K^+ ion. However, these literature values are measured for ions rather than salts and not in the presence of porous brick medium. Moreover the principal thermodynamic variables of solution concentration, temperature and pressure all have influence to the actual hydration number [227].

Although the calculated apparent hydration numbers for the whole salt displayed in Fig. 23 are not absolute they offer an explanation for the measured effective diffusion coefficients ranking. As before, better knowledge of the system in terms of the real hydrodynamic radii of the hydrated ions and the water molecule coupled to a parameter that adjusts to reflect changes in the value of the apparent hydration number would improve correlation with the experimental results. Nonetheless, the increasing salt ion hydration reduces ion movement as the total burden required to be transported by the salt ions increases, resulting in changes to diffusivity in the measured porous salt diffusion system. The significantly larger diameters of the hydrated ions compared to the bare ions may, in part, also explain the relatively small diffusion coefficients measured in smaller pore size porous media like OLB.

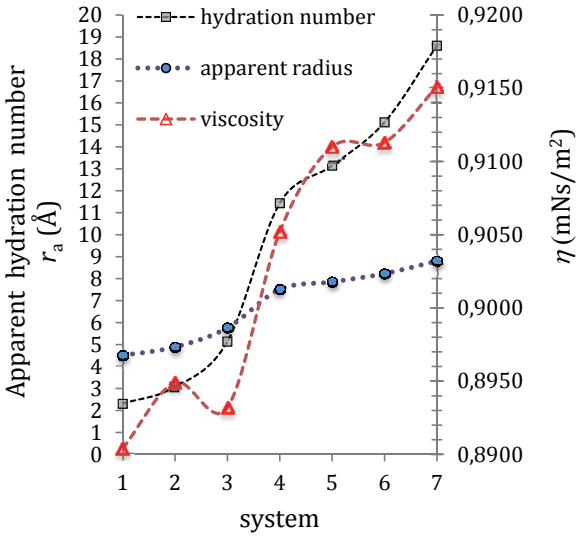

Fig. 23. The estimated total radius of the diffusing binary salt, the viscosity of the solution and the evaluated apparent hydration number, h_a, of the salt. The binary diffusion systems are numbered accordingly to the salt: 1 (KCl), 2 (NaCl), 3 ($NaNO_3$), 4 ($CaCl_2$), 5 ($MgCl_2$), 6 (Na_2SO_4) and 7 (Na_2CO_3).

A similar increase in the sequence of the diffusion coefficients was also reported for porous sodium bentonite [156] and for montmorillonite clay [228, 229], where there is also a clear correlation between the unhydrated ionic radius and apparent diffusivity observed - although the apparent diffusion coefficient measured for the Na^+ ion was still greater than that measured for K^+ ion. Partly the same trend has been observed for salt diffusion coefficients measured in concrete, whereas in this work the effective binary diffusion coefficient measured for KCl was larger than that measured for NaCl despite having the same Cl^- counter ion. The reason for the contradictory ranking of, $D_{NaCl} < D_{KCl} < D_{CaCl_2}$, where the most hydrated salt had the largest diffusion coefficient, reported in concrete could result from chloride binding in the concrete matrix and the more complex, non-binary diffusion processes reported [161].

6.7 Quasi-steady diffusion through brick media

In publication IV the diffusion of salt in a fully saturated brick is studied under isothermal conditions by means of DM and mathematical methods. When a sample is completely saturated, the convective transport can be neglected. The mathematical methods involved analytical and numerical calculations of the diffusion process in combination with the measured data. The work outlined in publications II and III, and also in references [95-100], was extended by developing an analytical solution which gives the temporary salt concentration in the diffusion chamber under examination.

The brick material separates two chambers of volumes V_α and V_β containing NaCl solutions of concentrations $c_\alpha(t)$ and $c_\beta(t)$. By following the concentration change in chamber α, the diffusion coefficient of the salt in the porous brick can be determined. The brick material has thickness L, geometric area A, and porosity ε. The mass conservation requires that (see section 4.1 in [112]):

$$J_{brick}A = V_\alpha \frac{dc_\alpha}{dt} = -V_\beta \frac{dc_\beta}{dt} \tag{62}$$

Under quasi-steady-state conditions, the flux density J_{brick}, defined over the total geometrical brick area A, can be assumed to be independent of position. Glass et al. [93] have concluded that the estimation error of D can be neglected if the time required to reach the quasi-steady-state conditions is less than 20% of the total measurement duration time. The lag time t_0 represents the lower boundary of the time required to achieve the quasi-steady-state condition [90]. For all of the measurements evaluated, the measurement duration time was longer than $5t_0$ - typically $10t_0$ - and in some experiments even $100t_0$. Therefore the estimation error of D could be neglected. Furthermore all the analytical and numerical validation calculations were applied only after the $t > t_0$ condition was true.

The diffusion equation:

$$J_{brick}A = -\varepsilon AD \frac{\partial c}{\partial x} \tag{63}$$

can be integrated with respect to position to obtain $c(x)$. If $x = 0$ denotes the brick surface in contact with chamber α, and $x = L$ the surface in contact with chamber β, the boundary conditions are $c(0) = c_\alpha(t)$ and $c(L) = c_\beta$ (see Fig. 1 in publication IV). If the volume ratio of the chambers V_β/V_α is large enough, the concentration changes in chamber β can be neglected, and c_β can be considered independent of time. In our experiments this condition was satisfied because $V_\beta/V_\alpha > 93$.

The initial salt concentration in chamber α is $c_{\alpha 0}$, and its time variation is given by the following analytical solution derived in publication IV:

$$c_\alpha = c_\beta - \left(c_{\alpha 0} - c_\beta\right) e^{-t/d} \tag{64}$$

where

$$d = \frac{V_\alpha L}{\varepsilon A D} + \frac{L^2}{2D} \tag{65}$$

is the relaxation time.

The measurement data was divided into three groups and compared with the analytical and numerical data - these groups are summarized in publication IV (Tables I-III) for different specimen and chamber properties. In the simulation the brick specimen, the brick and salt type, the initial salt concentration in chamber α and in the brick sample were varied. The results of groups II and III especially demonstrate that the theories developed for NaCl diffusion in NRB are applicable to other types of salts and bricks. The simulation results are also showed graphically in publication IV (Figs. 2-4). It is worth noting that the experimental period for sample 7 (in Fig. 4) is over 3 months when compared to regular experiments that had durations of about one week. As it can be seen the figures a good correlation between the measured data and the analytical and numerical solutions was achieved demonstrating the accuracy of the proposal analytical solution.

The last figure in publication IV outlines the concentration profiles of NaCl in NRB (Fig. 5). The diffusion time required for the linear concentration profile in brick sample 1 was simulated to be over 10 h. The delay results from the ceramic brick medium salt binding effect, which gives way to a linear concentration profile after about 10 h. Hence in the quasi-steady-state the possible sorption places are filled, the sorption-desorption cycles are in equilibrium and the salt flow is controlled solely by the concentration gradient of the salt. This timescale presented for the linear concentration profile inside the porous medium was validated only for NRB sample 1 with dimensions of L = 10.4 mm and Φ = 25 mm and under the stated conditions. The required time period for the linear profile will change with ambient conditions and dimensions of the specimen. For example, in closed capillary tests the brick specimens were had dimensions of $L \approx$ 40 mm and $\Phi \approx$ 12 mm that result in a larger binding effect. This binding effect should also be taken into account in the diffusion coefficients calculated from the non-steady-state method, especially in comparison to the diffusion coefficients measured with steady-state method in publications II–V. This sorption effect is discussed further in Section 6.10.

The analytical solution of Eq. (64) gave the temporary salt concentration in the monitored diffusion chamber α, which were compared to the measured data under different environmental conditions. In publication V the diffusion of salt in fully saturated brick is studied as a function of salt nature, concentration and temperature by means of DM and mathematical methods. The analyses performed in publication IV were extended to include more measurement data under varying

test conditions in order to simulate the real environmental circumstances. (**N.B.** In Eq. (8) of publication V there should be minus sign between the two first bracket expressions instead of the plus sign.) It is worth noting that the data presented have been verified by numerous experiments and simulations, which have not been shown in publications IV and V due to space limitations although some of the earlier measurement data and model development by the author are presented in references [99, 100].

The measurements presented in publication V were divided into three groups in order to see the validation and analysis results of the measured D. In group I the variation parameter is the temperature and the specimen properties, measurements and simulations are given in publication V (Table 2 and Fig. 2). As can be seen, the ambient temperature also has a big influence on the diffusion coefficient in a porous brick medium. The equation for the temperature dependence of the binary diffusion coefficient of NaCl in the temperature region between 8 and 25 °C was statistically found to be $D_e = (0.03252\,t^2 + 0.604\,t + 14.7) \times 10^{-7}$ cm^2/s, were t denotes the temperature value in the Celsius scale. This second order fitting gives values that are very similar to the linear fitting of $D_e = (1.67\,t + 7.18) \times 10^{-7}$ cm^2/s derived in publication III.

In group II the different salt types commonly found in brick structures were investigated and the diffusion coefficients were validated in aqueous solutions of KCl, $NaNO_3$, $CaCl_2$, $MgCl_2$, Na_2SO_4 and Na_2CO_3 (in addition to NaCl) in NRB at 25 °C. The specimen properties, measurements and simulations are given in Tables 1 and 3 and Fig. 4 in publication V (**N.B.** the figures in Table 1 had shifted from their initial place during publication) and Table 6 in this thesis.

In the last group (III) the solution concentration was varied and the sample and chamber properties, measurements and simulations are given in Table 4 and Fig. 6 in publication V (**N.B.** the figures of D, V_α and V_β in Table 4 were erroneously switched during publication). The concentration dependence of the diffusion coefficients of NaCl was measured in NRB at 25 °C and it was found that the relation between the integral binary diffusion coefficient and concentration in NRB can be given with the second order equation of $D_e = (3.912C^2 - 12.61C + 49.84) \times 10^{-7}$ where C is the concentration value in mol/dm^3 units. The fitting was performed in the mean concentration region between (0.05-3.08) mol/dm^3. For a comparison of the influences of the different salts, temperature and concentration of the ambient solution to the salt distribution in brick medium a comparable concentration profile was constructed for the same specimen and at the same time moment (see Figs. 3, 5 and 7 in publication V). By comparing the profiles it can be observed that the effect of temperature is the most important, followed by the effect of different salts. The influence of the concentration of the same salt solution is approximately three times smaller on the diffusion coefficient in porous ceramic brick meaning that as a first approximation the effect of the concentration dependence of the diffusion coefficient of the salt can be ignored.

For diaphragm or diffusion cells some reservations can be expressed as the techniques can be subject to hydrostatic effects or osmotic pressures the existence of which would have a marked impact on the results from the diffusion measurements. The presence of these osmotic pressures or hydrostatic effects all depend on the experimental arrangements and the materials used in the experiments. In this work, the hydrostatic pressure difference generated by different solution concentrations and also the different densities in both chambers was equalized with different heights of the solution levels. The hydrostatic equilibrium was quickly reached after about 20 min, which is much shorter than that required to achieve the quasi-steady-state condition (at least 10 h). The additional concern of osmotic pressure build up over the porous brick medium also does not occur as all the brick materials investigated - NRB, OLB and ODB - were tested and found to be very permeable for both water and salt prior to diffusion experiments. Moreover, no salt impermeability was discovered a fact that could also be deduced from their pore size distributions when compared to the membrane materials used in osmotic studies [219].

6.8 Integral and differential interdiffusion of ^{22}NaCl in brick media

In the third and unpublished part of this thesis, the CCM was for the first time applied to the measurement of the diffusion coefficient in a porous medium. The apparatus and the method were adapted for use in the porous brick medium as well as the calculation of the results of the differential and integral interdiffusion and tracer diffusion coefficients of ^{22}NaCl that are presented in Chapter 5.

When measuring the integral interdiffusion coefficient, the upper half of the brick cylinder was filled at the beginning of the experiment with pure water ($C_1 = 0$) and the lower half of the brick cylinder with NaCl solution of concentration C_2 mixed with a very small amount of radioactive ^{22}NaCl tracer. These two different solutions were in total internal equilibrium prior to the filling of the brick cylinder and the start of the experiment. The mean concentration $C_{\text{mean}} = 0.5\, C_2$ of NaCl in the experiments was varied between 0.0005 to 3.08 mol/dm^3.

The integral binary diffusion coefficients obtained with this non-stationary-state CCM are known as integral apparent interdiffusion coefficients, D^i_{app}, (see Section 4.6). By comparing their measured values (Table 9) to the effective interdiffusion coefficients, D_e, measured with the stationary-state DM an interesting observation can be made. These measured values diverge from one another the more dilute the electrolyte concentration in the brick pores. As the values of D_e below a salt concentration 0.05 mol/dm^3 could not be measured accurately enough with the DM, the differences in dilute concentration of 5×10^{-4} mol/dm^3 were unable to be compared. By extrapolating the trends of the diffusion coefficients of D_e and D^i_{app}, their difference ($D_e - D^i_{\text{app}}$) would still continue to increase below 0.05 mol/dm^3. It is worth noting that the determination errors for the single experiments increased even by an order of magnitude in this dilute 5×10^{-4} mol/dm^3 concentration region as can be seen from Table 9. This deviation

probably results from the big sorption effect in relation to the small diffusion flow and to a lesser extent specimen inhomogeneity.

Both of these integral diffusion coefficients, D^i_{app} and D_e, describe the binary diffusion of NaCl inside the porous NRB at under the same conditions. By taken the binding of part of the salt flux into account, an explanation for this difference between the diffusion coefficients could be obtained and this is achieved by the adsorption capacity S (Section 6.10).

Table 9. Experimental integral apparent interdiffusion coefficients D^i_{app} in 10^{-5} cm^2/s units of NaCl in NRB, calculated with the linear least-square method in the mean concentration region of (0.0005-3.08) mol/dm^3 at 298.15 ± 0.01 K. The errors of the single experiment measurements (ca. 3×10^{-9} cm^2/s) are not shown because they are lower than the dispersion error when evaluating the mean diffusion coefficient.

C (mol/dm^3)	5.00×10^{-4}	0.0500	0.300	1.00	3.08
single exp. D^i_{app}	0.201±0.002	0.330	0.376	0.393	0.465
	0.197±0.004	0.336	0.368	0.374	0.473
	0.199±0.001	0.338	0.379	0.378	0.466
	0.204±0.002	0.352	0.361	0.394	0.498
	0.211±0.001	0.336		0.377	0.462
		0.347			0.451
		0.336			
		0.350			
		0.352			
mean D^i_{app}	0.202±0.002	0.342±0.003	0.371±0.004	0.388±0.006	0.469±0.007

Table 10. Experimental differential apparent interdiffusion coefficients D^d_{app} in 10^{-5} cm^2/s units of NaCl in NRB, calculated with the linear least-square method for mean concentrations, $C_{\mathrm{mean}} = (C_1+C_2)/2$, between 0.05 and 3.08 mol/dm^3 at 298.15 ± 0.01 K. The errors of the single experiment measurements (2×10^{-9} cm^2/s) are not shown because they are lower than the dispersion error when evaluating the mean diffusion coefficient.

C_{mean} (mol/dm^3)	0.050	0.30	1.00	3.08
$C_2 - C_1$(mol/dm^3)	0.020	0.20	0.60	1.56
D^d_{app} single exp.	0.290	0.326	0.347	0.324
	0.297	0.318	0.349	0.319
	0.291	0.325	0.360	0.315
			0.364	0.321
D^d_{app} mean	0.293±0.002	0.323±0.003	0.355±0.004	0.320±0.002

When measuring the differential interdiffusion coefficient, the upper half of the brick cylinder was filled at the beginning of the experiment with inactive NaCl solution with concentration C_1 and the lower half of the brick cylinder with NaCl solution of concentration C_2 mixed with a very small amount of radioactive ^{22}NaCl tracer. These two different solutions were in total internal equilibrium prior to filling of the brick cylinder and the start of the experiment. The mean NaCl concentration $C_{\mathrm{mean}} = 0.5(C_2 + C_1)$ was varied between 0.05 to 3.08 mol/dm^3. The differential binary diffusion coefficients obtained with this

non-stationary-state CCM are termed differential apparent interdiffusion coefficients, D^{d}_{app} and the values of these measured diffusion coefficients are given in Table 10.

As there were no literature values available, these D^{d}_{app} values were compared to the measured D^{i}_{app} values. However, due to the smaller (~3-5 times) concentration gradient for the differential diffusion process when compared to the integral diffusion process the measured coefficients differ one another. The separation varies as a function of concentration and is at minimum approximately when the mean concentration is 1 mol/dm^3. As a result of the sorption effect the D^{d}_{app} coefficients decreased strongly with decreasing salt concentration as was also observed with the D^{i}_{app} coefficients measured. In addition, reliable values of D^{d}_{app} for concentrations lower than 0.05 mol/dm^3 could not be measured, probably as a result of a too small concentration gradient and the sorption phenomena. All the binary diffusion coefficients of NaCl in brick at 25 °C results determined with the closed capillary and diaphragm methods are plotted in Fig. 24 as a function of concentration to illustrate the differences between these measured coefficients. Moreover, the same figure also includes the interdiffusion coefficients measured in the absence of a porous medium [130, 216].

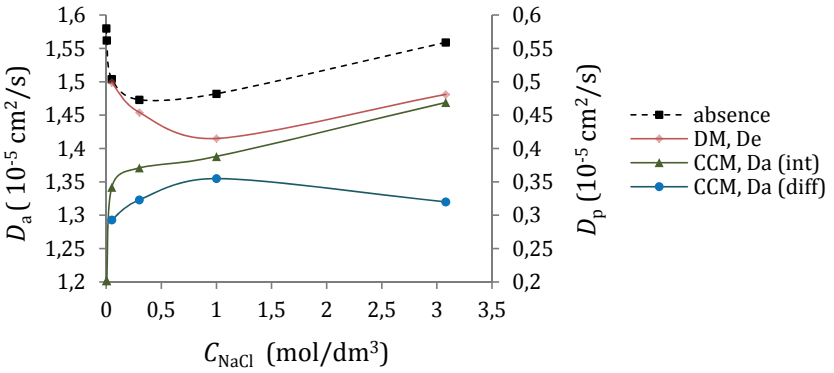

Fig. 24. Experimental interdiffusion coefficients of the binary NaCl-H_2O system in a porous brick medium and in the absence of a porous medium as a function of NaCl concentration at 298.15 (±0.01) K. There are three set of data in the presence of brick medium, (right axis, D_p). The DM,De data are effective diffusion coefficients measured with the stationary state DM. The Da(int) and Da(diff) data are apparent integral of D^{i}_{app} and the apparent differential D^{d}_{app} values measured with the non-stationary-state CCM. The D_a values (left axis), i.e., in the absence of porous medium, were taken from literature [130, 216].

From the binary values, measured below a concentration of 10^{-4} mol/dm^3, available in the literature, it is evident that water ionization has an effect [130] as the values are smaller than those calculated by the Onsager-Fuoss equation [11]. The trend of the measured diffusion coefficients without the sorption effect seems to be very similar as the values increase with decreasing concentration both in the presence of porous brick (D_e) and in the absence of a porous medium. These

differences between the diffusion coefficients of D^{i}_{app} and D^{d}_{app} result primarily from their deviation from D_e in the dilute concentration region caused by the binding effect of the brick medium. Both of the plotted integral interdiffusion coefficients D_e and D^{i}_{app} are considered in more detail in Section 6.10.

6.9 Tracer diffusion: ^{22}NaCl-NaCl-H_2O in brick media

As with the differential interdiffusion coefficient measurements determination of the tracer diffusion coefficient involved filling the upper half of the brick cylinder with the inactive solution of concentration C and the lower half with the radioactive solution of the same concentration. As the concentration of the supporting NaCl electrolyte was exactly the same in both sides of the brick cylinder the only gradient was that of the ^{22}NaCl added to the lower solution and the amount of tracer was small enough so as not to influence to the total concentration of the NaCl, for example, in the 0.005 mol/dm^3 supporting electrolyte - most dilute used - the amount of pure ^{22}NaCl tracer was calculated to be 0.0104%. The experimental ternary tracer diffusion system was NaCl(1)-^{22}NaCl(2)-H_2O(0). The tracer diffusion coefficients obtained with this non-stationary-state CCM are known as apparent tracer diffusion coefficients, D^{t}_{app}. The measured diffusion coefficients are given in Table 11 and plotted with the tracer diffusion coefficients measured in an unbounded aqueous solution as a function of concentration in Fig. 25.

Table 11. Experimental apparent tracer diffusion coefficients D^{t}_{app} of ^{22}NaCl in NRB, calculated with the linear least-square method, at different concentrations C of the NaCl supporting electrolyte at 298.15 ± 0.01 K. The literature values D_{a}(10^{-5} cm^2/s) correspond to Na^+ ions in free water [19]. The errors of the single experiment measurements are not shown when they are smaller than 5×10^{-9} cm^2/s because the dispersion error determines the uncertainty of the mean diffusion coefficient.

C (mol/dm^3)	0.00500	0.0500	0.300	1.00	3.08
single exp. D^{t}_{app}	0.247±0.002	0.306	0.312	0.312	0.268±0.001
	0.255±0.001	0.299	0.302	0.314	0.276±0.002
	0.249±0.001	0.305	0.303	0.295	0.277±0.002
	0.248±0.002	0.297	0.310	0.310	0.286±0.002
	0.240±0.023	0.308		0.308	0.266±0.002
	0.235±0.001				
mean D^{t}_{app}	0.246±0.003	0.303±0.002	0.307±0.002	0.308±0.003	0.275±0.004
D_{a}	1.317	1.291	1.271	1.231	1.023

As can be seen, the trend in the measured tracer diffusion coefficients is similar to that measured in the absence of porous medium at concentrations between 0.3 - 3.08 mol/dm^3, with only the absolute values smaller in the presence of the brick medium due to the hindered movement of Na^+ ions inside the brick matrix. In the dilute region in the absence of porous brick, values of $D_{\mathrm{Na+}}$ increase toward the Onsager limiting law value of 1.334×10^{-5} cm^2/s with decreasing salt concentration. In contrast, in the presence of porous brick, the values of D^{t}_{app},

decreases strongly because of the sorption effects with decreasing salt concentration. As the concentration gradient, $\nabla C\left({}^{22}NaCl\right)$, in the case of tracer diffusion is the same the only reason for increasing deviation with decreasing salt concentration as measured between tracer diffusion coefficients in absence and presence of porous brick is the salt binding effect of the pore walls. The relation D_{Na^+}/D_a^t increases from 3.72 to 5.35 when the concentration decreases from 3.08 to 5×10^{-4} mol/dm^3.

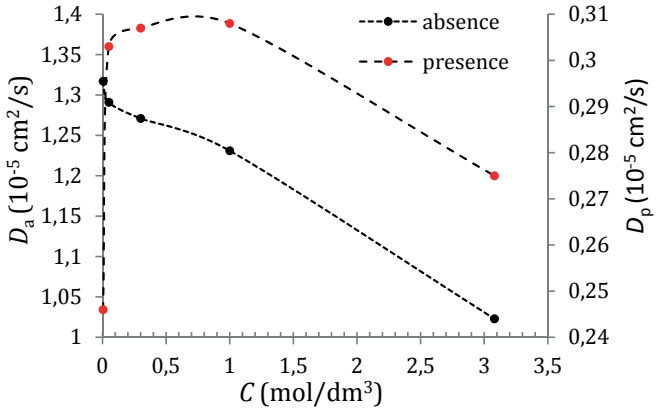

Fig. 25. Experimental tracer diffusion coefficients D_p of ^{22}NaCl in presence of porous brick as a function of the supporting NaCl electrolyte concentration at 298.15 ± 0.01 K. The values in absence of porous brick D_a were taken from literature [19].

6.10 Adsorption capacity and adsorption isotherm

The measurement of the amount of salt sorbed on the pore walls from the pore solution inside a macroscopic porous medium is a complicated task as it is not as simple as crushing the exposed brick and dissolving the sorbed salt into solution for subsequent analysis. It should be possible, however, to analyze the surface and solution concentrations inside the brick medium without breaking the native structure and morphology in order to make concentration analyses under real equilibrium conditions. One possible method is to force out the fully saturated pore solution from the brick specimen under high pressure and analyze the concentration (cf. the initial salt concentration) after the equilibrium has been reached. The drawbacks of this method include the presence of dead end pores and closed cracks as well as the change of the sorption desorption balance inside the brick during the squeezing process. This problem of accurate sorption analyses was beyond the scope of the work outlined here, however, in Section 4.4 some preliminary analyses were still performed in order to aid the interpretation of the diffusion measurements made by different methods. The results of these experiments, both with residual radioactivity and SEM+EDS techniques, indicated an average of 2-3% sorption of NaCl on the surface of the NRB-specimen.

It has also been shown in Section 4.6 that the sorption processes discovered do have an influence on the diffusion coefficients measured using non-steady-state methods. Sorption occurs on the pore walls when salt penetrate from the high concentration side to the low or zero concentration side in the porous medium, therefore, the effect of sorption must be taken into account when studying NaCl diffusion in brick with the CCM. The binding forces and mechanisms retarding the observed salt diffusion in brick media have not been investigated but probably include physical adsorption, chemisorption or absorption. Nevertheless, based on the negative surface charge densities, q = −(4.43-3.75) mC/m^2, with the pore-size area of (0.2-1.0) μm of NRB [140, 150] the physical van der Waals adsorption of Na^+ counter-ions on the NRB-surface is more likely to be the main sorption process and this is accompanied by Cl^- adsorption in order to preserve the electroneutrality. In this work, all of the binding effects of salt on the porous brick are considered as sorption as the salt binding and the attainment of the sorption equilibrium are assumed to be fast processes that are reached immediately as the diffusion proceeds.

By comparing the diffusion coefficients measured under the same conditions with the non-steady-state CCM and with the stationary DM the influence of the sorption can be evaluated. It was shown that $D_{\mathrm{app}} \propto D_{\mathrm{e}}$ with the relation derived in Eq. (51) and this relation can also be presented in the form:

$$S = \frac{D_e}{D_{app}^i} - 1 \tag{66}$$

where S is the adsorption capacity, Eq. (48), and D_{e} and $D_{\mathrm{app}}^{\mathrm{i}}$ stand for the effective integral diffusion coefficient measured with stationary-state methods and the apparent integral diffusion coefficient measured with non-stationary-state methods, respectively.

Since D_{e} and D_{app}^{i} have been measured for different electrolyte concentrations, the adsorption capacity can be determined from Eq. (66) and Tables 7 and 9 and fitted with the least-squares method to the following exponential form:

$$S = 0.0675\ {C_{mean}}^{-0.708} \tag{67}$$

where C_{mean} is the total mean concentration inside the diffusion system; the correlation coefficient for the fitting was 0.980. This equation shows that the adsorption capacity of salt decreases strongly with increasing salt concentration. It is also possible to use the experimental data to find the adsorption capacity as a function of the free salt concentration:

$$S = 0.063\ {C_f}^{-0.65} \quad . \tag{67}$$

The correlation coefficient of this new fitting was 0.979. The free NaCl was evaluated from Eq. (66) and the relation $C_{\mathrm{mean}} = C_{\mathrm{s}} + C_{\mathrm{f}}$, Eq. (47). The adsorption isotherm of NaCl in NRB at 25 °C can be obtained from the definition

of the adsorption capacity, $S = \mathrm{d}C_\mathrm{s}/\mathrm{d}C_\mathrm{f}$, Eq. (48), by integration of Eq. (67) with respect to C_f and the result is:

$$C_s = 0.18\, {C_f}^{0.35}. \tag{68}$$

This adsorption isotherm has a similar form to the Freundlich isotherm. The adsorption equation of Freundlich - in the form of $x_\mathrm{ads} = \alpha c^{\beta}$, where the x_ads is the mass or amount of solute adsorbed per unit mass of the adsorbent - was originally proposed on a purely empirical basis and in general no physical meaning can therefore be drawn from the coefficients α and β [153]. When describing the process of sorption inside the macroscopic brick medium the concentration C_s in Eq. (68) is a more convenient quantity than x_ads - usually used in the case of particle or powder adsorption - as the morphology rather than mass of the brick influences to the amount of sorption. The morphology of the brick specimen (ε, τ, ξ) is already taken into account in the sorption capacity function Eq. (66), from where the sorption isotherm is derived. Both the evaluated sorption capacity and sorption isotherm functions are plotted in Fig. 26, as a function of the free salt concentration evaluated from the mean salt concentration used in the diffusion measurements.

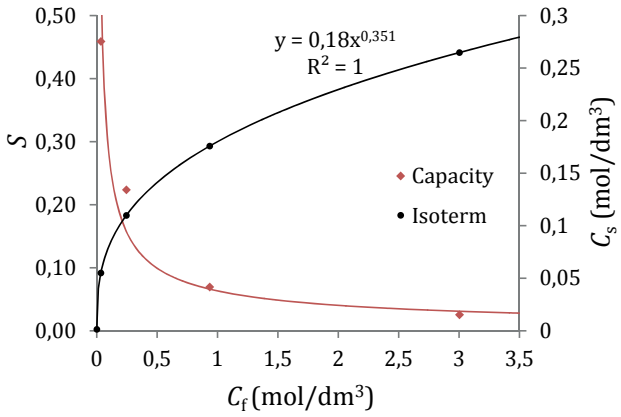

Fig. 26. Calculated sorption capacity S and adsorbed NaCl concentration C_s as a function of the free NaCl concentration in NRB at 298.15 ± 0.05 K.

It has also been found that the Freundlich isotherm fits data of chloride binding in different types of cement very well, in the free chloride concentration region of 0.01 to 1 mol/dm^3, whereas the Langmuir equation diverged from experimental data [163]. For the chloride binding in cements the values of α = 3.57-5.87 and β = 0.29-0.38 have been proposed at low free chloride concentrations [230]. Usually, the empirical constant β is between 0.1 and 0.5 or when in the $1/\beta$ form it varies between 10 and 2. It has also been shown that the Freundlich isotherm is to be expected if the binding energy varies continuously from site to site on the solid surface [231].

Nevertheless, the calculated Freundlich-like adsorption isotherm Eq. (68) is a useful equation for both quantifying the behavior of NaCl salt sorption and for explaining the different diffusion coefficient values measured with the closed capillary and the modified diaphragm diffusion cell measurements in the porous fired NRB medium. The determined value for the constant β (or $1/\beta$) of 0.35 (2.9) is also a typical mean value describing the adsorption data at the solid-solution interface, at least in a restricted range of solution concentration [231]. The value of constant α = 0.18 is small when compared to the values measured in cement or concrete for the binding of chlorides - there were no pre-existing literature values for porous brick media. However, this difference can be easily explained from the fact both concrete and cement have larger surface areas with more sorption sites compared to the NRB. Nevertheless, it might be more correct in this case of salt sorption on brick to use the term apparent sorption isotherm instead of the true sorption isotherm due to the use of the exceptional determination method presented. Overall it would be very interesting to compare Eq. (68) to the adsorption isotherm determined from the concentration analyses of the pore surface and pore solution of the brick in equilibrium, if possible.

7 CONCLUSIONS

There were three main objectives of this thesis, the first one was to develop the existing measuring techniques and calculation method of the diffusion coefficients in the closed capillary method (CCM) in aqueous solutions. The goal was also to measure accurately the required tracer diffusion coefficients of ^{22}NaCl in aqueous $MgCl_2$ solutions over a large concentration range and for the first time, verify the Onsager Limiting Law for the tracer diffusion of ^{22}NaCl in a 2:1 supporting electrolyte.

The second objective was to develop and test the measuring techniques, the apparatus and the calculation method of the diffusion coefficient with the modified diaphragm cell method (DM) for aqueous solutions in a porous ceramic brick medium. The aim was also to apply this newly developed methodology to the measurement of diffusion coefficients of salts commonly found in different porous brick media as a function of concentration and temperature. In addition to the practical diffusion experiments the diffusion of salts in fully saturated brick by means of mathematical methods involving analytical and numerical calculations was also studied. The goal was to construct a mathematical model and obtain an analytical solution, which characterizes the salt diffusion process with the experimental data.

The final objective of the thesis was to optimize and apply the CCM for measurements of the diffusion coefficients in porous media for the first time. Moreover, we aimed at comparing the diffusion coefficients in porous media measured with the non-stationary-state CCM with those measured earlier with the stationary-state DM. This comparison would allow the CCM as an absolute method to be tested because, in contrast to the DM, porosity values for the brick specimens are not required prior to the diffusion experiments. This exclusion of, in many ways, contradictory porosity measurements would allow the simplification of the measurements and remove one source of error. On the other hand, the possible influence of the effect of the sorption on the diffusion coefficients to be measured in the non-stationary CCM also has its own complications that needed to be addressed.

The main results from the practical work are collated in Table 12 and show the most important, experimentally measured diffusion coefficients are collected and include the determined maximum and mean standard errors of the mean. Moreover, approximately half of the data the presented as part of these measurement series have not been published previously.

The following conclusions can be drawn from the experimental work performed as a result of the objectives outlined for this thesis. The first conclusions focus mainly on the tracer diffusion measurements made with the CCM in aqueous solutions. In publication I, a new diffusion cell was developed as well as tested and a new statistically improved calculation method was presented. The tracer diffusion coefficients were discovered to be most accurately determined, with a precision of $\leq \pm 0.076\%$, by the new linear least-square calculation method. In

addition, the tracer diffusion coefficients of ^{22}NaCl were measured in aqueous $MgCl_2$ solutions at 25.00 ±0.01 °C, over a wide concentration range between 1 mol/dm^3 and 10^{-4} mol/dm^3. The Onsager Limiting Law was also demonstrated to be applicable for the tracer diffusion of ^{22}NaCl in low (10^{-4}-10^{-2}) mol/dm^3 concentration region of $MgCl_2$ for the first time for 2:1 supporting electrolyte and the Nernst limiting value $D^{\infty} = 1.334\times10^{-5}$ cm^2/s for Na^+-ion was extrapolated with a precision of $\pm0.002\times10^{-5}$ cm^2/s. Moreover, it was found that the reason for the departure of the measured tracer diffusion coefficients from the Onsager Limiting Law at concentration > 10^{-2} mol/dm^3 was demonstrated to be mainly as a consequence of the growing viscosity of the supporting electrolyte.

In addition to the results detailed in the publication I of this thesis, measurements were carried out at the infinite dilute region where $C(MgCl_2) = 10^{-5}$-10^{-6} mol/dm^3 and the values measured exceeded the Nernst limiting value. In order to interpret these results the Nernst-Planck equations for ionic flows were resolved taking the ionization of water into account. It was shown that at this order of dilution the concentration of the tracer, the supporting electrolyte and the ions resulting from the ionization of water become comparable and that the tracer flow would contain contributions from the cross-term coefficients demonstrating that the measured diffusion coefficients were not pure tracer diffusion coefficients. The effect of the tracer concentration was ruled out with a series of measurements made with increasing NaCl tracer concentrations and by extrapolating then the straight line fit to zero and the extrapolation gave the value of $D^{\infty}_{Na+} = (1.341 \pm 0.008) \times 10^{-5}$ cm^2/s. This value greater than the Nernst limiting value was interpreted as support for the calculated contributions resulting from the high cross-term coefficients of hydrogen and hydroxyl ions.

To study further the contribution of the ionization of water, also interdiffusion coefficients were measured in a binary NaCl-H_2O system at extreme dilution of the order of 10^{-6} mol/dm^3. As a result the experimental interdiffusion coefficients measured were lower than Onsager-Fuoss limiting law predicts, but in good agreement with the values calculated from the Nernst-Planck equations taking into account the ionization of water. This observation in a binary diffusion system also supports the extrapolated tracer diffusion value D^{0}_{Na+}, which was found to be higher than the Nernst limiting value in a ternary tracer system at infinite dilution.

Table 12. The calculated standard errors of the mean (in %) for all different diffusion coefficients measured in this work according to the methods and test series. The mean and single experimental values of the diffusion coefficients are given in the original tables, the number of the table given in the last column. The previously published measurement series, in publications I-V, are highlighted with a green background. The abbreviations abs, pre, CCM and DM stand for: in the absence and presence of porous medium, closed capillary and diaphragm diffusion cell method, respectively.

Diffusion coefficient (variable)	Diffusing species	C range (mol/dm^3)	Electrolyte/ porous medium	Standard error (%)	Av. st. error (%)	Method	Table
$D(C)$	^{22}Na+	10^0 - 10^{-4}	$MgCl_2$/abs	$\leq \pm 0.08$	± 0.06	CCM	2
$D(C)$	^{22}Na+	10^{-5} - 10^{-6}	$MgCl_2$/abs	$\leq \pm 0.07$	± 0.04	CCM	3
$D(C)$	^{22}NaCl	2×10^{-6} - 10^{-6}	NaCl/abs	$\leq \pm 0.25$	± 0.23	CCM	4
D_e(brick)	NaCl	0.05	NaCl / pre	$\leq \pm 3$	± 1.8	DM	5
D_e(salt)	salt	0.05	Salt / pre	$\leq \pm 0.8$	± 0.4	DM	6
$D_e(C)$	NaCl	3.08 - 0.05	NaCl / pre	$\leq \pm 1.2$	± 0.8	DM	7
$D_e(t)$	NaCl	0.05	NaCl / pre	$\leq \pm 1.4$	± 1.1	DM	8
$D^i_{app}(C)$	^{22}NaCl	3.08 - 5×10^{-4}	NaCl / pre	$\leq \pm 1.5$	± 1.2	CCM	9
$D^d_{app}(C)$	^{22}NaCl	3.08 - 0.05	NaCl / pre	$\leq \pm 1.2$	± 0.8	CCM	10
$D^i_{app}(C)$	^{22}Na+	3.08 - 0.005	NaCl / pre	$\leq \pm 1.3$	± 1.0	CCM	11

In the second part of this thesis the interdiffusion of salts in porous ceramic brick media were investigated with both experimental measurements and mathematical methods. In publication II, the developed DM apparatus was outlined and diffusion measuring techniques optimized for brick specimens. The diffusion coefficients were calculated under quasi-steady-state conditions using regression analysis. The diffusion coefficients of NaCl were measured in different ceramic brick materials of OLB, ODB and NRB at 25.00 ± 0.05 °C.

In publication III, the measurements were continued with porous engineering NRB and the diffusion coefficients of NaCl were also measured as a function of concentration and temperature. The measurements were performed at concentrations between 0.05 to 3.08 mol/dm^3 and temperatures ranging from 8 to 25 °C, respectively. In addition, the diffusion coefficients of the salts KCl, $NaNO_3$, $CaCl_2$, Na_2SO_4, $MgCl_2$ and Na_2CO_3, commonly found in building materials, were measured in aqueous solutions in NRB at 25 °C with the precision better than ±0.80%.

In contrast to publications II and III, where the focus was on developing the experimental techniques and measuring the diffusion coefficients, in publications IV and V, the emphasis was on the mathematical methods needed for the simulation work. In publication IV, both the numerical computer simulation and data analysis were carried out for the first part of the experimental diffusivity data at constant concentration and temperature. For the numerical analysis an implicit finite difference technique was used. The nonlinear differential equations used for modeling the salt diffusion in porous brick media started from the mass diffusive equation and initial and boundary conditions were discretized with the resultant system of algebraic equations solved by an iterative method. For salt diffusion in fully saturated brick under isothermal conditions, a mathematical model for a

finite-sized sample was developed and an approximate analytical solution was given. This solution identifies a characteristic number of fundamental importance for the salt transport process in the brick and in the chambers.

In publication V, the numerical computer simulation and data analysis were extended to include more experimental diffusivity data from different salts under varying environmental conditions like varying concentrations and temperature. The analytical solution developed and verified was used to give the temporary salt concentration in the monitored diffusion chamber α. The simulations were divided into three different groups, which were then compared to the measurement data and a good correlation was achieved. It was shown that the analytical solution has applications in a wide number of fields with DM. Also salt concentration profiles in the brick medium were simulated and given graphically for different temperature, salt and concentration. It was demonstrated that the precise diffusion coefficients could be used in a simulation program to solve the aqueous salt profiles in a brick medium under different environmental conditions.

In addition to the published results, a material parameter correlating the relation of salt diffusion coefficients in the presence and absence of porous material was presented for the investigated porous brick media OLB, ODB and NRB. The material parameters found predicted the experimentally measured effective diffusion coefficients as a function of brick type, salts and concentrations with an accuracy of ±7%. However, for changes of temperature the predictions with this parameter were worse. Furthermore, the ranking for the effective diffusion coefficients measured for different salts were demonstrated to depend on the viscosity and the apparent hydration number of the salt in the aqueous pore solution of the brick medium.

In the final part of this thesis the CCM was, for the first time, applied to the measurement of the diffusion coefficients in a porous medium. The optimal diffusion cell with optimal counting efficiency of the apparatus was developed for porous ceramic brick specimens. With this modified CCM the differential and integral interdiffusion and tracer diffusion coefficients of ^{22}NaCl were measured in NRB as a function of concentration at 25.00 ± 0.01 °C with a precision better than ±1.5%. By comparing the apparent diffusion coefficients, D^{i}_{app}, obtained with this non-stationary-state CCM with the effective diffusion coefficients, D_{e}, measured in publications II-V with the stationary-state DM a deviation was discovered that could be explained by the sorption effect. This interpretation is also supported by the simple pore tube model developed in this thesis and the results from the sorption experiments. By taking the sorbed part of the salt flux into account a Freundlich like sorption isotherm, $C_{\mathrm{s}} = 0.18\, C_{\mathrm{f}}{}^{0.35}$, could be presented with the help of the calculated adsorption capacity $S = (\mathrm{d}C_{\mathrm{s}}/\mathrm{d}C_{\mathrm{f}})_{\mathrm{eq}}$ of NaCl in NRB at 25 °C.

Overall the main conclusion of this experimental thesis is that the methods of DM and CCM developed here are both excellent techniques for the salt diffusion coefficient measurements in fully saturated porous fired brick. Both of these methods also have the potential to be adapted to other porous building materials

like mortar and lime-sand-brick as well as for most porous sedimentary rocks like shale, sandstone and limestone. The drawback to these techniques is the increase in the time it would take to measure less porous materials as the measurement duration for fired brick media is already considerable at > 120 h. The lack of published diffusion measurement data in porous brick materials made direct comparison of the diffusion coefficients measured in this thesis difficult. Comparable determinations of experimental D_e and D_{app} values are waited for with a great enthusiasm.

It is worth noting however that as CCM is an absolute method additional porosity measurements for the medium being studied are not needed, thus saving time and removing one source of error. The precondition for CCM is that the measured salt solutions still must capillary-soak into the porous medium investigated in order to establish the initial concentration distribution for the concentration gradient although the value of initial concentration distribution may still be arbitrary.

The fundamental difference between CCM and DM in the case of salt diffusion in porous media led to the different measured values of the interdiffusion coefficient. It was concluded that the ratio of these coefficients is given by the relation $D_{\mathrm{ss}}/D_{\mathrm{app}} = \varepsilon(1 + S)$. This result could be confirmed when more accurate sorption results become available.

MAIN SYMBOLS AND ABBREVIATIONS

ε	porosity
ε_r	dielectric constant
η	viscosity
η_0	viscosity of water
κ	conductance
κ^{-1}	Debye length
λ	decay constant
λ_i	molar conductivity of species i
λ_i^0	molar conductivity of species i at infinite dilution
ξ	constrictivity factor
τ	tortuosity
τ_a	apparent tortuosity
Φ	electric potential; diameter
A	area;
A^t	activity at time t
A^0	activity at time zero
A_{pore}	pore area
c_α	concentration in chamber α
$c_{\alpha 0}$	initial concentration in chamber α
c_β	concentration in chamber β
c_i	concentration of ionic species i
C_{f}	free NaCl concentration
C_i	concentration of component i
C_{mean}	total mean NaCl concentration
C_{s}	adsorbed NaCl concentration
CCM	closed capillary method
d	characteristic number
$d(u)$	mobility function (dimensionless)
D_{a}	diffusion coefficient in absence of porous medium
D_{app}	apparent diffusion coefficient
$\text{D}_{\text{app}}^{\text{i}}$	integral apparent interdiffusion coefficient
$D_{\text{app}}^{\text{d}}$	differential apparent interdiffusion coefficient
$D_{\text{app}}^{\text{t}}$	apparent tracer diffusion coefficient
D_{e}	effective interdiffusion coefficient
D_{fe}	free effective diffusion coefficient
D_{fss}	free stationary state diffusion coefficient
D_{ii}	main-term diffusion coefficient
D_{ij}	cross-term diffusion coefficient
D_i	diffusion coefficient of ionic species i
D_i^0	diffusion coefficient of ionic species i at infinite dilution
D_{p}	diffusion coefficient in presence of porous medium
D_{ss}	diffusion coefficient measured under stationary state
DM	diaphragm diffusion cell method
F	Faraday constant (96485 C mol^{-1})

h	counting efficiency; hydration number
h_a	apparent hydration number
I	intensity
I_c	ionic strength
I_m	constant intensity-term m
I_∞	intensity of the equilibrium concentration
j_i	diffusion flux density of ionic species *i*
J_i	diffusion flux density of component *i*
K_w	ionic product of the water (1.008×10^{-14} mol^2 dm^{-6} at 25 °C)
L	length of pore cylinder, capillary or brick specimen
n	number of components; n pieces of fluxes
N	pulse counts
N_A	Avogadro constant (6.023×10^{23} mol^{-1})
NRB	new Finnish red brick
ODB	old dark brick
OLB	old light brick
Q	diffusibility
r	radius; correlation coefficient
r_a	apparent radius
R	molar universal gas constant (8.314 J K^{-1} mol^{-1}); impedance
R_a	impedance in absence of porous medium
R_p	impedance in presence of porous medium
S	adsorption capacity
SEM	scanning electron microscopy
t	time; transport number, Celsius temperature
t_i^o	transport number of species i at infinite dilution
T	absolute temperature
u_i	electric mobility of species i
u_i^0	electric mobility of species i at infinite dilution
V	volume
z_i	charge number of ion i

REFERENCES

1. Graham, T., A short account of experimental researches on the diffusion of gases through each other, and their separation by mechanical means, *Quar. J. Sci., Lit. and art*, **27** (1829) 74-83.
2. Graham, T., On the law of the diffusion of gases, *Phil. Mag.,* **2** (1833) 175-190, 351-358.
3. Fick, A.E., Ueber diffusion, *Pogg. Ann.,* **94** (1855) 59-86.
4. Fick, A.E., On liquid diffusion, *Phil. Mag.,* **10** (1855) 30-39.
5. Adamson, A.W., Measurement of Na^+ ion diffusion by means of radiosodium, *J. Chem. Phys*., **15** (1947) 762-763.
6. Anderson, J.S. and Saddington, K., The use of radioactive isotopes in the study of the diffusion of ions in solution, *J. Chem. Soc*. (Suppl.), (1949) 381-386.
7. Stokes, R.H., An improved diaphragm-cell for diffusion studies and some tests of the method, *J. Am. Chem. Soc*., **72** (1950) 763-767.
8. Nielsen, J.M., Adamson, A.W. and Cobble, J.W., The selfdiffusion coefficients of the ions in aqueous sodium chloride and sodium sulphate at 25 °C, *J. Am. Chem. Soc*., **74** (1952) 446-451.
9. Onsager, L., Reciprocal relations in irreversible processes I., *Phys. Rev.*, **37** (1931) 405-426.
10. Onsager, L., Reciprocal relations in irreversible processes II., *Phys. Rev.*, **38** (1931) 2265-2279.
11. Onsager, L. and Fuoss, R.M., Irreversible processes in electrolytes. Diffusion, conductance, and viscous flow in arbitrary mixtures of strong electrolytes, *J. Phys. Chem.*, **36** (1932) 2689-2778.
12. Onsager, L., Theories and problems of liquid diffusion, *Ann. N.Y. Acad. Sci.*, **46** (1945) 241-265.
13. Albright, J.G. and Mills, R., A study of diffusion in the ternary system, labeled urea–urea-water, at 25° by measurements of the intradiffusion coefficients of urea, *J. Phys. Chem.*, **69** (1965) 3120-3126.
14. Albright, J.G., Equations for the description of isothermal diffusion in multicomponent systems containing pairs of chemically equivalent components, *J. Phys. Chem.*, **72** (1968) 11-15.
15. Liukkonen, S., *A study of self-diffusion in a binary electrolyte-water system*, Ph.D. thesis, Helsinki University of Technology, *Acta Polytech. Scand*., **113** (1973) 1-49.
16. Schönert, H., Transport of isotopes in systems with reversibly reacting species. I., *Ber. Bunsenges. Phys. Chem*., **82** (1978) 726-731.
17. Lobo, V.M.M., *Electrolyte solutions: Literature data on thermodynamic and transport properties, vol I*, Ed. The author, Coimbra, Portugal, 1984.
18. Lobo, V.M.M. and Quaresma, J.L., *Electrolyte solutions: Literature data on thermodynamic and transport properties, vol II*, Univ. Coimbra, Portugal, 1981.
19. Mills, R. and Lobo, V.M.M*., Self-diffusion in electrolyte solutions – a critical examination of data compiled from the literature*, Elsevier, Amsterdam, 1989.

20. Albright, J.G., Mathew, R., Miller, D.G., and Rard, J.A., Isothermal diffusion coefficients for NaCl-$MgCl_2$-H_2O at 25°. 1. Solute concentration ratio of 3:1, *J. Phys. Chem.*, **93** (1989) 2176-2180.
21. Anderson, D.E. and Graf, D.L., Multicomponent electrolyte diffusion, *Annu. Rev. Earth Planet. Sci*., **4** (1976) 95-121.
22. Miller, D.G., Ting, A.W., Rard, J.A. and Eppstein, L.B., Ternary diffusion coefficients of the brine systems NaCl (0,5M)-$NaSO_4$ (0,5M)-H_2O and NaCl (0,489M)-$MgCl_2$ (0,051M)-H_2O (seawater composition) at 25°C, *Geochim. Cosmochim. Acta,* **50** (1986) 2397-2403.
23. Altenberger, A.R. and Friedman, H.L., Theory of conductance and related isothermal transport coefficients in electrolytes, *J. Chem. Phys.*, **78** (1983) 4162-4173.
24. Mou, C.Y., Thacher, T.S. and Lin, J.L., A statistical mechanical theory of the self-diffusion coefficient of simple ions in electrolyte solutions, *J. Chem. Phys.*, **79** (1983) 957-963.
25. Thacher, T.S., Lin, J.L. and Mou, C.Y., Theory of Onsager phenomenological coefficients for isothermal linear transport processes in electrolyte solutions, *J. Chem. Phys.*, **81** (1984) 2053-2063.
26. Kremp, D., Ebeling, W., Krienke, H. and Sandig, R., HNC-type approximation for transport processes in electrolytic solutions, *J. Stat. Phys.*, **33** (1983) 99-106.
27. Zhong, E.C. and Friedman, H., Self-diffusion and distinct diffusion of ions in solution, *J. Phys. Chem.*, **92** (1988) 1685-1692.
28. DeGroot, S.R. and Mazur, P., *Non-equilibrium thermodynamics*, North-Holland Publ. Co., Amsterdam, 1962.
29. Haase, R., *Thermodynamics of Irreversible Processes*, Addison-Wesley Publishing Company, London, 1969.
30. Miller, D.G., Application of irreversible thermodynamics to electrolyte solutions. I. Determination of ionic transport coefficients l_{ij} for isothermal vector transport processes in binary electrolyte systems, *J. Phys. Chem.*, **70** (1966) 2639-2659.
31. Miller, D.G., Application of irreversible thermodynamics to electrolyte solutions. II. Ionic coefficients l_{ij} for isothermal vector transport processes in ternary electrolyte systems, *J. Phys. Chem.*, **71** (1967) 616-632.
32. Miller, D.G., Application of irreversible thermodynamics to electrolyte solutions. III. Equations for isothermal vector transport processes in n-component systems, *J. Phys. Chem.*, **71** (1967) 3588-3592.
33. Hertz, H.G., Harris, K.R., Mills, R. and Woolf, L.A., Velocity correlations in aqueous electrolyte solutions from diffusion, conductance, and transference data. Part 2. Applications to concentrated solutions of 1-1 electrolytes, *Ber. Bunsenges. Phys. Chem*., **81** (1977) 664-670.
34. Woolf, L.A. and Harris, K.R., Velocity correlation coefficients as an expression of particle-particle interactions in (electrolyte) solutions, *J.C.S. Faraday I*, **74** (1978) 933-947.
35. Miller, D.G., Explicit relations of velocity correlation coefficients to Onsager l_{ij}'s, to experimental quantities, and to infinite dilution limiting laws for binary electrolyte solutions, *J. Phys. Chem.*, **85** (1981) 1137-1146.

36. Rard, J.A. and Miller, D.G., Ternary mutual diffusion coefficients of NaCl-$SrCl_2$-H_2O at 25°C. 1. Total concentrations of 0.5 and 1.0 moldm^3, *J. Phys. Chem.*, **91** (1987) 4614-4620.
37. Rard, J.A. and Miller, D.G., Ternary mutual diffusion coefficients of NaCl-$SrCl_2$-H_2O at 25°C. 2. Total concentrations of 2.0 and 3.0 moldm^3, *J. Phys. Chem.*, **92** (1988) 6133-6140.
38. Paduano, L., Mathew, R., Albright, J.G., Miller, D.G. and Rard, J.A., Isothermal diffusion coefficients for NaCl-$MgCl_2$-H_2O at 25°C. 2. Low concentrations of NaCl with a wide range of $MgCl_2$ concentrations, *J. Phys. Chem.*, **93** (1989) 4366-4370.
39. Mills, R., Easteal, A.J. and Woolf, L.A, Viscosities and intradiffusion coefficients in the ternary system NaCl-$MgCl_2$-H_2O at 25°C, *J. Solution Chem.*, **16** (1987) 835-840.
40. Price, W.E. and Woolf, L.A, Intradiffusion coefficients of all species in aqueous gallium perchlorate solutions and solution viscosities at 25°C, *J. Solution Chem.*, **22** (1993) 873-882.
41. Leaist, D.G., Ternary diffusion in aqueous NaCl + $MgCl_2$ solutions at 25°C, *Electrochim. Acta*, **33** (1988) 795-799.
42. Rard, J.A. and Miller, D.G., Isopiestic determination of the osmotic and activity coefficients of aqueous mixtures of NaCl and $MgCl_2$ at 25°C, *J. Chem. Eng. Data,* **32** (1987) 85-92.
43. Bianchi, H., Corti, H.R. and Fernandez-Prini, R., The conductivity of concentrated aqueous mixtures of NaCl and $MgCl_2$ at 25°C, *J. Solution Chem.*, **18** (1989) 485-491.
44. Mathew, R., Paduano, L., Albright, J.G., Miller, D.G. and Rard, J.A., Isothermal diffusion coefficients for NaCl-$MgCl_2$-H_2O at 25°C. 3. Low $MgCl_2$ concentrations with a wide range of NaCl concentrations, *J. Phys. Chem.*, **93** (1989) 4370-4374.
45. Mathew, R., Albright, J.G., Miller, D.G. and Rard, J.A., Isothermal diffusion coefficients for NaCl-$MgCl_2$-H_2O at 25°C. 4. Solute concentration ratio of 1:3, *J. Phys. Chem.*, **94** (1990) 6875-6878.
46. Wendt, R.P. and Shamim, M., Isothermal diffusion in the system water - magnesium chloride - sodium chloride as studied with the rotating diaphragm cell, *J. Phys. Chem.*, **74** (1970) 2770-2783.
47. Albright, J.G, Mathew, R. and Paduano, L., private communication, as cited in Ref. 19, p. 127.
48. Gosting, L.J., Hanson, E.M., Kegeles, G. and Morris, M.S., Equipment and experimental methods for interference diffusion studies, *Rev. Sci. Instr*., **20** (1949) 209-215.
49. Ambrosone, L., Vitagliano, V., Della Volpe, C. and Sartorio, R., Non ideality of free diffusion boundaries, *J. Solution Chem.*, **20** (1991) 271-291.
50. Rard, J.A. and Miller, D.G., Ternary mutual diffusion coefficients of $ZnCl_2$-KCl-H_2O at 25°C by Rayleigh interferometry, *J. Solution Chem.*, **19** (1990) 129-148.
51. Tyrrell, H.J.V. and Harris, K.R., *Diffusion in liquids*, Butterworths, London, 1984.

52. Fontanella, M., Micali, N., Wanderlingh, F. and Tettamanti, E., Diffusion processes in multicomponent systems, I NMR investigations of a LiCl solution, *Phys. Chem. Liq.*, **15** (1986) 283-293.
53. Fontanella, M.E, Micali, N., Salvato, G. and Wanderlingh, F., Diffusion processes in multicomponent systems, II Macroscopic investigation of a LiCl solution, *Phys. Chem. Liq.*, **15** (1986) 295-308.
54. Marbach, W. and Hertz, H.G. Self- and mutual diffusion coefficients of some n-alkanes at elevated temperatures and pressures*, Z. Phys. Chem*., **193** (1996) 19-40.
55. Mills, R. and Woolf, L.A., *The diaphragm cell*, ANU Press, Canberra, 1968.
56. Wang, J.H., Tracer-diffusion in liquids, III., *J. Am. Chem. Soc*., **74** (1952) 1612-1615.
57. Timmerhaus, K.D. and Drickamer, H.G., Self-diffusion in CO_2 at moderate pressures, *J. Phys. Chem.*, **19** (1951) 1242-1243.
58. Noszticzius, Z., Öndiffúziós állandó mérése elektrolitoldatokban*, Kémiai Közlemények*, **32** (1969) 115-120.
59. Wang, J.H., Tracer-diffusion in liquids, I., *J. Am. Chem. Soc.*, **74** (1952) 1182-1186.
60. Wang, J.H., Tracer-diffusion in liquids, II., *J. Am. Chem. Soc.*, **74** (1952) 1611-1612.
61. Mills, R., A remeasurement of the self-diffusion coefficients of sodium ion in aqueous sodium chloride solutions, *J. Am. Chem. Soc.*, **77** (1955) 6116-6119.
62. Patil, S.F., Rajurkar, N.S. and Borhade, A.V., Self-diffusion of cobalt and manganese ions in aqueous electrolyte solutions, *J. Chem. Soc. Faraday Trans.*, **87** (1991) 3405-3407.
63. Wang, J.H. and Kennedy, J.W., Self-diffusion coefficients of sodium ion and iodide ion in aqueous sodium iodide solutions, *J. Am. Chem. Soc*., **72** (1950) 2080-2083.
64. Devell, L., Measurements of the self-diffusion of water in pure water, H_2O-D_2O mixtures and solutions of electrolytes, *Acta Chem. Scand*. **16** (1962) 2177-2188.
65. Liukkonen, S., Passiniemi, P., Noszticzius, Z. and Rastas, J., Theory of tracer diffusion measurements in liquid systems, *J.C.S. Faraday I*, **72** (1976) 2836-2843.
66. Noszticzius, Z., Liukkonen, S., Passiniemi, P. and Rastas, J., Optimal conditions and measuring functionals in the measurements of diffusion coefficients, *J.C.S. Faraday I*, **72** (1976) 2537-2544.
67. Passiniemi, P., Liukkonen, S. and Noszticzius, Z., Closed capillary method for tracer diffusion measurements in liquids, *J.C.S. Faraday I*, **73** (1977) 1834-1839.
68. Passiniemi, P., Accurate tracer diffusion coefficients of Na^+ and Cl^- ions in dilute aqueous sodium chloride solutions measured with the closed capillary method, *J. Solution Chem.*, **12** (1983) 801-813.
69. Passiniemi, P. and Noszticzius, Z., Fitting the solution of the diffusion equation to measured data in tracer-diffusion experiments, *Finn. Chem. Lett*., No. 8 (1976) 189-191.

70. Guggenheim, E.A., On the determination of the velocity constant of a unimolecular reaction, *Phil. Mag*., **2** (1926) 538-543.
71. Ahl, J. and Liukkonen, S., Determination of Tracer Diffusion Coefficients of ^{22}NaCl as a function of Magnesium Chloride Concentration in Water at 25 °C, *Czech. J. Phys*. **49** (1999) 867–872.
72. von Konow, T., *Saltvittring i tegel – saltvittringsmekanismer [Deterioration in bricks due to salts – mechanisms of salt deterioration]*, Technical Research Centre of Finland, Research Notes 1003, Espoo, 1989.
73. Vuorio, M., *Thermodynamic behaviour of aqueous solutions in porous building materials*, M. Sc. thesis, Helsinki University of Technology, Espoo, 1998.
74. Larsen, E.S and Nielsen, C.B.*,* Decay of bricks due to salt, *Mater. Struct*., **23** (1990) 16-25.
75. Nielsen, C.B., *Salts in porous building materials*, Technical Report 243/91, Denmark, 1991.
76. Grogan, J.C. and Conway, J.T. (eds.), *Masonry: Research, Application and Problems*, ASTM Special Technical Publication 871, 1985.
77. Brownell, W.E., *The causes and control of efflorescence on brickwork*, Structural Clay Products Institute, Research Report 15, 1969.
78. Merrigan, M.W., Efflorescence: cause and control, *TMS Journal*, **5** (1986) G19-G22+T39.
79. Chapman, R.W., Salt weathering by sodium chloride in the Saudi Arabian desert, *Amer. J. Sci*., **280** (1980) 116-129.
80. Binda, L., and Baronio, G., Measurement of the resistance to deterioration of old and new bricks by means of accelerated aging tests, *Durability Build. Mater*., 2, 1984, 139-154.
81. Yakovlev, G.I. and Gailyus, A., Salt corrosion of ceramic brick, *Glass and Ceramic*, **62** (2005) 321-323.
82. Hornain, H., Marchand, J., Duhot, V. and Morainville-Regourd, M., Diffusion of chloride ions in limestone filler blender cement pastes and mortars, *Cement Concrete Res*., **25** (1995) 1667-1678.
83. Andrade, C., Calculation of chloride diffusion coefficients in concrete from ionic migration measurements, *Cement Concrete Res*., **23** (1993) 724-742.
84. Saetta, A.V., Scotta, R.V. and Vitaliani, R.V., Analysis of chloride diffusion into partially saturated concrete, *ACI Mater. J.*, **90** (1993) 441-451.
85. Nagesh, M. and Bishwajit, B., Modelling of chloride diffusion in concrete and determination of diffusion coefficients, *ACI Mater. J.*, **95** (1998) 113-120.
86. Truc, O., Ollivier, J.P. and Carcasses, M., A new way for determining the chloride diffusion coefficient in concrete from steady state migration test, *Cement Concrete Res*., **30** (2000) 217-226.
87. Northrop, J.H. and Anson, M.L., A method for the determination of diffusion constants and the calculation of the radius and weight of the hemoglobin molecule, *J. Gen. Physiol*., **12** (1929) 543-554.
88. McBain, J.W. and Dawson, C.R., The diffusion of potassium chloride in aqueous solution, *Proc. Roy. Soc. London A*, **148** (1935) 32-39.

89. Hartley, G.S. and Runnicles, D.F., The porous diagram method of measuring diffusion velocity, and the velocity of diffusion of potassium chloride in water, *Proc. Roy. Soc. London A*, **168** (1938) 401-419.
90. Garbarini, G.R., Eaton, R.F, Kwei, T.K. and Tobolsky, A.V., Diffusion and reverse osmosis through polymer membranes, *J. Chem. Educ*., **48**, 4 (1971) 226-230.
91. Buenfeld, N.R. and Newman, J.B., The permeability of concrete in a marine environment, *Mag. Conc. Res.,* **36** (1984) 67-80.
92. Buenfeld, N.R. and Newman, J.B., Examination of three methods for studying ion diffusion in cement pastes, mortars and concrete, *Mater. Struct*., **20** (1987) 3-10.
93. Glass, G.K. and Buenfeld, N.R., Theoretical assessment of the steady state diffusion cell test, *J. Mater. Sci*., **33** (1998) 5111-5118.
94. Lempinen, A., Fechner, H. and Grunewald, J., *Salt Diffusion in Building Materials*, Building Physics '96 – 4 th Nordic symposium, (1996) 619-626.
95. Ahl, J., *The measurement of salt diffusion in water in porous brick materials*, Technical Report, Laboratory of Structural Engineering and Building Physics, Helsinki University of Technology, 1998.
96. Ahl, J., *Salt transport in brick structures. Part I*, Technical Report, Laboratory of Structural Engineering and Building Physics, TASK III, Be96-3290 meeting in Helsinki, Helsinki University of Technology, 1998.
97. Ahl, J., *Salt diffusion in brick structures*, Technical Report, Laboratory of Structural Engineering and Building Physics, Helsinki University of Technology, 1999.
98. Ahl, J., *Salt transport in brick structures. Part II*, Technical Report, Laboratory of Structural Engineering and Building Physics, Helsinki University of Technology, 1999.
99. Lü, X., Ahl, J. and Viljanen, M., Estimation of Salt Diffusion Coefficient in Brick, *10th International Symposium for Building Physics*, 1999, pp. 699-707.
100. Lü, X. and Viljanen, M., Determination of Salt Diffusion Coefficient in Brick: Analytical Methods, *Transport Porous Med.*, **49** (2002) 241–246.
101. Pikal, M.J., Isotope effect in tracer diffusion. Comparison of the diffusion coefficients of $^{24}Na^{+}$ and of $^{22}Na^{+}$ in aqueous electrolytes, *J. Phys. Chem*., **76** (1972) 3038-3040.
102. Weingärtner, H., Diffusion in liquid mixtures of light and heavy water, *Ber. Bunsenges. Phys. Chem*., **88** (1984) 47-50.
103. Weingärtner, H., Self diffusion in liquid water. A reassessment, *Z. Phys. Chem*. Neue Folge, **132** (1982) 129-149.
104. Longsworth, L.G., Temperature Dependence of Diffusion in Aqueous Solutions, *J. Phys. Chem*., **58** (1954) 770-773.
105. Longsworth, L.G., The mutual diffusion of light and heavy water, *J. Phys. Chem*., **64** (1960) 1914-1917.
106. See, D.M. and White, R.E., A simple method for determining differential diffusion coefficients from aqueous electrolyte diaphragm cell data at temperatures below 0 °C, *J. Electrochem. Soc*., **146** (2) (1999) 677-679.
107. Cussler, E.L., *Multicomponent diffusion*, The Netherlands: Elsevier, Amsterdam, 1976.

108. Cussler, E.L., *Diffusion – Mass transfer in fluid systems*, Cambridge University Press, Cambridge, 1984.
109. Mills, R., The self-diffusion of chloride ion in aqueous alkali chloride solutions at 25°C, *J. Phys. Chem.*, **61** (1957) 1631-1634.
110. Albright, J.G., Equations for the description of isothermal diffusion in multicomponent systems containing pairs of chemically equivalent components, *J. Phys. Chem.*, **72** (1968) 11-15.
111. DeGroot, S.R., Thermodynamics of irreversible processes, North-Holland, Amsterdam (1958).
112. Kontturi, K.; Murtomäki, L. and Manzanares, J. A. *Ionic Transport Processes in Electrochemistry and Membrane Science*, Oxford University Press, Oxford (2008).
113. Nernst, W., *Z. Phys. Chem*., Zur Kinetik der in Lösung befindlichen Körper. Erste Abhandlung. Theorie der Diffusion, **2** (1888) 613-637.
114. Nernst, W., Die elektromotorische Wirksamkeit der Jonen, *Z. Phys. Chem*., **4** (1889) 129-181.
115. Planck, M., Uber die Potentialdifferenz zwischen zwei verdünnten Lösungen binarer Elektrolyte, *Ann. Phys.*, **40** (1890) 561-576.
116. Robinson, R.A. and Stokes, R.H., *Electrolyte solutions – The measurement and interpretations of conductance, chemical potential and diffusion in solutions of simple electrolytes*, 2nd ed. revised, Butterworths, London, 1965.
117. Lee, K. and Kay, R.L., Transference numbers for magnesium chloride at 25 °C, *Aust. J. Chem*., 33 (1980) 1895-1902.
118. Bianchi, H., Corti, H.R. and Fernandez-Prini, R., The conductivity of dilute aqueous solutions of magnesium chloride at 25 °C, *J. Solution Chem*., **17** (1988) 1059-1065.
119. Lobo, V.M.M, Ribeiro, A.C.F. and Verissimo, L.M.P., Diffusion coefficients in aqueous solutions of magnesium nitrate at 298 K*, Ber. Bunsenges. Phys. Chem*., **98** No.2 (1994) 205-208.
120. Kay, R.L. and Evans, D.F., The effect of solvent structure on the mobility of symmetrical ions in aqueous solution*, J. Phys. Chem*., **70** (1966) 2325-2335.
121. Kohlrausch, F. Das elecrtische Leitungsvermögen der wässerigen Lösungen von den Hydraten und Salzen der leichten Metalle, sowie von Kupfervitriol, Zinkvitriol und Silbersalpeter. *Ann. Physik*, **6** (1879) 1-50.
122. Rastas, J., *Ueber die Tracerdiffusion in wässrigen Elektrolytlösungen vom Standpunkt der Thermodynamik der irreversiblen Prozesse*, Ph.D. thesis, Helsinki, *Acta Polytech. Scand*., Ch. 50,1966.
123. MacInnes, D.A., *The principles of electrochemistry*, 2nd ed., Reinhold Publishing Corporation, New York, 1947.
124. Debye, P. and Hückel, E., Zur Theorie der Elektrolyte. I. Gefrierpunktserniedrigung und verwandte Erscheinungen, *Physik. Z.*, **24** (1923) 185-206.
125. Debye, P. and Hückel, E., Zur Theorie der Elektrolyte. II. Das Grenzgesetz für die elektrische Leitfähigkeit, *Physik. Z.*, **24** (1923) 305-325.
126. Onsager, L., Zur Theorie der Elektrolyte 1. *Physik. Z.*, **27** (1926) 388-392.
127. Onsager, L., Zur Theorie der Elektrolyte 2. *Physik. Z.*, **28** (1927) 277-298.
128. Gosting, L.J. and Harned, H.S., The application of the Onsager theory of ionic mobilities to self-diffusion, *J. Am. Chem. Soc*., **73** (1951) 159-161.

129. Hamann, C.H., Hamnett, A. and Vielstich, W., *Electrochemistry*, 2nd ed., Wiley, Weinheim, 1998.
130. Mills, R., The effect of the ionization of water on diffusional behavior in dilute aqueous electrolytes, *J. Phys. Chem*., **66** (1962) 2716-2718.
131. Woolf, L.A., Miller, D.G. and Gosting, L.J., Isothermal Diffusion Measurements on the System H2O-Glycine-KCl at 25°C; Tests of the Onsager Reciprocal Relation, *J. Amer. Chem*. Soc., **84** (1962) 317-331.
132. Woolf, L.A., Multicomponent diffusion in a system consisting of a strong electrolyte. Solute at low concentrations in an ionizing solvent, *J. Phys. Chem*., **76** (1972) 1166-1169.
133. Passiniemi, P., Liukkonen, S. and Noszticzius, Z., Electrolyte diffusion at very low concentrations in ionized water, *J.C.S. Faraday I*, **76** (1980) 2552-2557.
134. Murtomäki, L., Kallio, T., Lahtinen, R. and Kontturi, K., *Sähkökemia*, Kopijyvä Oy, Jyväskylä, 2009.
135. Livingston, R.A., *Geochemical methods applied to the reproduction of handmolded brick*, Proceedings, 8th International brick/block masonry conference, ed. J. de Courcy, Elsevier, New York, 1988.
136. Soveri, U., The mineralogical composition of argillaceous sediments of Finland, *Annales Academiae Scientiarum Fennicae*, Series A III, **48** (1956) 1-32.
137. Hyyppä, J., *Savi ja sen teollinen käyttö*, Geologiska forskningsanstalten, Esbo, Geotekniska publikationer, **65** (1960), pp.25-40.
138. Leppävuori, E., Prokki, H., Kanerva, P. and Vähäkallio, P., *Rakennusaineet*, Otakustantamo, Helsinki, 1979.
139. Zhang, B. and Liu, X. Effects of fractal trajectory on gas diffusion in porous media, *AIChE J.*, 49 (2003) 3037-3047.
140. Syrjänen, T., *Suitability of electro-osmosis for dehydratation of brick wall,* M. Sc. thesis, Helsinki University of Technology, Espoo, 1995.
141. Roels, S., Elsen, J., Carmeliet, J. and Hens, H., Characterisation of pore structure by combining mercury porosimetry and micrography, *Mater. Struct*., **34** (2001) 76-82.
142. Adamson, A.W.*, Physical chemistry of surfaces*, John Wiley & Sons, New York, 1990, pp. 567-571.
143. Shao, P., Huang, R.Y.M., Feng, X. and Anderson W., Gas-Liquid displacement method for estimating membrane pore-size distributions, *AIChE J.*, **50** (2004) 557-565.
144. Hoogschagen, J., Diffusion in porous catalysts and adsorbents, *Ind. Eng. Chem*., **47** (1955) 906-913.
145. Moridis, G.J., Semianalytical solutions for parameter estimation in diffusion cell experiments, *Water Resour. Res*., **35** (1999) 1729-1740.
146. Weerts, A.H., Bouten, W. and Verstaten, J.M., Simultaneous measurement of water retention and electrical conductivity in soils: Testing the Mualem-Fridman tortuosity model, *Water Resour. Res*., **35** (1999) 1781-1787.
147. Samson, E., Marchand, J. and Snyder, K.A., Calculation of ionic diffusion coefficients on the basis of migration test results, *Mater. Struct*., **36** (2003) 156-165.

148. Brakel, J. van and Heertjes, P.M., Analysis of diffusion in macroporous media in terms of a porosity, a tortuosity and a constrictivity factor, *Int. J. Heat Mass Transfer*, **17** (1974) 1093-1103.
149. Tumidajski, P.J., Schumacher, A.S., Perron, S., Gu, P. and Beaudoin J.J., On the relationship between porosity and electrical resistivity in cementitious systems, *Cem. Concr. Res.*, **26** (1996) 539-544.
150. Viljanen, M., Liukkonen, S., Bergman, J. and Syrjänen, T., *Test construction Report*, National Board of Public Building, Helsinki, 5/1994.
151. Smith, J.M., *Chemical Engineering Kinetics*, 3rd ed., McGraw-Hill, New York, 1981.
152. Takahashi, R., Sato, S., Sodesawa, T. and Nishida, H., Effect of pore size on the liquid-phase pore diffusion of nickel nitrate, *Phys. Chem. Chem. Phys.*, **4** (2002) 3800-3805.
153. Shaw, D.J., *Introduction to colloid and surface chemistry*, 3rd ed., Butterworths, London, 1986.
154. Olin, M., *Diffusion in crushed rock and in bentonite clay*, Ph.D. thesis, Helsinki University of Technology, VTT Publications 175, Espoo, 1994.
155. Ferreiro, E.A. and de Bussetti, S.G., Adsorption on Na-montmorillonite of 1,10-phenanthroline and quinoline in Single and binary aqueous solution, *Z. Phys. Chem*., **217** (2003) 1143-1152.
156. Muurinen, A., *Diffusion of anions and cations in compacted sodium bentonite*, Ph.D. thesis, Helsinki University of Technology, VTT Publications 168, Espoo, 1994.
157. Gosman, A. and Blažiček, J., Study of the diffusion of trace elements and radionuclides in soils. Capillary modification of the thin layer method. Diffusion of ^{137}Cs, *J. Radioanal. Nuc. Chem. Art*., **182** (1994) 179-191.
158. Kontturi, K., Savonen , A. and Vuoristo, M., Study of adsorption and ion-exhange properties of some porous membranes, *Acta. Chem. Scand*, **48** (1994) 1-11.
159. Kontturi, A.K, Kontturi, K., Mafé, S., Manzanares, J.A., Niinikoski, P. and Vuoristo, M., Convective diffusion in porous membranes with adsorbed charges*, Langmuir*, **10** (1994) 949-954.
160. Tumidajski, P.J., application of Danckwerts' solution to simultaneous diffusion and chemical reaction in concrete, *Cem. Concr. Res*., **26** (1996) 697-700.
161. Zhang, T. and Gjørv, O.E., Diffusion behavior of chloride ions in concrete, *Cem. Concr. Res*., **26** (1996) 907-917.
162. Nilsson, L-O., *Chloride penetration into concrete structures*, Nordic Miniseminar, ed. Nilsson, L-O., Chalmers University of Technology, Publication P-93:1, Göteborg, 1993, p. 17.
163. Tang, L., *Chloride transport in concrete - measurement and prediction,* Ph.D. thesis, Chalmers University of Technology, Publication P-96:6, Göteborg, 1996.
164. Tumidajski, P.J. and Chan, G.W., Effect of sulfate and carbon dioxide on chloride diffusivity, *Cem. Concr. Res*., No.4, **26** (1996) 551-556.
165. Gust, S., Hämeenoja, E., Ahl, J., Laitinen, T., Savonen, A. and Sundholm, G., Effect of organic additives on the lead/acid negative plate, *J. Power Sources*, **30** (1990) 185-192.

166. Abdurakhmanov, A.K., Éminov, A.M. and Maslennikova, G.N., Stages of ceramic structure formation in the presence of additives, *Glass Ceramics*, No.9-10, **57** (2000) 354-356.
167. Nilsson, L-O., *A theoretical study on the effect of non-linear chloride binding on chloride diffusion measurements in concrete*, Chalmers University of Technology, Publication P-92:13, Göteborg, 1992.
168. Carmeliet, J., Descamps, F. and Houvenaghel, G., A multiscale network model for simulating moisture transfer properties of porous media, *Transport Porous Med.*, **35** (1999) 76-88.
169. Nilsson, L-O., Massat, M. and Tang, L., *The effect of non-linear binding on the prediction of chloride penetration into concrete structures, in Durability of concrete*, ed. Malhotra, V.M., ACI Special Publication SP-145, 1994, pp.469-486.
170. Atkinson, A. and Nickerson, K.,The diffusion of ions through water-saturated cement, *J. Mater. Sci*., **19** (1984) 3068-3078.
171. Andrade, C. and Sanjuán, M.A., Experimental procedure for the calculation of chloride diffusion coefficients in concrete from migration tests, *Adv. Cem. Res.*, **6** (1994) 127-134.
172. Gosman, A., Liukkonen, S. and Passiniemi, P., Adsorption and diffusion at low electrolyte concentrations, *J. Phys. Chem*., **90** (1986) 6051-6053.
173. *Andrade*, C., Calculation of chloride diffusion coefficients in concrete from ionic migration measurements*, Cem. Concr. Res*., **23** (1993) 724-742.
174. Whiting, D., *Rapid determination of the chloride permeability of concrete*, Federal Highway Administration, Report no. FHWA/RD-81/119, 1981.
175. Page, C.L., Short, N.R. and Tarras, A., Diffusion of chloride ions in hardened cement pastes, *Cem. Concr. Res*., **11** (1981) 395-406.
176. Ollivier, J.-P., Arsenault, J., Truc, O. and Marchand, J., Determination of chloride binding isotherms from migration tests, *Mario Collepardi Symposium on Advances in Concrete Science and Technology*, Rome, 1997.
177. MacDonald, K.A. and Northwood, D.O., Experimental measurements of chloride ion diffusion rates using a two-compartment diffusion cell: Effects of material and test variables, *Cem. Concr. Res*., **25** (1995) 1407-1416.
178. Gilleece, P.R.V., Basheer, A.E. and Long, A.E., The effect of concentration on the accelerated chloride ion migration tests for modified concretes, *Proceedings of the International RILEM workshop*, St-Rémy-les-Chevreuse, France, 1995, p.161.
179. Tang, L. and Nilsson, L-O., Rapid determination of the chloride diffusivity in concrete by applying an electrical field, *ACI Mater. J. Tech. Paper* (1992) 49-53.
180. Andrade, C., Sanjuán, M.A., Recuero, A. and Río, O., Calculation of chloride diffusivity in concrete from migration experiments, in non steady-state conditions, *Cem. Concr. Res*., **24** (1994) 1214-1228.
181. Andrade, C., Castellote, M., Alonso, C. and González.C., Non-steady-state chloride diffusion coefficients obtained from migration and natural diffusion tests. Part I: comparison between several methods of calculation, *Mater. Struct*., **33** (2000) 21-28.
182. Dresner, L. and Kraus, K.A., Ion exclusion and salt filtering with porous ion-exhange materials, *J. Phys. Chem*., **67** (1963) 990-996.

183. Dresner, L., Electrokinetic phenomena in charged capillaries, *J. Phys. Chem*., **67** (1963) 1635-1641.
184. Rice, C.L and Whitehead, R., Electrokinetic flow in a narrow cylindrical capillary, *J. Phys. Chem*., **69** (1965) 4017-4024.
185. Levine, S., Marriott, J.R., Neale, G. and Epstein, N., Theory of electrokinetic flow in fine cylindrical capillaries at high zeta-potentials, *J. Colloid Interface Sci*., **52** (1975) 136-149.
186. Anderson, J.L. and Koh, W-H., Electrokinetic parameters for capillaries of different geometries, *J. Colloid Interface Sci*., **59** (1977) 149-158.
187. Olivares, W., Croxton, T.L and McQuarrie, D.A., Electrokinetic flow in a narrow cylindrical capillary, *J. Phys. Chem*., **84** (1980) 867-869.
188. Pintauro, P.N. and Verbrugge, M.W., The electric-potential profile in ion-exchange membrane pores, *J. Membrane Sci*., **44** (1989) 197-212.
189. Bockris, J.O'M. and Reddy, A.K.N, *Modern Electrochemistry*, 2nd ed., Plenum Press, New York, 1998.
190. Maekawa, M., *Surface chemistry and electrochemistry of membranes*, ed. Sørensen, T.S., Marcel Dekker, Inc., New York, 1999, pp.247-269.
191. Harned, H.S. and Nuttal, R.L., The diffusion coefficient of potassium chloride in dilute aqueous solution, *J. Am. Chem. Soc.*, **69** (1947) 736-740.
192. Zhukhovtskii, A.A, Krykov, S.N. and Geodakyan, V.A., in Primenie Radioaktivnykh Izotopov v Metallurgii, ed. Kidin, I.N., vol. XXXIV, Moscow, 1955.
193. Ahl, J., *Tracer-diffusion of sodium[^{22}Na]chloride in $MgCl_2$-H_2O-solutions*, Licentiate's thesis, Helsinki University of Technology, Espoo,1996.
194. Chakrabarti, H. and Changdar, S.N., Accurate measurement of tracer diffusion coefficients in aqueous solutions with sliding cell technique*, Appl. Radiat. Isot.*, **43** (1992) 405-412.
195. Simonin, J.P, Mills, R., Perera, A., Turg, P. and Tallet, F., Closed capillary method for diffusion of biological macromolecules, *J. Solution Chem.*, **15** (1986) 1015-1030.
196. Crouthamel, C.G., Gatrousis, C. and Goslovich, S.J., *A Compilation of gamma-ray spectra, in Applied gamma-ray spectrometry*, ed. Crouthamel, C.G., Pergamon Press, New York, 1960, pp.19,172,173.
197. Willard, H.H., Merritt, L.L., Jr., Dean, J.A. and Settle, F.A., Jr., *Instrumental methods of analysis*, 6th ed., D. Van Nostrand Company, New York, 1981, pp. 289-315.
198. Passiniemi, P., *Theory and measurements of tracer diffusion in electrolytes. Tracer diffusion coefficients of ^{22}NaCl and Na^{36}Cl in aqueous sodium chloride at 298,15 K measured with closed capillary method*, Ph.D. thesis, Helsinki University of Technology, Espoo, 1982.
199. Schönert, H., Phenomenological description of the transport of isotopes in electrolytic systems, *Electrochim. Acta*, **27** (1982) 1043-1048.
200. Carslaw, H.S. and Jaeger, J.C., *Conduction of heat in solids*, Oxford University Press, London, 2nd ed., 1959, p. 228.
201. Courant, R. and Hilbert, D., *Methods of mathematical physics*, *vol. I*, Interscience, New York, 1953, pp.324,370.
202. Passiniemi, P., Simple method for determining water diffusion coefficient in conducting polymers, *Synth. Met*., **69** (1995) 685-686.

203. Passiniemi, P., General theory for determination of diffusion coefficients of solvents and gases in polymers, *Polymer*, **36** (1995) 341-344.
204. Press, W.H., Flannery B.P., Teukolsky, S.A. and Vetterling, W.T, *Numerical recipes: The art of science computing*, Cambridge University Press, New York, 1989, pp. 498-546.
205. Logan, S.R., How to determine the best straight line, *J. Chem. Educ.,* No.10 **72** (1995) 896-898.
206. Crank, J., *The mathematics of diffusion*, 2nd ed., Oxford, Clarendon Press, 1975.
207. Rastas, J. and Kivalo, P., Determination by the open-end capillary method of the diffusion coefficient of tracers in electrolytic solutions, *Acta Polytech. Scand. Chem. Ser.*, **35** (1964).
208. Liukkonen, S., Rastas, J., Hassinen, E. and Kivalo, P., Eine modification der offenen Kapillarenmethode nach Thomas zur bestimmung des tracerdiffusionskoeffizienten in wässrigen elektolytlösungen, *Acta Polytech. Scand. Chem.*, **55** (1966).
209. Christian, G., D., *Analytical chemistry*, 4th ed., John Wiley & Sons, Inc., New York, 1986, pp.59-96
210. Della Monica, M., Conductance equation for concentrated electrolyte solution, *Electrochim. Acta,* **29** (1984) 159-160.
211. Stokes, G.G., On the theories of the internal friction of fluids in motion and of the equilibrium and motion of elastic solids, *Trans. Camb. Phil. Soc.,* **8** (1845) 287-305.
212. Einstein, A., On the movement of small particles suspended in stationary liquids required by the molecular-kinetic theory of heat, *Ann. Phys*., **17** (1905) 549-560.
213. Gordon, A.R., The diffusion constant of an electrolyte, and its relation to concentration, *J. Chem. Phys.*, **5** (1937) 522-526.
214. Broersma, S., Stokes' and Einstein's law for nonuniform viscosity, *J. Chem. Phys.*, **28** (1958) 1158-1168.
215. Della Monica, M., Ceglie, A. and Agostiano, A., A conductivity equation for concentrated aqueous solutions, *Electrochim. Acta,* **29** (1984) 933-937.
216. Lobo, V.M.M. and Quaresma, J.L., *Handbook of electrolyte solutions, Part B, Physical Sciences Data 41*, Elsevier Science Publishers B.V., Amsterdam, 1989, pp.1602-1691.
217. Koryta, J., Dvořák, J. and Kavan, L., *Principles of electrochemistry*, 2nd ed., John Wiley & Sons Ltd., Chichester, 1993, pp.121-124.
218. Mortimer, R.G., *Physical chemistry*, The Benjamin/Cummings Publishing Company, Inc., California, 1993, pp.730-736.
219. Mulder, M., *Basic principles of membrane technology*, Kluwer Academic Publishers, Dordrecht, 1993, pp.110-120.
220. Petersen, E.E., Diffusion in a pore of varying cross section, *AIChE. J.*, **4** (1958) 343-345.
221. Currie, J.A., Gaseous diffusion in porous media, Parts 1 and 2, *Br. J. Appl. Phys*., **11** (1960) 314-324.
222. Michaels, A.S., Diffusion in a pore of irregular cross section, *AIChE. J*, **5** (1959) 270-271.

223. Einstein, A., Elementare theorie der brownsche bewegung, *Z. Elektrochem*. **14** (1908) 235-239.
224. Conway, B.E. and Ayranci, E, Effective ionic radii and hydration volumes for evaluation of solution properties and ionic adsorption, *J. Solution Chem.*, **28** (1999) 163-192.
225. Ayranci, E. and Conway, B.E., Size, shape and charge effects in the partial molal volume, compressibility and electrostriction behaviour of sulphur and chlorine oxyanions in water, *J. Chem. Soc. Faraday Trans. I*, **79** (1983) 1357-1372.
226. Lide, D.R., CRC *Handbook of chemistry and physics*, 72nd ed., CRC Press, Inc., Boca Raton, FL, 1991.
227. Horvath, A.L., *Handbook of aqueous electrolyte solutions*, Ellis Horwood Limited, Chichester, 1985, pp.19-33.
228. Cremers, A., *Ionic movement in a colloidal environment*, D. Sc. thesis, University Louvain, Belgium, 1968.
229. Nye, P.H., Diffusion of ions and uncharged solutes in soils and clays, *Adv. Agronomy*, **31** (1979) 225-272.
230. Tang, L. and Nilsson, L-O., Effect of curing conditions on chloride diffusivity in silica fume high strength concrete, *Proceedings of the 9th international congress on the chemistry of cement*, New Delhi, Nov., Vol. V, 1992, pp.100-106.
231. Hunter, R.J., *Introduction to modern colloid science*, Oxford University Press, New York, 1993, pp.164-193.

Diffusion is a fundamental irreversible transport process and often the rate determining step in many industrial and natural processes. The backbone of diffusion is the precise measurement of diffusion coefficients. Still, experimental diffusion coefficients are often lacking. There was a need for tracer diffusion measurement data in ternary system to test the theoretical Onsager limiting law and also need for diffusion coefficients in porous media to be used in a simulation program to predict moisture and salt concentration profiles under different environmental conditions. The diffusion coefficients of common salts were measured in porous fired bricks as a function of concentration and temperature with the numerical computer simulation and data analysis. A mathematical model was presented. The Diaphragm Cell and the Closed Capillary methods developed in this thesis are both excellent techniques for the diffusion coefficient measurements in porous materials. The Onsager limiting law was verified for the first time for a 2:1 electrolyte.

ISBN 978-952-60-5846-7
ISBN 978-952-60-5847-4 (pdf)
ISSN-L 1799-4934
ISSN 1799-4934
ISSN 1799-4942 (pdf)

Aalto University
School of Chemical Technology
Department of Chemistry
www.aalto.fi

BUSINESS + ECONOMY

ART + DESIGN + ARCHITECTURE

SCIENCE + TECHNOLOGY

CROSSOVER

DOCTORAL DISSERTATIONS

Aalto-DD 134/2014